PB-237 704

DETERMINATION OF ENERGETIC CHARACTERISTICS OF URBAN-RURAL SURFACES IN THE GREATER ST. LOUIS AREA

W. F. Dabberdt, et al

Stanford Research Institute

Prepared for:

National Environmental Research Center

April 1974

DISTRIBUTED BY:

NTIS

National Technical Information Service
U. S. DEPARTMENT OF COMMERCE

BIBLIOGRAPHIC DATA SHEET	1. Report No. EPA-650/4-74-007	2.	PB 237 704

4. Title and Subtitle

DETERMINATION OF ENERGETIC CHARACTERISTICS OF URBAN-RURAL SURFACES IN THE GREATER ST. LOUIS AREA

5. Report Date: April 1974 (date of issue)

6.

7. Author(s): W. F. Dabberdt and P. A. Davis

8. Performing Organization Rept. No.

9. Performing Organization Name and Address
Stanford Research Institute
Atmospheric Sciences Laboratory
333 Ravenswood Avenue
Menlo Park, California 94025

10. Project/Task/Work Unit No.

11. Contract/Grant No.: 68-02-1015

12. Sponsoring Organization Name and Address
The Environmental Protection Agency
National Environmental Research Center
Research Triangle Park, North Carolina 27711

13. Type of Report & Period Covered: Final

14.

15. Supplementary Notes

16. Abstracts

The role of surface geophysical characteristics (e.g., albedo, thermal admittance, Bowen ratio, emissivity) in the partitioning of energy at the complex and heterogeneous metropolitan earth-air interface has been evaluated through a unique application of Lettau's climatonomy theory. The climatonomical methodology permits the determination of effective surface descriptors on the basis of the observed diurnal response of the surface temperature to the observed forcing function of available solar energy. The method has significant potential as a tool for applied studies of climatic effects and modifications relating to land-use. Aircraft measurements, made at 2-3 hour intervals from altitudes of 460 m and 1220 m above ground, included downwelling and upwelling solar radiation, surface radiative temperature, and air temperature. Continuous records of downwelling solar and atmospheric irradiances were obtained at a single surface station located adjacent to the flight track. Balloon soundings of the lower atmosphere also were used in the analysis.

The feasibility of implementing the climatonomical approach was evaluated on the basis of experimental data obtained on 9 August 1972. Albedos showed a maximum near 16 percent over the rural sites comprising farms, fields, and woods with a minimum near 13 percent over the older urban residential and commercial/industrial sites. Urban surface temperatures were higher than the rural surface temperatures with the maximum difference (10-15 deg C) occuring in the early afternoon. The estimated thermal admittance ranged from a minimum near 20 mly sec $^{-\frac{1}{2}}$ deg^{-1} for urban and suburban sites to about 85 for the wooded sections. The estimated inverse Bowen ratio ranged from 0.22 in the urban area to 3.9 for farmland.

17. Key Words and Document Analysis. 17a. Descriptors

microclimatology; climatology; solar radiation; albedo; surface temperature

Reproduced by
NATIONAL TECHNICAL
INFORMATION SERVICE
U S Department of Commerce
Springfield VA 22151

17b. Identifiers/Open-Ended Terms

surface energy budget

17c. COSATI Field/Group: 04/02 micrometeorology; 04/02 climatology; 20/04 boundary layer; 20/08 albedo; 20/13 thermodynamics

18. Availability Statement	19. Security Class (This Report)	21. No. of Pages
Release unlimited	UNCLASSIFIED	109
	20. Security Class (This Page) UNCLASSIFIED	22. Price 5.25-2.25

EPA-650/4-74-007

DETERMINATION OF ENERGETIC CHARACTERISTICS OF URBAN-RURAL SURFACES IN THE GREATER ST. LOUIS AREA

by

W. F. Dabberdt and P. A. Davis

Stanford Research Institute
Menlo Park, California 94025

Contract No. 68-02-1015
Project No. 26AAI/16
Program Element No. 1AA003

EPA Project Officer: James L. McElroy

Meteorology Laboratory
National Environmental Research Center
Research Triangle Park, North Carolina 27711

Prepared for

OFFICE OF RESEARCH AND DEVELOPMENT
U.S. ENVIRONMENTAL PROTECTION AGENCY
WASHINGTON, D.C. 20460

April 1974

This report has been reviewed by the Environmental Protection Agency and approved for publication. Approval does not signify that the contents necessarily reflect the views and policies of the Agency, nor does mention of trade names or commercial products constitute endorsement or recommendation for use.

ABSTRACT

The role of surface geophysical characteristics (e.g., albedo, thermal admittance, Bowen ratio, emissivity) in the partitioning of energy at the complex and heterogeneous metropolitan earth-air interface has been evaluated through a unique application of Lettau's climatonomy theory. In contrast to the conventional approach that first specifies an inventory of "appropriate" surface descriptors and then attempts to evaluate or interpret observed climatic features, the climatonomical methodology permits the determination of the surface descriptors on the basis of the observed diurnal response of the surface to the observed forcing function of available solar energy. Features of various land-use types (e.g., farmland, suburban residential, commercial) can then be evaluated in the context of the surface energy budget. For example, if the subsurface heat flux is treated by assuming the medium is a homogeneous conductor, then an effective thermal admittance is derived that satisfies the assumption and the observed diurnal response of surface temperature.

During three designated experimental periods, totalling some 50 hours, that began with clear skies and reasonably steady meteorological conditions, aircraft data-collection missions were flown repetitively at 2-3 hour intervals from altitudes of 460 m and 1220 m mgl* along a selected flight track across the St. Louis area. Aircraft data included temporal and spatial measurements of downwelling and upwelling solar radiation, the effective surface radiative temperature, and the air temperature. Continuous records of downwelling solar and atmospheric irradiances were obtained at a single surface station located adjacent to the flight track.

*Above mean ground level.

The feasibility of implementing the climatonomical approach was evaluated on the basis of experimental data obtained on 9 August 1972; abrupt weather changes occurred during the other two periods and limited their suitability for extensive analysis. Albedos over the various land-use types showed a maximum near 16 percent over the rural sites comprising farms, fields, and woods with a minimum near 13 percent over the older urban residential and commercial/industrial sites. Urban surface temperatures were higher than the rural surface temperatures with the maximum difference (10-15 degrees C) occurring in the early afternoon. Aircraft albedo and surface temperature measurements, the surface irradiance measurements, and two balloon soundings of the lower atmosphere were used in the climatonomical analysis to determine both thermal addmittance and the inverse Bowen ratio for each of nine land-use sites. The thermal admittance ranged from a minimum near 20 mly $sec^{-1/2}{}_{^oC}{}^{-1}$ for urban and suburban sites to about 85 for the wooded sections. The inverse Bowen ratio ranged from 0.22 in the urban area to 2.9 for farmland.

On the basis of the results, the method is judged feasible and attractive for exploring additional factors, such as the effect of natural surface alterations (e.g., wetness and ground cover) on the surface energy budget. The method has significant potential as a tool for applied studies of climatic effects and modifications relating to land-use planning.

CONTENTS

ABSTRACT iii

LIST OF ILLUSTRATIONS vii

LIST OF TABLES xi

FOREWORD xiii

I INTRODUCTION 1

A. Objectives 1

B. Scope 3

II EXPERIMENTAL PROCEDURES 5

A. Surface Observations 5

B. Aircraft Observations 6

C. Data Processing 13

1. Solar radiation 13
2. Surface temperature 15

III METEOROLOGICAL CONDITIONS 19

A. 9 August 1972 19

B. 11 August 1972 21

C. 23 April 1973 22

IV AIRCRAFT OBSERVATIONS 25

A. Solar Data 25

B. Surface Temperatures 32

C. Air Temperatures 37

V CLIMATONOMICAL ANALYSIS 41

A. Climatonomy Theory 41

B. Method of Approach 47

V CLIMATONOMICAL ANALYSIS (continued)

C. Application and Results 61

VI CONCLUSIONS AND RECOMMENDATIONS 75

APPENDIX

A AIRCRAFT DATA SUMMARY A-1

REFERENCES R-1

ILLUSTRATIONS

11	Aero Commander Aircraft of Colorado State University a) Aero Commander 500 B (left) alongside a Cessna 182 Skylane (right) b) Interior View of Equipment Rack in Aero Commander	8
2	Flight Tracks, Check Points, and Locations Selected for Harmonic Analysis of Data	10
3	Variations in Response between Wide-Angle and Narrow-Angle Solarimeter Measurements of Surface Reflectance and between 4-Degree and 20-Degree Radiometric Measurements of Surface Temperature	14
4	Total Solar and Atmospheric Radiation Incident on Horizontal Surface, Granite City, Illinois, 9 August, 1972	20
5	Total Solar and Atmospheric Radiation Incident on Horizontal Surface, Granite City, Illinois, 11 August, 1972	23
6	Aircraft Solar Measurements, 1400 CDT Flight, 9 August, 1972	26
7	Height Variations of Measured Incident Solar Radiation, 11 August 1972	29
8	Normalized Aircraft Solar Measurements, 1700 CST Flight, 23 April 1973	31
9	Aircraft Radiometric Surface Temperature Measurements, 1400 CDT Flight, 9 August 1972	33
10	Normalized Aircraft Radiometric Surface Temperature Measurements, 1700 CST Flight, 23 April 1973	34
11	Urban and Rural Surface Temperature Variations with Time (a) 9 August 1972 (b) 23 April 1973	36

ILLUSTRATIONS (Continued)

12 Aircraft Air Temperature Measurements, 1400 CDT Flight, 9 August 1972 38

13 Site R-1 50

14 Site R-2 50

15 Site R-3 50

16 Site R-4 50

17 Site R-5 51

18 Site R-6 51

19 Site R-7 51

20 Site R-8 51

21 Site R-9 52

22 Near-Surface Meteorological Stations Operated by Illinois State Water Survey, August 1972 57

23 Comparison of Two-Harmonic Temperature Wave at Station 022 and Two-Harmonic Regression Analysis for Site R-1 Using Data Points 60

24 Effective Surface Radiative Temperature from Two Aircraft Altitudes at Nine Sites on 9 August 1972 62

25 Diurnal Variation of Derived Departures (from daily average) of Atmospheric, Latent, and Subsurface Heat Flux Densities for Three Land-Use Types: Farmland, Commercial/Industrial, and Suburban Residential 74

ILLUSTRATIONS (Concluded)

A-1 Aircraft Solar Measurements, 0930 CDT Flight, 9 August 1972 . . . . . A-6

A-2 Aircraft Solar Measurements, 1145 CDT Flight, 9 August 1972 . . . . . A-7

A-3 Aircraft Solar Measurements, 1400 CDT Flight, 9 August 1972 . . . . . A-8

A-4 Aircraft Solar Measurements, 1630 CDT Flight, 9 August 1972 . . . . . A-9

A-5 Aircraft Solar Measurements, 1915 CDT Flight, 9 August 1972 . . . . . A-10

A-6 Aircraft Solar Measurements, 0900 CDT Flight, 11 August 1972 . . . . . A-11

A-7 Aircraft Solar Measurements, 1130 CDT Flight, 11 August 1972 . . . . . A-12

A-8 Aircraft Solar Measurements, 1400 CDT Flight, 11 August 1972 . . . . . A-13

A-9 Aircraft Solar Measurements, 1630 CDT Flight, 11 August 1972 . . . . . A-14

A-10 Aircraft Radiometric Surface Temperature Measurements, 9 August 1972 . . . . . A-15

A-11 Aircraft Air Temperature Measurements, 9 August 1972 . . . . . A-17

A-12 Aircraft Radiometric Surface Temperature Measurements, 11 August 1972 . . . . . A-19

A-13 Aircraft Air Temperature Measurements, 11 August 1972 . . . . A-21

A-14 Aircraft Radiometric Surface Temperature Measurements, 23 April 1973 . . . . . A-23

TABLES

1	Chronological Summary of Aircraft Operations in St. Louis	11
2	Description of Surface Areas Selected for Analysis	53
3	Results of Harmonic Analysis of 9 August 1972 Surface Observations of Downwelling Short- and Long-Wave Radiation at Granite City, Illinois	54
4	Comparison of the 24-Point Harmonic and 8-Point Regression Analyses of the Near-Surface Ambient Temperature on 9 August 1972 in the Greater St. Louis Area	58
5	Albedo Values for the Nine Surface Areas as Measured on 9 August 1972 from the Two Aircraft Altitudes	66
6	Climatonomic Parameters for 9 August 1972, in the Greater St. Louis Area	67
7	Derived Amplitude Terms for Atmospheric Sensible, Latent, and Subsurface Heat Flux Densities	73

FOREWORD

A large number of people contributed a variety of skills and services to this program: Contract Manager for the study was Dr. James L. McElroy, Meteorology Laboratory, National Environmental Research Center, EPA, Research Triangle Park, N.C.; Ms. Patricia Buder, Research Meteorologist, and Mr. Hisao Shigeishi, Mathematician, SRI, contributed significantly in the analysis and processing of the data; Dr. Edward Uthe, Atmospheric Physicist, SRI, provided the surface radiation data during August 1972; Dr. William Marlatt, Mr. Don Hill, and Mr. Duane Adams, Colorado State University, provided the aircraft and instrumentation services under subcontract to SRI; Mr. Stan Changnon, Illinois State Water Survey, provided near-surface temperature records for August 1972; the National Weather Service, Lambert Field, St. Louis, provided forecast information and EMSU soundings; and Dr. Clifford Murino, Vice President for Research, St. Louis University, kindly assisted by providing facilities at the University for maintaining and operating the surface radiation station during April 1973, in cooperation with Professor Donald E. Martin, Director of Meteorology, and Mr. Louis J. Hull, both of St. Louis University.

I INTRODUCTION

A. Objectives

It is well recognized that the complex air-earth interface plays an important role in the behavior of the atmospheric planetary boundary layer and in the differences in the structure of the rural and urban surface energy budgets. Understanding these differences (and the subsequent partitioning of the net radiation) is further complicated by the local heterogeneity of individual surface types (i.e., land-use patterns) and the attendant difficulties in parameterization of the interface energy fluxes. Conventional approaches toward solution of the problem implicitly consider the local areas to be homogeneous on the broader scale, and then proceed to first specify the appropriate surface geophysical descriptors (e.g., albedo, thermal admittance, roughness) and subsequently compute the energy fluxes. One of the major difficulties in this approach is the a priori specification of surface descriptors.

To overcome this obstacle, we have developed and tested a method whereby these descriptors are determined through an examination of variations of the surface energy budget as a function of land use, and the subsequent analysis of these variations in terms of the associated differences in the geophysical features of the surface. Included among the surface characteristics are radiative (albedo, emissivity), thermal (heat capacity, conductivity), and structural (aerodynamic roughness, height-area-orientation) properties. Radiative and thermal characteristics are affected by surface wetness, but the importance of evapotranspiration makes it necessary to add surface "type" as a characteristic, particularly to distinguish such features as cropland, meadows, parks, and the like.

To be useful in modeling, the influence of the surface characteristics on the surface energy budget must be identified, even before associated feedback reactions with the boundary layer can be considered fully.

The basic objective of this study was the examination of the variations of the surface energy budget throughout the greater St. Louis metropolitan area (ranging from rural farmlands to suburbia to the urban core) so as to evaluate these variations in terms of associated differences in the thermal, radiative and aerodynamic geophysical features of the surface. Toward this end, we have drawn heavily from the climatonomy theory of H. and K. Lettau[*1] (1971). In climatonomy, temporal climatic variations are described analytically as unique response functions to a prescribed forcing function. More specifically, climatonomy may be summarized as the quantitative determination of mean values and temporal-spatial variations of: (1) temperature, the primary response function, and (2) energy fluxes, the secondary responses (e.g., atmospheric and subsurface sensible heat exchange, net effective infrared emissions, evaporation) at a planetary surface in response to the solar forcing function (i.e., available incident solar radiation).

A major purpose of this study was to examine the feasibility of obtaining representative empirical data on the spatial and diurnal variations in the effective geophysical surface characteristics of selected heterogeneous areas with different surface types. Variations in the diurnal response of surface temperature are reflected in the secondary responses and depict the influence of the surface on the establishment of rural-urban differences in the surface energy budget. This information should provide a more meaningful classification of distinct surface types in terms of climatic responses to incident radiation.

---

[*] References are listed at the end of this report.

B. Scope

The experimental program focused on the acquistion of data on the spatial and temporal (i.e., diurnal) distribution of surface temperature, and solar and terrestrial radiation for a variety of surface types. The data may be conveniently categorized according to source:

- Frequent aircraft observations
- Continuous surface observations
- Supplemental, conventional observations.

The aircraft observations consisted of flights at two-to-three hourly intervals over a 90-km path centered over the St. Louis urban core; to obtain as much independent data as possible, the initial and return legs of each flight were made at different altitudes. The primary aircraft data included both upwelling and downwelling solar irradiance and effective surface radiative temperature. Supplemental aircraft observations included surface photography and ambient temperature. Representative measurements of the albedo (based on upwelling irradiance measurements) and surface temperature (based on upwelling radiance measurements) are difficult to acquire except from a moving platform aloft. In fact, over a very non-homogeneous surface the only effective means of observing surface temperature is by radiometric techniques applied in a nearly transparent spectral region. At this stage of investigation no emphasis was given to a study of direct influences of the atmospheric boundary layer itself on the radiative processes. Instead, site representative measurements of total downwelling irradiance were made at one surface so as to incorporate directly any atmospheric influence. The other principle data requirement is the boundary layer wind profile; this was available twice-daily from the nearby Environmental Meteorological Support Unit (EMSU) station operated by the National Weather Service (NWS).

Surface geophysical features derived through the analysis of the surface response to the radiative forcing function were limited to two parameters: thermal admittance and inverse Bowen ratio. This limitation is a result of the number and type of measured values; to derive additional geophysical features would require additional measurements, such as the latent or sensible heat fluxes. Even so, certain simplifying assumptions had to be made: photosynthetic and anthropogenic fluxes of heat were not treated explicitly in the theory; however, their actual impacts on the observations are implicit in the data and thus are reflected in the derived values. On the other hand, the August data used in the analysis have the advantage that contributions from both processes to the surface energy balance are most likely minimal.

II EXPERIMENTAL PROCEDURES

A. Surface Observations

Although it would be desirable to obtain measures of the downwelling irradiance at the surface simultaneously over each of the various urban and rural surface types, it was necessary to accept a single site only. However, for the clear conditions selected for study, a single location should provide a representative measure of the forcing function at all locations, except in situations with extreme variations in pollutant loading. An Eppley Precision Spectral Pyranometer (PSP) was mounted free of sky obstructions to measure the total direct-plus-diffuse solar irradiance on a horizontal surface. During August 1972 this instrument was installed at the Granite City Army Depot as part of an SRI METROMEX experiment.[2] At the same site the atmospheric radiation incident on a horizontal surface was recorded from an Eppley Pyrgeometer Infrared Radiometer (PIR). Nearby observations of pressure, wind velocity, temperature, and wet bulb temperature also were available; the SRI lidar used during METROMEX provided a relative measure of local particle loading of the lower atmosphere. Data from other METROMEX experiments were available for other locations in the St. Louis area.

The surface site was established at St. Louis University during a second field program at St. Louis in April 1973. The same Eppley PSP was used for the measurement of downwelling solar irradiance, but the atmospheric radiation was inferred from concurrent measurements with a C.S.I.R.O. Net Radiometer (NR). The latter instrument was installed with a blackened dome covering its bottom sensing surface. This dome contains a thermocouple junction; a reference thermocouple junction immersed in a reference bath at a known temperature is used to determine the black

body radiation incident on the lower surface of the NR. Thus, the residual difference between the black body radiation and the measured net radiation gives the downwelling irradiance only. At night, the downwelling irradiance is simply the desired atmospheric radiation. During the day, the separately measured total insolation (from the PSP measurement) must be subtracted from the downwelling irradiance derived from the NR to obtain the atmospheric radiation. A nuisance with operation of the NR was the requirement to supply nitrogen from a tank to maintain dry-air pressure for inflation of the upper polyethelene dome of the instrument. Some difficulty was encountered in maintaining a nearly constant pressure on the dome over an extended period of time without readjustment.

Data from the PSP and PIR during August 1972 and the PSP and NR during April 1973 were recorded on a two-channel Hewlett-Packard Moseley recorder.

B. Aircraft Observations

The two key measurements of the program were the diurnal variations of surface temperature and of albedo over the heterogeneous lower boundary of the urban-rural St. Louis area. It was concluded that the only feasible approach to the acquisition of these data was the use of a light aircraft for repeated low-level flights (throughout the 24-hour period) along the same flight track, thus covering the same surface features each time. The twin-engine Aerocommander aircraft (shown in Figure 1) owned by Colorado State University (CSU) was selected. This aircraft had been used extensively for low-level meteorological experiments and was equipped to acquire the type of measurements required in this study.

A daily routine of nine flights was selected for documentation of diurnal variations. Each flight lasted approximately one hour, allowing one-half hour for the departure leg and one-half hour for the return leg

along the same track. During August, take-off times originally were selected for 0000, 0300, 0600, 0830, 1100, 1330, 1600, 1830, and 2100 in Central Daylight Time. Because of greater daytime variability in surface properties flights were spaced more closely during the day than during the night. During April, take-off times (Central Standard Time) were set at 0100, 0400, 0630, 0900, 1130, 1400, 1630, 1900, and 2200. The flight schedule was designed to provide maximum data density during daylight hours when surface temperatures change most rapidly. This is particularly important because the analysis methodology required the specification of the diurnal variation of the meteorological parameters in terms of a Fourier expansion.

Flight tracks were chosen to sample a variety of land-use types and to approximately parallel the low-level wind flow; accordingly, they were based in large part on the clear-sky wind rose climatological data for the given times of year. Two flight levels (departure and return) were designated at 460 m and 1220 m above the mean ground level. The upper level, near the top of the boundary layer and the cloud-base level (for small cumulus clouds), provided an appropriate altutude for the aerial photography. In addition, by acquiring data at two levels, it is possible, in principle, to infer the effects of atmospheric attenuation on the measurements of surface temperature and albedo.

Figure 2 illustrates the flight tracks adopted for August 1972 and April 1973. These tracks were selected not only on the basis of wind roses, but were designed to avoid the critical air space near Lambert Field as well as some of the higher obstructions in the southwestern portion of the city. Nevertheless, each track crossed an interesting variety of land use patterns and visually identifiable checkpoints. River crossings are excellent checkpoints because they are identifiable in both the surface albedo and temperature records. River crossings along the April track were superior to those in August because

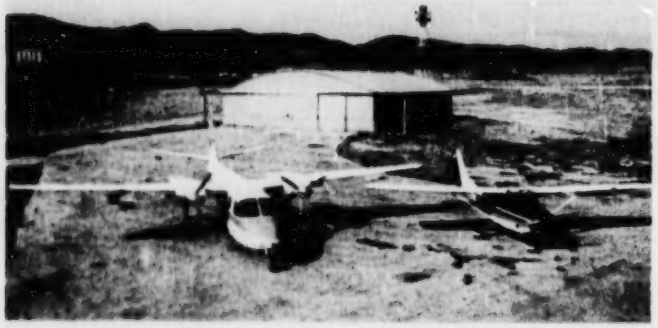

(a) AERO COMMANDER 500 B (LEFT) ALONGSIDE A CESSNA 182 SKYLANE (RIGHT)

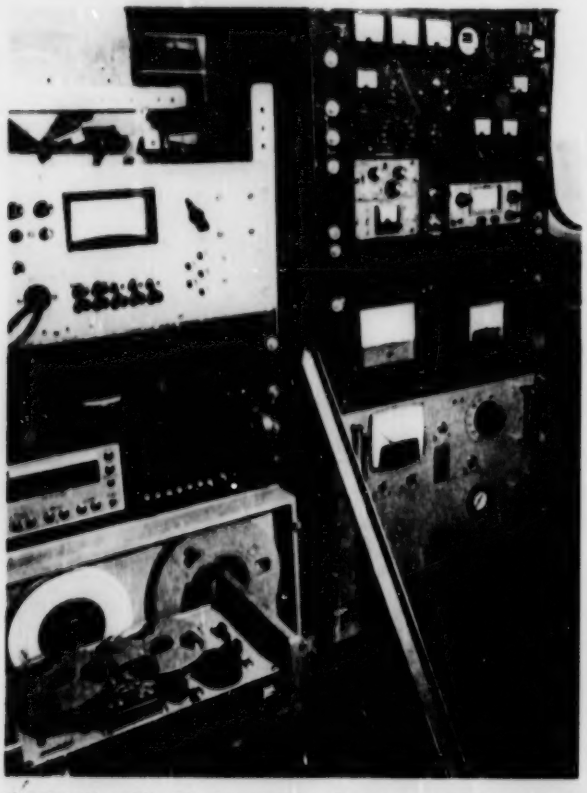

(b) INTERIOR VIEW OF EQUIPMENT RACK IN AERO-COMMANDER

SA-2322-11

FIGURE 1 AERO COMMANDER AIRCRAFT OF COLORADO STATE UNIVERSITY

of the right angle of the flight track to the rivers; when the track slants across a river a slight drift in position alters the distance between checkpoints. For the August 1972 flights the CSU aircraft was operated from the Alton Municipal Airport near the northern end of the flight track. During April 1973 the aircraft was operated from the Spirit of St. Louis Airport near the western end of that flight track. The checkpoints for both flight tracks that were used in the final data reduction are illustrated in Figure 2. Also illustrated along the August flight track are the positions for which a detailed time series analysis of data for 9 August 1972 was performed (discussed later). Although data were recorded in the time domain, checkpoints were used to convert all data to the distance domain. In this way variations in ground speed along the two legs of the flight were effectively removed by changing the data density per unit distance. Table 1* contains a listing of all flights conducted during the program.

Under a subcontract with Colorado State University, its pilot and technician obtained the following measurements from the aircraft:

(1) Subtrack photographs with two Hasselblad 70 mm cameras

(2) Total downwelling solar irradiance with an Eppley Pyranometer

(3) Total upwelling solar irradiance (reflected solar radiation) with a Yellott SOL-A-METER (solarimeter)

(4) Surface temperature with a Barnes PRT-5 radiometer (8 to 13 μm)

(5) Wet and dry bulb temperatures at flight altitude.

Aerial cameras were employed to document surface characterisitcs of regions used later for time series analysis, to verify checkpoint

---

*Times shown in this table are flight starting times in contrast to the text and figures where some average time is used to designate a specific flight.

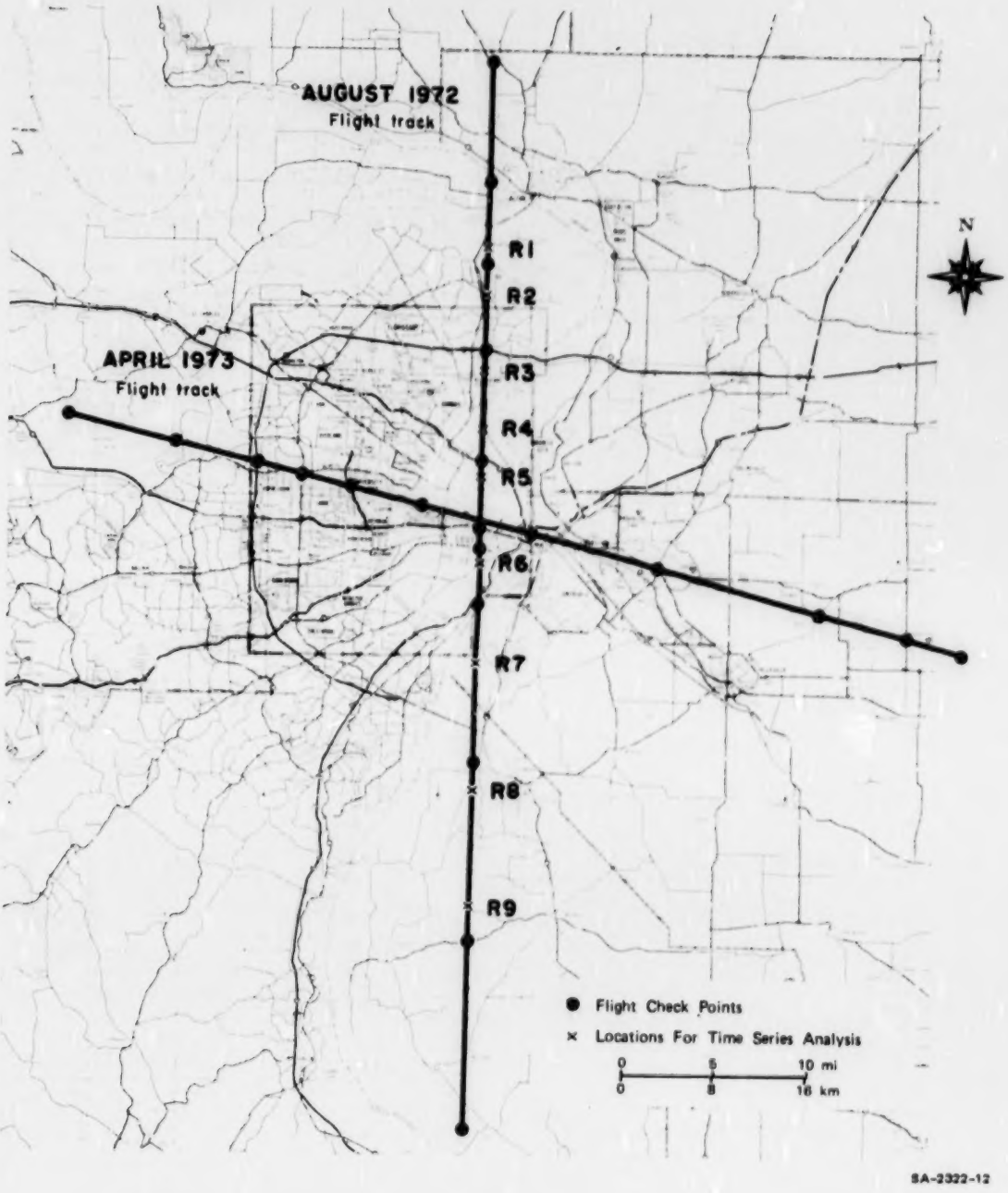

FIGURE 2 FLIGHT TRACKS, CHECK POINTS, AND LOCATIONS SELECTED FOR HARMONIC ANALYSIS OF DATA

Table 1

CHRONOLOGICAL SUMMARY OF AIRCRAFT OPERATIONS IN ST. LOUIS

DATE	START (Local Time)*	FLIGHT TRACK†	COMMENTS
9 August 1972	0345	N-S	
	0555	N-S	
	0850	N-S	
	1120	N-S	Photographs
	1330	N-S	
	1600	N-S	
	1845	N-S	
	2100	N-S	Aircraft malfunction; flight aborted
11 August 1972	0030	N-S	
	0330	N-S	
	0630	N-S	
	0900	N-S	Photographs
	1130	N-S	Photographs
	1400	N-S	Photographs
	1630	N-S	Photographs; rain showers along flight track
12 August 1972	1100	N-S	Check flight
17 April 1973	1400	E-W	PRT-5 test flight
23 April 1973	1630	E-W	Photographs
	1900	E-W	
	2200	E-W	
24 April 1973	0100	E-W	
	0400	E-W	
	0600	E-W	Photographs; extensive cloudiness
	0830	E-W	Extensive cloudiness
27 April 1973	1115	E-W	Photographs; rain showers developed

*August times are Central Daylight Time; April times are Central Standard Time.

†See Figure 2

locations and actual tracks followed in flight, and to assist in data interpretation as a function of time of day. Good 70 mm film transparencies were obtained over most of the August flight track; selected prints over specific areas during the flight of 9 August are presented later. Two Hasselblad cameras were used to obtain overlapping photographs at a 1220 m flight altitude at typical cruising speed, but complete coverage over the 90 km track on a single flight leg required changing film during flight. With only a single technician aboard the aircraft, other duties normally would not allow sufficient time for changing film.

For the April 1973 flights, along the E-W track shown in Figure 2, two additional Hasselblad cameras and an observer were added to the flight program. No complete daytime series of observations was acquired during the April program, although rather complete photographic coverage of the entire E-W track was obtained during an unsuccessful flight near noon on 27 April. Despite the inferior quality of some of those prints, land-use forms and flooded areas (especially along the western end of the track) were clearly depicted. In general, the surface types were very similar to those covered along the other track for the August flights.

Data from the pyranometer and solarimeter were recorded onboard on separate Moseley strip-chart recorders. The PRT-5 radiometric measurements, dry and wet bulb temperatures, and time were recorded on a seven-channel PEMCO analog recorder. One of the channels was used as an event marker to indicate overflights of checkpoints along the flight track.

Albedos were determined simply as the ratio of upwelling to downwelling irradiance. Although the pyranometric measurements of downwelling irradiance were associated with a time constant on the order of 15 seconds (about 1 km travel distance), such rapid variations in the downwelling irradiance during clear-skies were not anticipated. The time constant for upwelling irradiance measurements, on the other hand, was on the

order of milliseconds (similar to the time constant for the PRT-5 radiometer). For the April flights a narrow-angle (20-deg) solarimeter was added to provide more restricted views that were more compatible with the radiometric surface temperature scenes acquired by the PRT-5. Furthermore, for the April program, the field of view of the PRT-5 was expanded from 4 to 20 degrees with a lens. Thus, the infrared radiometric resolution was degraded while the spatial resolution of the reflected solar radiation measurements was increased for compatibility.

Figure 3a shows (in relative ordinates) samples of recorded radiometric temperature response as measured along the April flight track under cloudy skies on 17 April (not a data run). Although the two trace segments were not acquired simultaneously, they successfully illustrate that the coarser resolution provides appropriate data for comparison with solar measurements. Figure 3b provides a comparison of the narrow-angle and wide-angle solarimeter data from a flight altitude of 460 m. In absolute form the data from the narrow-angle solarimeter (converted to hemispheric) appear to read lower than the wide-angle data. Because of residual uncertainties in the calibration data, results in Figure 3b are plotted in normalized fashion. It is apparent that the enhanced responsiveness of the narrow-angle solarimeter makes it preferable to the wide-angle instrument.

C. Data Processing

1. Solar Radiation

Records of the downwelling irradiance measurements at the surface were digitized manually and instrument calibration data were applied to the digitized data. Strip chart records of the solar measurements aboard the aircraft were checked for quality, timing, and zero-reference drift. Airborne strip chart speeds were maintained at 2 in/min; pyranometer data were recorded over a 10 mv amplitude range

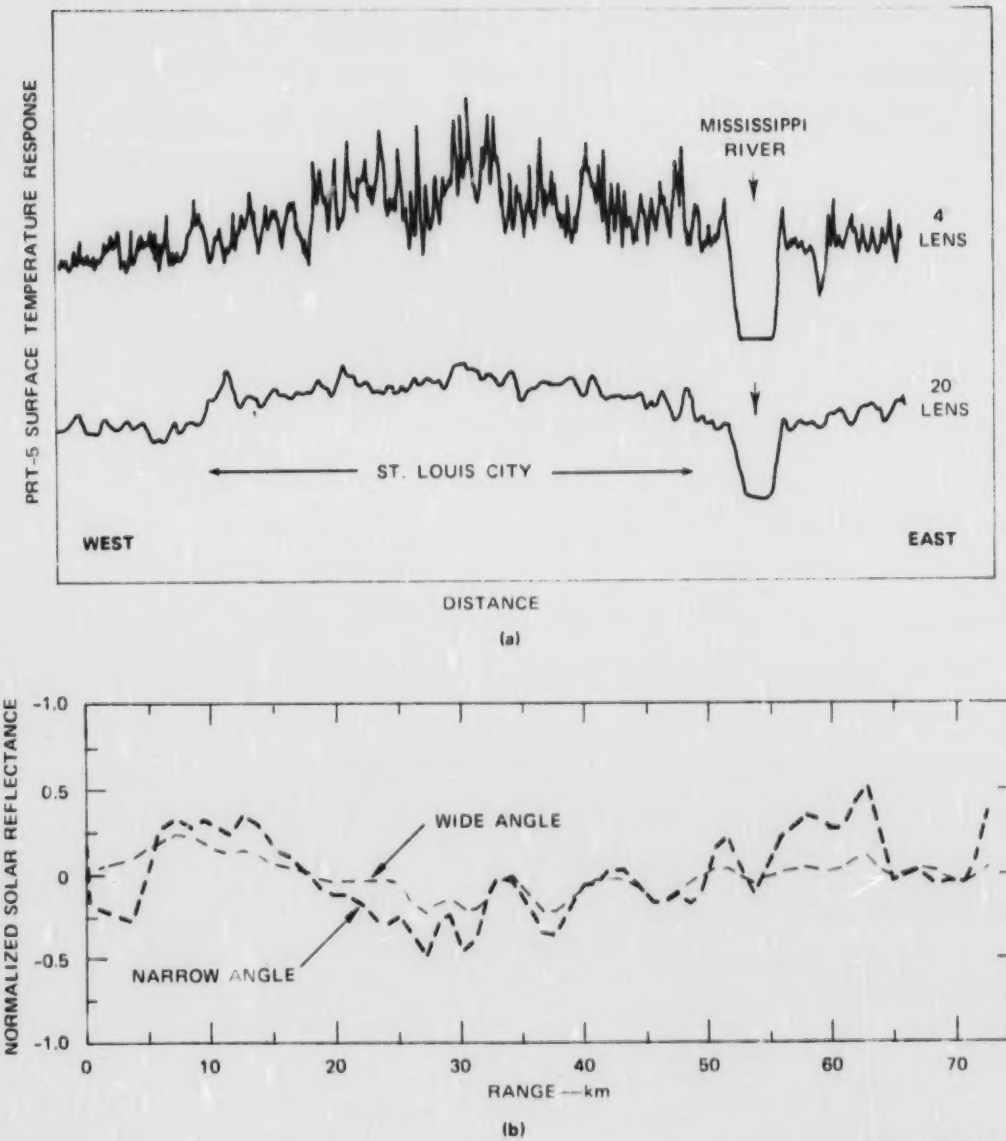

FIGURE 3 VARIATIONS IN RESPONSE (a) BETWEEN 4-DEGREE AND 20-DEGREE RADIOMETRIC MEASUREMENTS OF SURFACE TEMPERATURE AND (b) BETWEEN WIDE-ANGLE AND NARROW-ANGLE SOLARIMETER MEASUREMENTS OF SURFACE REFLECTANCE

whereas solarimeter data were expanded to a full-scale 5 mv range. Fifteen-second averaged samples were punched on computer cards for processing on SRI's CDC 6400 computer. Calibration, conversion to the units of cal cm^{-2} min^{-1}, albedo calculations, and graphing of results were accomplished on the computer in conjunction with the CDC 280 CRT display and microfilm system. Most difficulty was encountered with the data plotting program. It was necessary to identify data points closest to available checkpoints on each flight. Subsequently, the spacing of data points between checkpoints was preset in accordance with the known range between checkpoints. In this way it was possible to align data from the two flight levels over the proper points in range and ensure correspondence with data from the PEMCO recorder. The biggest difficulty with the river crossings occurred when the flight track from one leg strayed to the east or west of the other leg (on the August flights). Such a drift would force the appearance in the data plots of a misplacement in the river locations on a fixed range scale. The alternative was to shift the river crossings to exactly the same range points with an attendant artificial compression or expansion of data points over short stretches. In final form the upwelling and downwelling irradiances and the albedos along a single flight leg were plotted (using a three-point triangular slit function) separately from those along the other flight leg. Data from the return leg were plotted in reverse order so that the ordinates and abscissas of both graphs matched for easy comparison. Listings of all plotted data points were obtained also as a function of range.

2. Surface Temperature

Data from the analog tapes from the PEMCO recorder were digitized at a high rate at Colorado State University. Resultant digital tapes were processed on the CDC 6400 at SRI. First, revised digital tapes were prepared, during which time one-second averages of

the digital count in each channel were computed, stored and listed. These listings were used to screen the data and assign checkpoint locations. During the final computer run the digital counts from the intermediate tape were averaged over five-second intervals, converted to volts and then to temperature, and plotted on the same abscissa (range along flight track) used to plot the solar data. Range zero always referred to the first checkpoint on the flight track (the northern end for the August flights and western end for the April flights), the extreme right side of the plot always contained data from the southernmost (August) or easternmost (April) end of the flight track. Two graphs were plotted for each flight, but instead of separating them according to flight altitude (leg) as with the solar data, one graph contained the surface temperatures measured from the PRT-5 during both flight legs and the other graph contained the dry bulb temperature for both flight legs. The arrangement was selected because of the usefulness of direct comparison of temperature measurements of the same type from different altitude. Since the surface temperatures measured from both altitudes were expected to be extremely close in magnitude, 10°C was added to all measurements from one flight altitude to displace the record on the plotted graph.

The most serious data reduction problem encountered was the zero drift on the particular PEMCO recorder used, apparently as a result in part of inadequate warm-up during the frequent short-duration flights. Thus, while adequate calibration data were available for converting voltages to temperature, it was extremely difficult to obtain a reliable quantitative zero reference to convert digital count to voltage. During the April 1973 flights the situation was improved by installing voltage boxes to supply known voltages to all channels at least three times during a flight. For the August 1972 data, corrections had to be based on post-flight laboratory displays of zero drift, apparent changes in

river surface temperature on a given flight, and on observed background changes in the digital count on the event channel when not in use. Deducted time-dependent changes in digital count to all channels had to be added during the final processing stage.

III METEOROLOGICAL CONDITIONS

A. 9 August 1972

During the afternoon of 8 August 1972 a weak frontal system passed through the St. Louis area. A following period of at least 36 hours of clear weather was anticipated. It was decided to initiate flights at 0300 CDT on 9 August 1972; at the time light winds from the NNW prevailed. A minimum (shelter-height) surface temperature of 15°C occurred at about 0540 CDT. By 0900 surface winds had shifted toward the NE. Some cirrus clouds were present in the morning and some cumulus activity occurred in the afternoon. The flight initiated at 2100 CDT was aborted because of an aircraft alternator malfunction. This incident terminated the mission during what subsequently developed as the best opportunity for a 24-hour period of observation under reasonably steady meteorological conditions. Particle loading of the atmosphere, as revealed by time-height displays of lidar backscatter signals, was relatively light for the area for this time of year.

Figure 4 shows the total insolation as well as the atmospheric infrared irradiance at the Granite City surface site on 9 August 1972. The influence of morning cirrus clouds and small afternoon cumulus clouds on the downwelling solar irradiance is apparent in the trace. The maximum in the curve of atmospheric radiation occurs more than an hour after the maximum incoming solar radiation, but the trace generally shows little variation. An even greater phase lag was anticipated. A careful examination of the PIR data suggested that measurements of the atmospheric radiation were not reliable over short time scales; apparently, the instrument responded to short-term solar heating of the instrument window rather than solely to the true local infrared scene aloft.

Preceding page blank

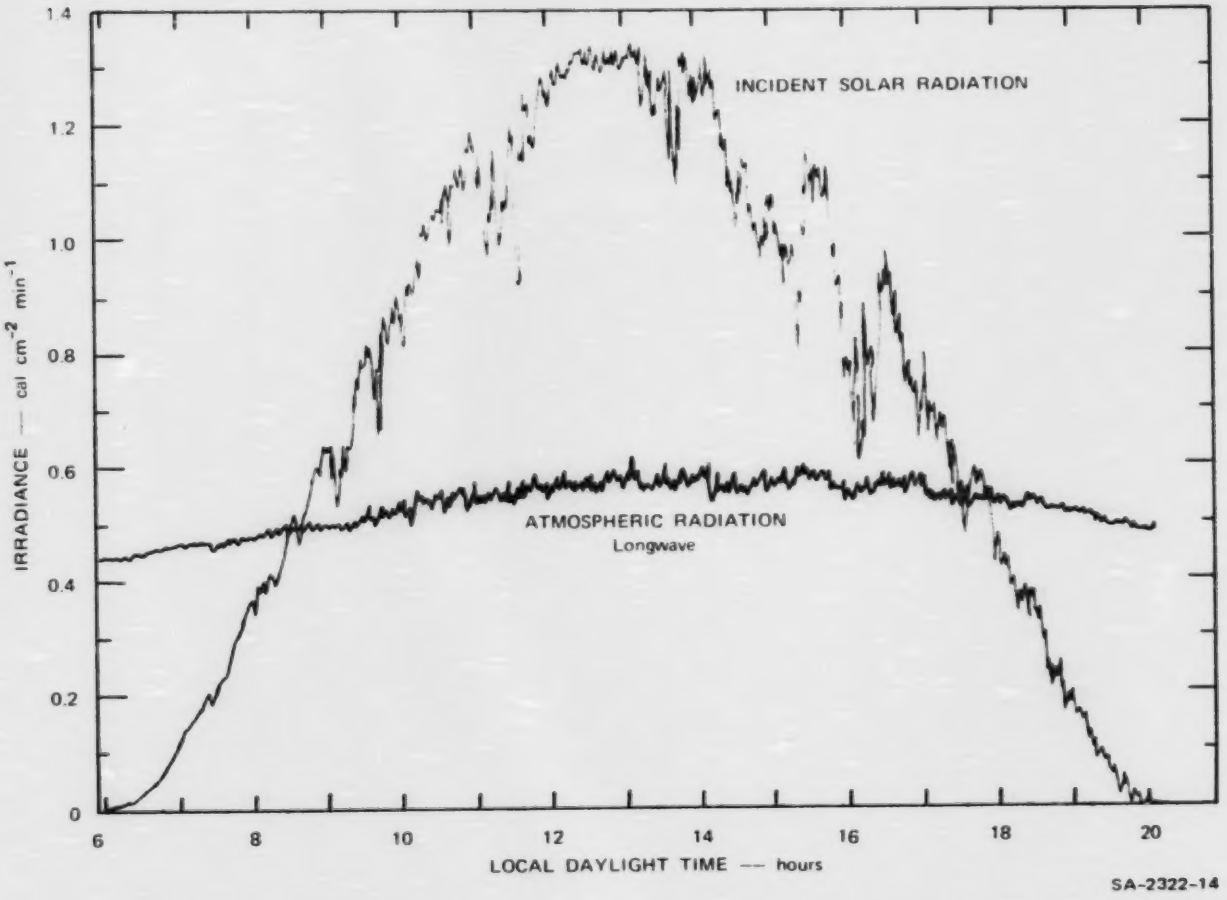

FIGURE 4 TOTAL SOLAR AND ATMOSPHERIC RADIATION INCIDENT ON HORIZONTAL SURFACE, GRANITE CITY, ILLINOIS, 9 AUGUST 1972

B. 11 August 1972

On 10 August the region of highest pressure in the area had shifted to the southeast, enabling a return flow of warmer air with higher humidity from the south. The forecast for 11 August called for fair weather but with cumulus activity in the afternoon leading to perhaps a 4/10 sky cover. Inasmuch as the flight track used on 9 August was suitable, another series of observations was initiated with the first flight at 0030 on 11 August. At that time surface winds were light from the SSE. A minimum temperature of about 17.4°C was observed at 0530. By daylight a considerable cover of cirrus clouds prevailed but, since solar heating was evident, the mission continued. Surface winds increased during the morning with directions shifting through S to SSW and then to SW. At the same time the cirrus cover dissipated. The winds subsided in the afternoon but small cumulus began forming by 1330. By 1530 winds had become variable and considerable convective activity had increased the cumulus cloud cover to about 5/10. The maximum temperature at the Granite City site was 32.2°C. At 1545 CDT cumulonimbus clouds developed nearby and extended almost overhead by 1630, the starting time of afternoon flight. Shortly thereafter the winds at the Granite City site shifted to the N and then the NE while remaining light. Some showers had occurred in the city and the mission was aborted after the 1630 flight.

Figure 5 shows the total solar radiation and atmospheric infrared radiation measured at Granite City during the daytime of 11 August. The curve for total insolation illustrates the deterioration of the forcing function of the surface energy balance near 1600. Although particle loading of the atmosphere was somewhat more extensive than on 9 August 1972, 11 August was not a day with strong pollution.

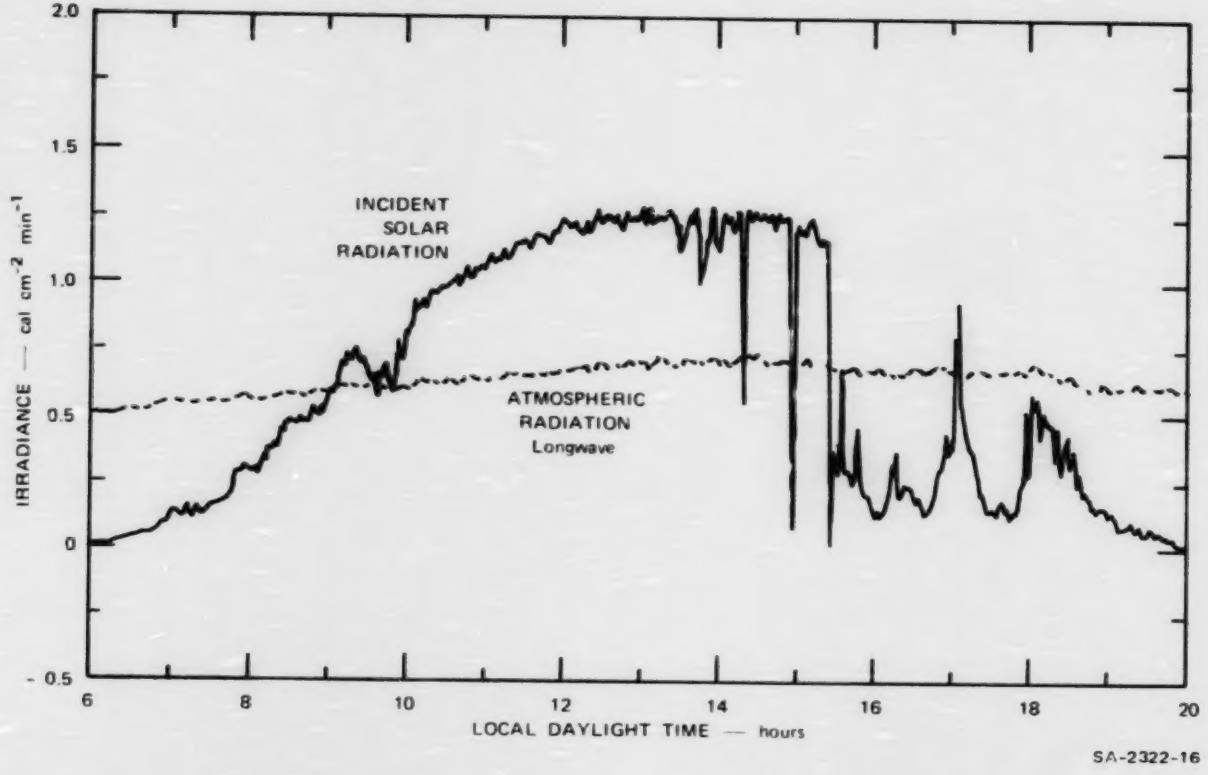

FIGURE 5 TOTAL SOLAR AND ATMOSPHERIC RADIATION INCIDENT ON HORIZONTAL SURFACE, GRANITE CITY, ILLINOIS, 11 AUGUST 1972

C. 23 April 1973

A second experimental program in the St. Louis area was arranged with Colorado State University to permit availability of their aircraft during a two-week period. Unfortunately, the desired optimum weather conditions did not prevail during this period. Unusually severe flooding affected the general area during the stay, thus rendering somewhat atypical the rural-urban differences in surface characteristics. No satisfactory 24-hour periods for the observational program occurred during the first week. During the following week the forecasting problem became very difficult due to periodic surges of moist air aloft with upper-level cloudiness, sometimes with light rain. As events developed, a suitable 24-hour period would have been possible following the rain on the night of 22 April 1973. The forecast for 23 April was for fair weather until late in the day again. However, when it began to appear that overcast conditions would not occur until sometime on 24 April it was possible to initiate a series of observations late in the day of 23 April. It was concluded that at least a series of observations during the cooling period following a dry daytime period would be worthwhile. The first flight could not be started before 1630 CST, at which time skies were clear with relatively light winds from the WNW. By about 0000 on 24 April cirrus clouds began moving in over the surface site at St. Louis University. Before sunrise winds shifted to the NE, and eventuall more to the E. By 0900 on 24 April a middle and high overcast condition had developed and further flights were cancelled. Inasmuch as only a very limited period of insolation was recorded before sunset and the nighttime record of atmospheric radiation was very steady (with only a slight increase from cirrus clouds after midnight), these observations were not presented herein.

IV AIRCRAFT OBSERVATIONS

A. Solar Data

Graphic records of all of the processed solar data obtained during the flight days of 9 August and 11 August 1972 are presented in the Appendix. Data samples illustrated in Figure 6 refer to the 1400 CDT flight of 9 August. The origin of the range scale shown in Figure 6 corresponds to the northernmost checkpoint in Figure 2. A broad portion of the Mississippi River was crossed at a range of about 10 km. Some irregularities in the measured downwelling solar irradiance in Figure 6 result from clouds existing above the aircraft. The dip in downward flux measured from the 460 m altitude at the 50 km point in range is associated with an artificial maximum albedo; this is the result of cloud shading the pyranometer but not the target area on the surface. A striking feature of the illustration, which is typical of all observations, is the lower albedo over the urban area (roughly, between 33 and 45 km range) relative to the surrounding suburban and rural areas. Although the spatial difference in albedo is only a few percent absolute, the reduced urban albedo surely is significant in terms of the surface energy budget. More of the solar radiation reaching the urban surface is available for heating the surface. In addition, the lack of significant evapotranspiration processes over the urban area means that even more solar radiation is available for heating. A complete explanation of the lower urban albedo requires a more careful examination, but the observed differences are probably accounted for by the structural "trapping" of solar radiation and shading of other surfaces in the urban area, combined with a surprising number of relatively dark urban roofs, areas with reflective soils outside the urban area, and an increase in

Preceding page blank

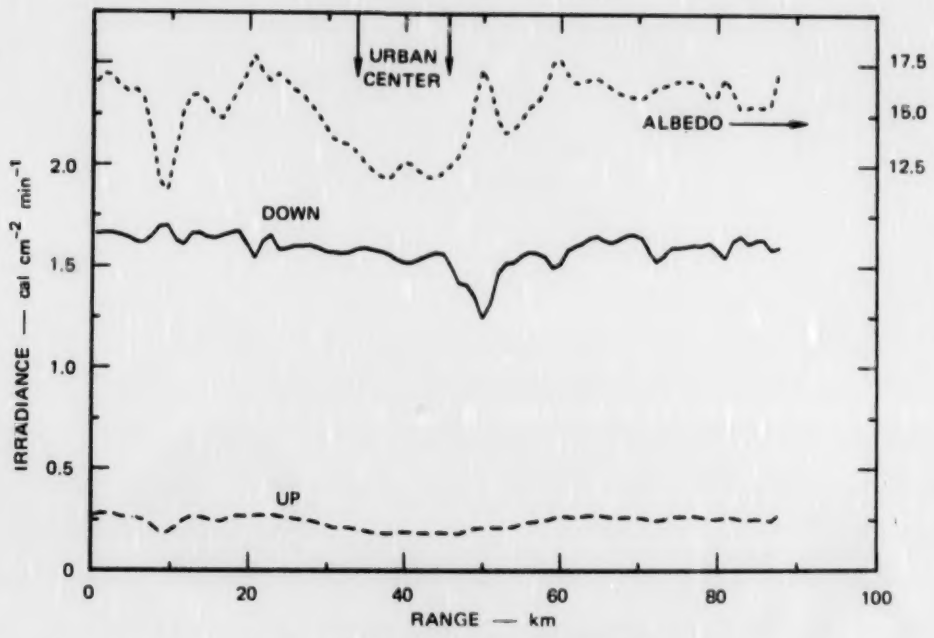

(a) FLIGHT ALTITUDE = 460 METERS

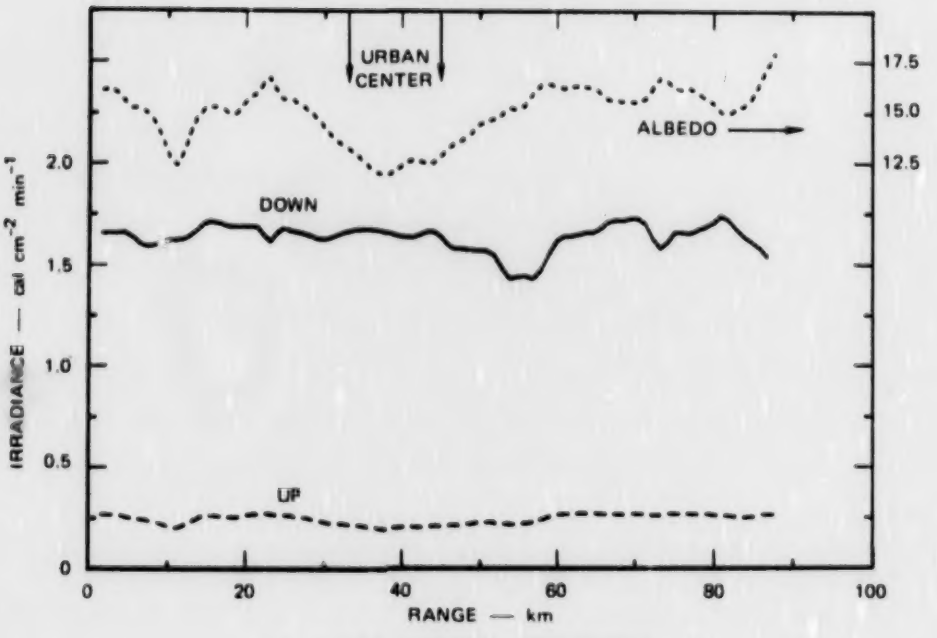

(b) FLIGHT ALTITUDE = 1220 METERS

SA-2322-17

FIGURE 6 AIRCRAFT SOLAR MEASUREMENTS, 1400 CDT FLIGHT, 9 AUGUST 1972

reflectance over rural areas at wavelengths just beyond the visible range. From higher altitude the albedo variations could appear more uniform, but would depend on the scattering/absorption properties of the urban aerosols.

Originally it was hoped to perform a detailed examination of possible diurnal variations in albedo (as function of surface type) as well as height variations in albedo as determined from the aircraft observations at two altitudes. It is possible, for example, that as the sun's elevation and azithmuth change during the day the complex changes in shading within urban structures could result in a diurnal variation of albedo. Both height and orientation of structures would be important. However, other factors (including surface wetness) also are involved in diurnal variations and the accurate repetitive measurement of small changes in albedo is a difficult task that requires a considerable body of data before final conclusions can be drawn.

The deduction of temporal changes in surface albedo on the basis of aircraft observation introduces some uncertainty due to time changes in atmospheric attenuation and turbidity. An attempt to remove this uncertainty was accomplished by overflights of each site at two altitudes (460 m and 1220 m) during each flight. Presumably, consistent identifiable differences in the measured albedos could be used to adjust to an appropriate surface albedo. Unfortunately the differences again are small and are subject to factors other than atmospheric attenuation. Thus the periodic observations from the two flight altutudes failed to establish any significant height or time variations (very low sun angles excluded) of surface albedo. Only the horizontal variations were significant and were related to variations in reflected solar radiation.

Time differences in the overflight of a given portion of the track by a single aircraft at two altitudes complicates the interpretation of

changes in measured solar radiation. Along the near end of the track, overflight at the second altitude may occur as much as 50 minutes later; the time delay is much shorter at the far end of the track. During this period of delay, time changes in the downwelling solar radiation (and possibly the albedo) occur regardless of atmospheric changes. With any cloudiness aloft, changes in cloud locations and in the cloud shadow location will influence the relative solar measurements over a given site. Furthermore, the actual scene being viewed changes with aircraft altitude. As the altitude is increased the viewed area increases rapidly and the type of surface viewed is changed by an amount dependent on the homogeneity of the surface. In addition, even the same objects in the field of view are not viewed at the same sun angles, except at the subpoint,* and differences in shading occur. How these factors influence the deduced atmospheric attenuation during the course of the day may be difficult to infer unless experiments are first conducted over a truly homogeneous surface of sufficient size to fill the field of view at both flight altitudes.

Although the observed relative spatial variations in albedo were real, absolute values may have been biased by calibration inaccuracies. Comparisons of surface and aircraft measurements of incident solar radiation indicated that the downwelling irradiance interpreted from aircraft measurements was too large. Assuming the validity of upwelling irradiance measurements on the aircraft, the absolute magnitudes of calculated albedos apparently were too small.

Figure 7 illustrates the downwelling irradiance measurements on 11 August 1972 at flight altitudes of 460 m and 1220 m. Differences in the measurements over urban and rural locations were insignificant during the time period illustrated. The indicated maxima in incident solar

*Subpoint refers here to the point on the ground directly beneath the aircraft.

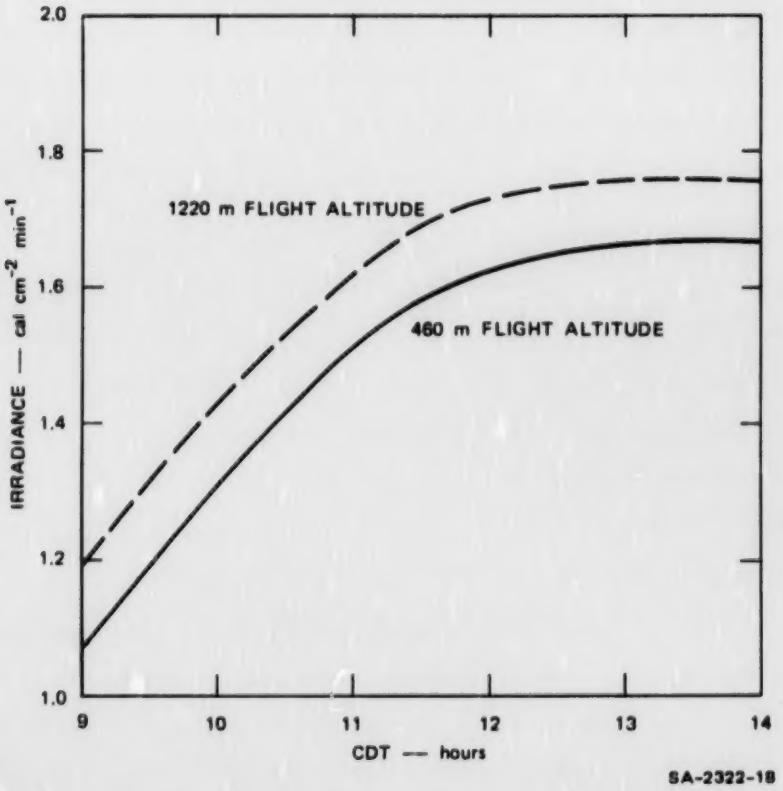

FIGURE 7 HEIGHT VARIATIONS OF MEASURED INCIDENT SOLAR RADIATION, 11 AUGUST 1972

radiation measured at 1220 m and at 460 m are 1.76 and 1.66 cal cm^{-2} min^{-1}, respectively. The maximum incident solar radiation measured at the surface (at the Granite City site) was only about 1.3 cal cm^{-2} min^{-1}. If it is assumed that complete homogeneity existed in the atmosphere below 1220 m and that the surface measurement was correct, then it must be concluded the absolute magnitudes of the aircraft measurements were overestimated by about 20%. If, in addition, the aircraft solarimeter measurements were assumed to be accurate, then the inferred albedos should be increased by about 25%. Relative differences, which are small, would be increased by the same amount.

Even with residual uncertainties in absolute magnitudes of solar components it is possible to examine relative variations in terms of ratios of departures from average to average. Data from both legs of the 1700 CST flight on 23 April 1973 are presented in such nondimensional ratios in Figure 8 for downwelling and upwelling irradiances and the inferred albedo. Only wide-angle solarimeter data were analyzed for presentation in Figure 8. The first leg (eastbound) of the flight was flown at an altitude of 460 m; a loss of pyranometer data occurred during this leg. Despite the data dropout, the decline in the normalized curve for the downwelling irradiance clearly reveals the reduction in incident radiation with decreasing solar elevation during the 22 minutes of flight. On the return leg (westbound) at an altitude of 1220 m, the decreasing solar elevation results in minimum incident radiation at the zero range on the flight track. The influence of small clouds is most evident in the traces for the 460 m flight; although the downwelling irradiance is reduced by the clouds the underlying surface is not shaded simultaneously so that albedo maxima result. Flooding of areas surrounding St. Louis, especially at the western end of the flight track, reduced the albedo but an albedo minimum is apparent again over the urban area. In general, the surface albedo ranges from about 10% below average to 10% above average.

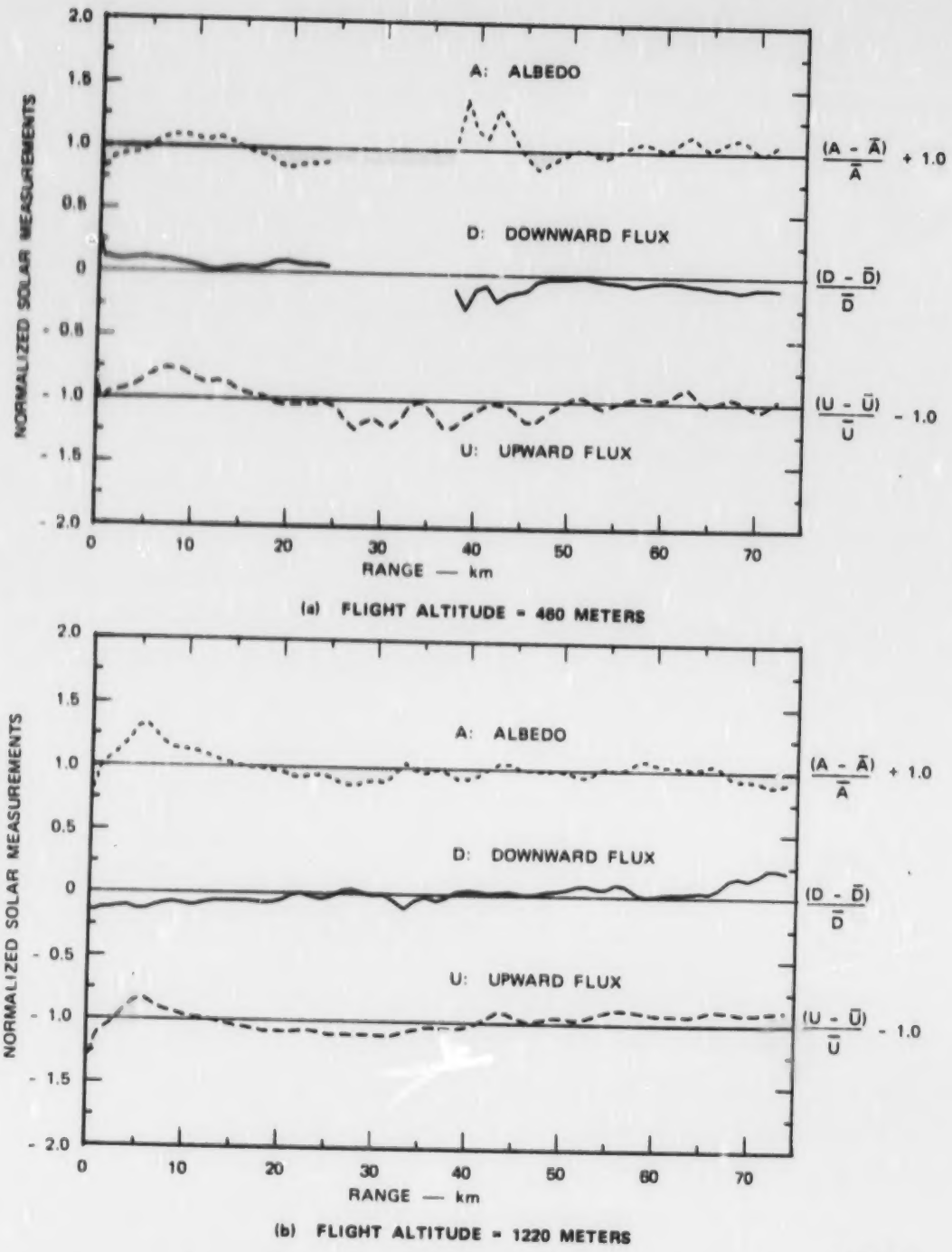

FIGURE 8 NORMALIZED AIRCRAFT SOLAR MEASUREMENTS, 1700 CST FLIGHT, 23 APRIL 1973

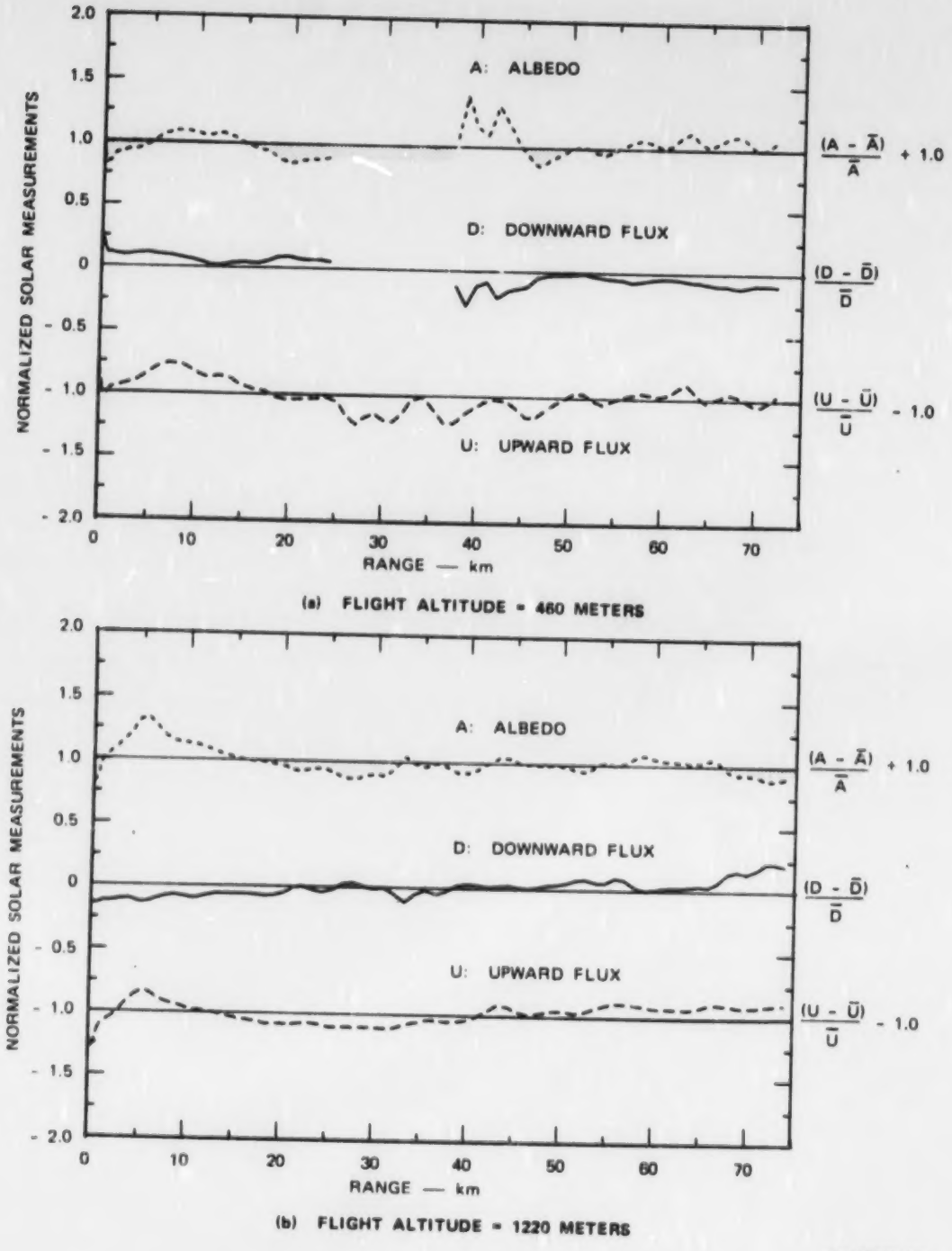

FIGURE 8 NORMALIZED AIRCRAFT SOLAR MEASUREMENTS, 1700 CST FLIGHT, 23 APRIL 1973

B. Surface Temperature

The measurement of surface temperature with the PRT-5 radiometer also was accomplished at the two flight altitudes. In principle, with proper allowance for actual time changes in surface temperatue during the overflights at two altitudes, the affect of atmospheric attenuation on the measured surface temperatue can be inferred from the difference observed from the two flight levels. However, the same factors that influence the albedo measurements at different heights also complicate the interpretation of temperature differences for the same site. Surface temperatures are strongly influenced by changes in solar heating; rapid fluctuations associated with shadows of cumulus clouds are much larger than differences of radiometric temperature associated with atmospheric attenuation. Of course, surface inhomogeneities contribute to variability in the PRT-5 records; nevertheless, the general picture that emerges is consistent with albedo measurements and expectations. Urban centers show higher temperature than the surrounding rural areas, as illustrated in the sample shown in Figure 9. Because of the small differences in radiometric surface temperature with flight altitude, the data from the 1220 m altitude have been displaced upward 10°C on the graph. Summaries of temperatures at selected sites along the track for each flight time were used in the time-series analyses discussed below.

Figure 10 illustrates the departures of the PRT-5 measurements of surface temperature from their means during each leg of the 1700 CST flight on 23 April 1973. The 460 m flight altitude (flown first) was associated with an apparent average surface temperature 1.6°C warmer than that for the 1220 m flight altitude. Consequently, the flooded area around the Missouri River (see flight track in Fig. 2), represented by the broad minimum near the origin of the track, appears with a larger temperature departure from normal in the 460 m flight record than in the 1220 m flight record. The same is true for the sharp minimum characterizing

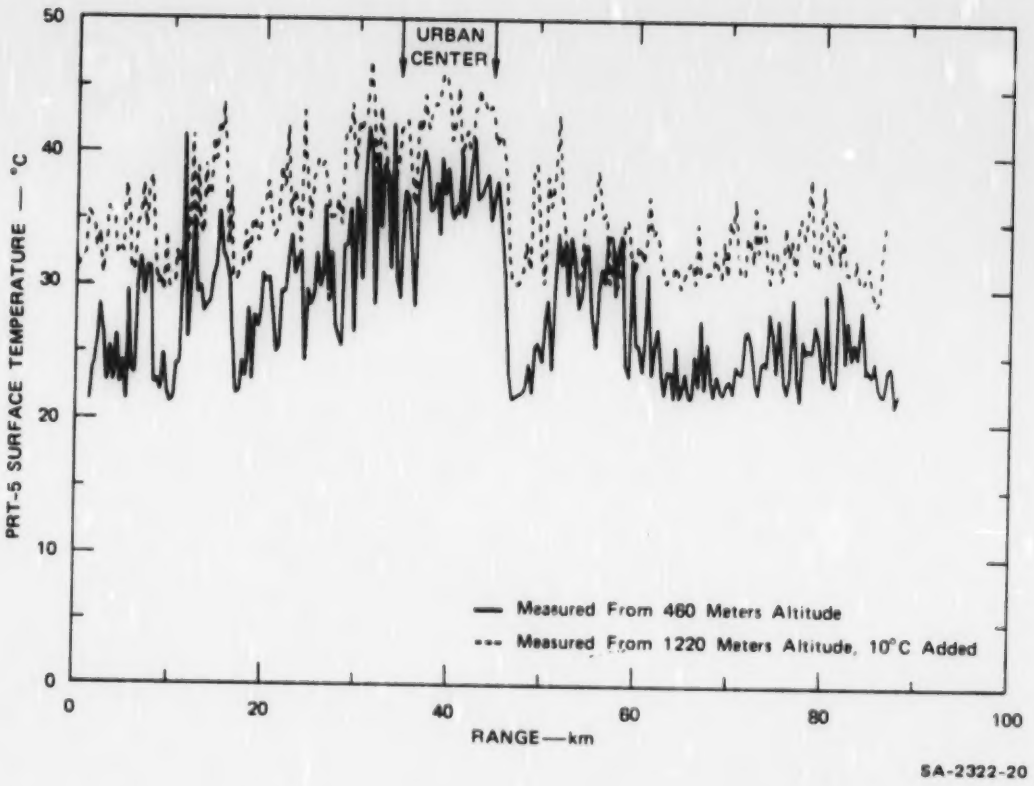

FIGURE 9 AIRCRAFT RADIOMETRIC SURFACE TEMPERATURE MEASUREMENTS, 1400 CDT FLIGHT, 9 AUGUST 1972

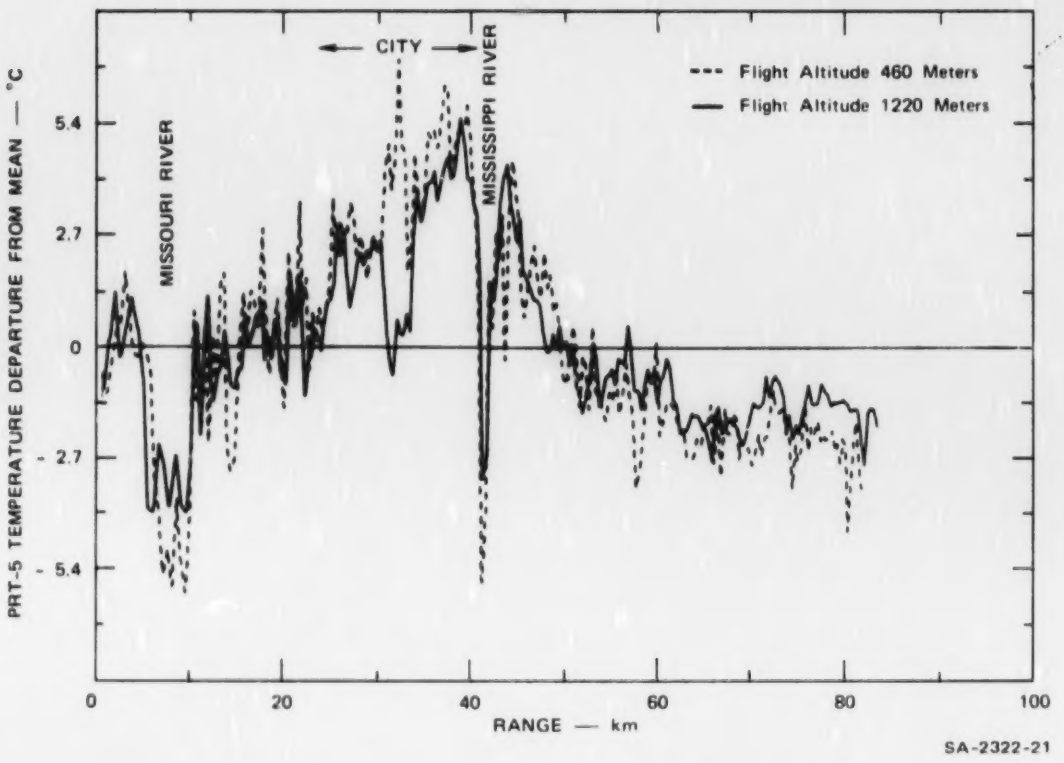

FIGURE 10 NORMALIZED AIRCRAFT RADIOMETRIC SURFACE TEMPERATURE MEASUREMENTS, 1700 CST FLIGHT, 23 APRIL 1973

the crossing of the Mississippi River near the center of the track. These results are reasonable since water body temperatures remain relatively uniform over short time intervals due to the large specific heat and effective mixing depth of the water. Thus, after accounting for the time change of the normal temperature for each track, the water temperatures measured from both altitudes differ by less than one degree and indicate that the atmospheric influence on the measurements was small at those localities. The temperature departures above normal are restricted to the urban area, which is significantly warmer than the rural areas to the east. Records from the two flight altitudes are in excellent agreement except for an unspecified feature in the western portion of the urban area.

Apparent spatial variations of the radiometric surface temperature could be influenced by marked gradients in surface emissivity (in the 10 to 12 μm spectral region) or by significant variations in atmospheric attenuation. No evidence is available to support a significant emissivity variation that accounts for observed horizontal temperature differences. Some insight into the possibility of differential atmospheric attenuation is provided by the airborne PRT-5 measurements from two altitudes.

Data acquired on 9 August 1972 were averaged over two segments of flight track representative of urban and rural surfaces. Results for the two flight altitudes are illustrated in Figure 11a, where smooth curves have been drawn through data points derived from seven flights. The pronounced daytime increase of the urban surface temperature relative to the rural surface temperature is clearly depicted. In all observations, the surface temperatures measured from the lowest altitude exceed those measured from the highest flight altitude, as anticipated by the presence of atmospheric attenuation. Only for the 1400 CDT flight does the urban temperature difference with flight altitude significantly exceed the

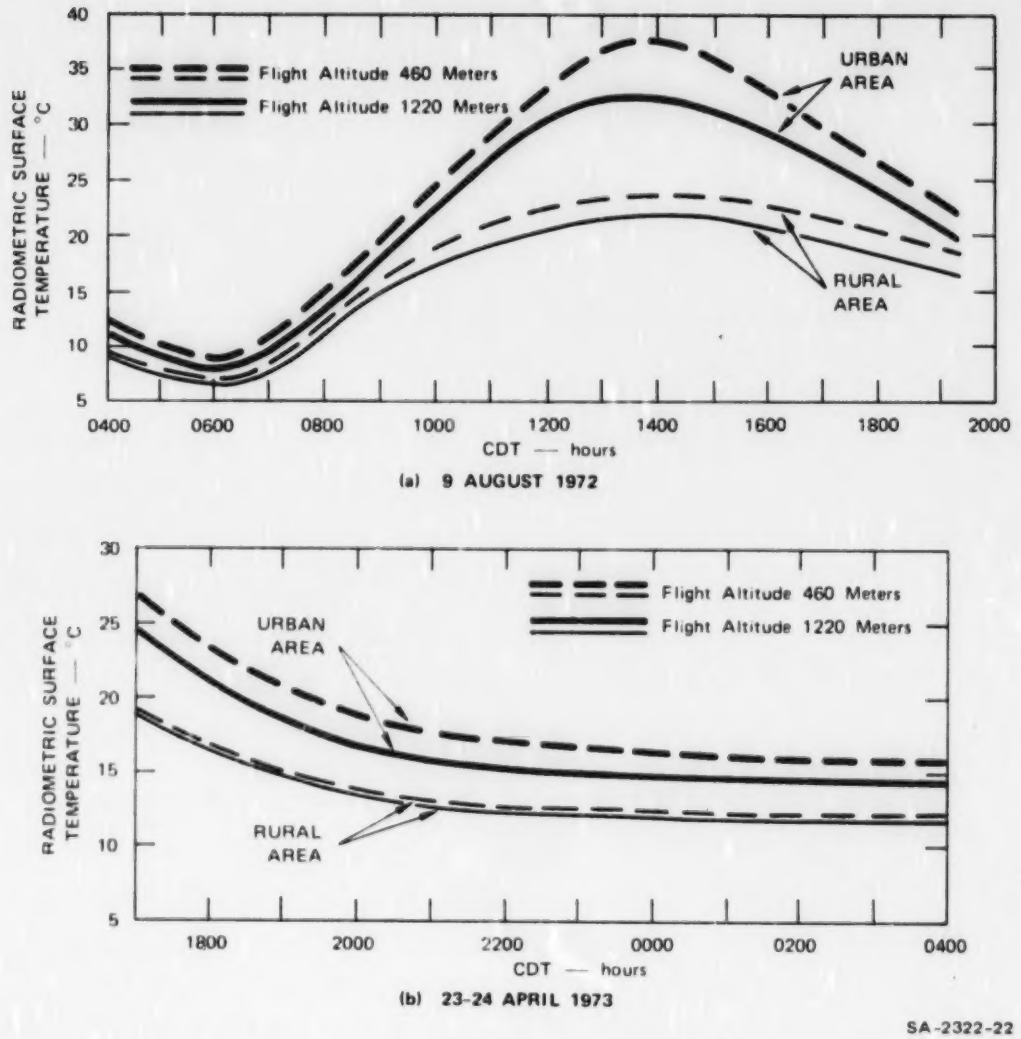

FIGURE 11 URBAN AND RURAL SURFACE TEMPERATURE VARIATIONS WITH TIME

rural difference. This suggests either greater attention in the urban atmosphere than in the rural atmosphere at 1400 CDT, with a suppression of the urban-rural surface temperature contrasts, or reduced attenuation below 460 m over the urban area at this time. (The same feature was not apparent at 1400 CDT on 11 August 1972.)

For the evening and night hours of 23 April 1973, PRT-5 data along the second flight track also were averaged over urban and rural areas. Results illustrated in Figure 11b show slightly more atmospheric attenuation over the urban area throughout the period. Presumably, the excess of urban surface temperatures over the rural surface temperatures should have been larger than those measured from the lowest flight altitude. Unfortunately, no data were available on differences in particle loading of the atmosphere over the two areas.

C. Air Temperature

Included in the aircraft observations were the air temperatures along the two flight altitudes. These data, although not specifically required for the surface analysis, are significant for several reasons. First, they provide a quick graphic display of thermal stability or changes in stability along the flight track. Second, harmonic analysis may be used to examine differences in the vertical exchange of sensible heat in the boundary layer. Finally, they are useful in assessment of atmospheric absorption and emission of infrared radiation, especially when combined with humidity measurements.

Samples of air temperature measurements at the two flight altitudes are shown in Figure 12; other data are included in the data summaries presented in the Appendix. The horizontal profiles of air temperature are sensitive to the relative accuracy of the measurements, to slight changes in flight altitude, and to the possibility of differential

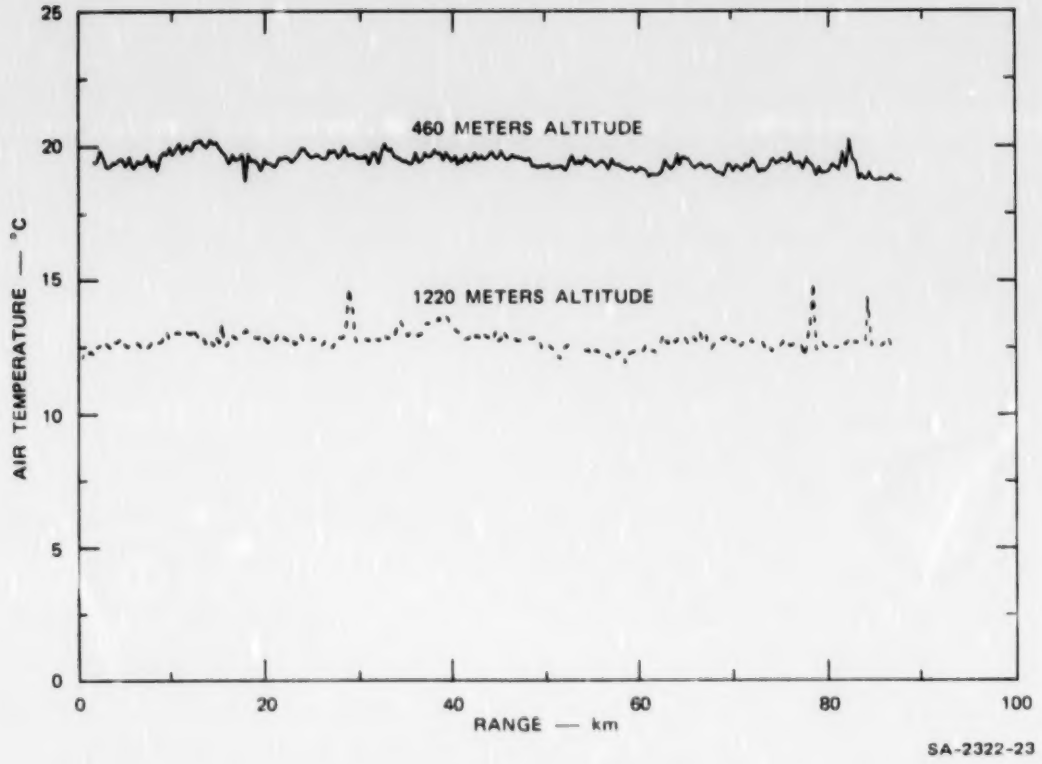

FIGURE 12 AIRCRAFT AIR TEMPERATURE MEASUREMENTS, 1400 CDT FLIGHT, 9 AUGUST 1972

advection along the tracks. Differences in the stability over urban and rural areas during different times of the day are of special interest, but often small in magnitude above the surface layer. The pronounced influence of convection on the temperature differences at the two flight levels is illustrated by the relatively large temperature differences in Figure 12. On many of the records slight changes in temperature with time (during the period of flight) are noticable. On the other hand, spikes that appear in the reduced air temperature data represent noise.

V CLIMATONOMICAL ANALYSIS

A. Climatonomy Theory

Professor Heinz Lettau was prompted in 1954 to coin the term climatonomy in order to emphasize quantitative aspects of the subject and to avoid misconceptions that might be associated with the word climatology. The distinction is intended as an analogy to the development of modern astronomy from the earlier astrology. Thus climatonomy denotes the use of numerical models to solve the local surface energy budget equation. A synopsis of climatonomy theory is presented below. Surface energy budget theory expresses the principle of the conservation of energy in the partitioning of the effective insolation at the earth-air interface. For the case of local homogeneity, the surface energy budget is given by

$$F_o = LW_o\uparrow - LW_o\downarrow + S_o + Q_o + E_o + P_o, \qquad (1)$$

where,

F_o ≡ solar forcing function (cal cm^{-2} min^{-1}); the effective shortwave radiation at the surface,

$LW_o\uparrow$ ≡ upwelling longwave radiation at the surface

$LW_o\downarrow$ ≡ downwelling longwave radiation at the surface

S_o ≡ subsurface heat flux density

Q_o ≡ atmospheric heat flux density

E_o ≡ evaporative heat flux density

P_o ≡ photosynthetic heat flux density.

By definition, heat flux away from the surface is defined as a positive flux. For the urban surface, photosynthetic energy transforms can usually be ignored, while on the overall average they may account for

Preceding page blank

5% to 10% of the available solar energy (Van Wijk).[3] In this exploratory study we have chosen to ignore this term, although further work should seek to evaluate this impact of vegetation on rural-urban climatic differences.

In climatonomy, the energy budget is examined over basic meteorological periods (e.g., diurnal and annual) through the use of "Fourier synthesis." Thus each term in Eq. (1) is represented by a mean value and harmonics. Expanding each term in Eq. (1) we obtain

$$F_o = \bar{F}_o + \sum_{i=1}^{m} \Delta_i F_o \cos (int - \delta_i), \tag{2a}$$

$$LW_o\uparrow = \overline{LW_o\uparrow} + \sum_{i=1}^{m} \Delta_i LW_o\uparrow \cos (int - \delta_i + \gamma_i^*), \tag{2b}$$

$$LW_o\downarrow = \overline{LW_o\downarrow} + \sum_{i=1}^{m} \Delta_i LW_o\downarrow \cos (int - \delta_i + \beta_i^*), \tag{2c}$$

$$S_o = \overline{S_o} + \sum_{i=1}^{m} \Delta_i S_o \cos (int - \delta_i + \psi_i^*), \tag{2d}$$

$$Q_o = \overline{Q_o} + \sum_{i=1}^{m} \Delta_i Q_o \cos (int - \delta_i + \varphi_i^*), \tag{2e}$$

$$E_o = \overline{E_o} + \sum_{i=1}^{m} \Delta_i E_o \cos (int - \delta_i + \chi_i^*), \tag{2f}$$

where t is time, i is the harmonic order, and n is the basic frequency when $n = 2\pi/\tau$ and τ is the basic period (i.e., one day). In Eq. (2), $\Delta_i()$ is the amplitude of the ith harmonic, δ_i is the phase angle for the ith harmonic of the forcing function, and $()_i^*$ is the phase lag of the various response functions to the solar phase. In the analyses that follow, zero time reference corresponds to midnight. As usual, the overbar denotes the time-averaged value over the basic period.

A basic premise of climatonomy is that the primary response to the solar forcing function is the surface temperature, and that the "climatic" functions are secondary responses, via the surface temperature, to the solar forcing function. In other words, each of the climatic functions

can be expressed in terms of surface temperature and hence Eq. (1) may be solved to yield a unique set of mean values plus variation of the response terms. It is thus appropriate to first introduce the Fourier representation for the surface temperature and then to rewrite the secondary response functions in terms of surface temperature, where

$$T_o = \overline{T_o} + \sum_{i=1}^{m} \Delta_i T_o \cos (int - \delta_i^*), \text{ and} \tag{3a}$$

$$T_o = \overline{T_o} + \sum_{i=1}^{m} (\Delta_i F_o / Z_i) \cos (int - \delta_i - \zeta_i), \tag{3b}$$

where,

$$Z_i \equiv \Delta_i F_o / \Delta_i T_o, \text{ and} \tag{4a}$$

$$\zeta_i \equiv \delta_i^* - \delta_i. \tag{4b}$$

Furthermore,

$$LW_o\uparrow = \overline{LW_o\uparrow} + \sum_{i=1}^{m} (\Gamma_i \Delta_i T_o) \cos (int - \delta_i - \zeta_i + \gamma_i), \tag{5a}$$

$$LW_o\downarrow = \overline{LW_o\downarrow} + \sum_{i=1}^{m} (B_i \Delta_i T_o) \cos (int - \delta_i - \zeta_i + \beta_i), \tag{5b}$$

$$S_o = \overline{S_o} + \sum_{i=1}^{m} (\Psi_i \Delta_i T_o) \cos (int - \delta_i - \zeta_i + \psi_i), \tag{5c}$$

$$Q_o = \overline{Q_o} + \sum_{i=1}^{m} (\Phi_i \Delta_i T_o) \cos (int - \delta_i - \zeta_i + \varphi_i), \tag{5d}$$

$$E_o = \overline{E_o} + \sum_{i=1}^{m} (X_i \Delta_i T_o) \cos (int - \delta_i - \zeta_i + \chi_i), \tag{5e}$$

where the following identities are introduced

$$\Delta_i LW_o\uparrow \equiv \Gamma_i \Delta_i T_o \ , \ \gamma_i^* \equiv -\zeta_i + \gamma_i; \tag{6a}$$

$$\Delta_i LW_o\downarrow \equiv B_i \Delta_i T_o \ , \ \beta_i^* \equiv -\zeta_i + \beta_i; \tag{6b}$$

$$\Delta_i S_o \equiv \Psi_i \Delta_i T_o \ , \ \psi_i^* \equiv -\zeta_i + \psi_i; \tag{6c}$$

$$\Delta_i Q_o \equiv \Phi_i \Delta_i T_o \ , \ \varphi_i^* \equiv -\zeta_i + \varphi_i ; \tag{6d}$$

$$\Delta_i E_o \equiv X_i \Delta_i T_o \ , \ \chi_i^* \equiv -\zeta_i + \chi_i . \tag{6e}$$

Introducing the identity (4a), Eq. (2a) is rewritten as

$$F_o = \overline{F_o} + \sum_{i=1}^{m} (Z_i \Delta_i T_o) \cos (int - \delta_i). \tag{7}$$

Lettau then introduces Eqs. (5) and (7) into (1), and expands the cosine functions in terms of cosine and sine terms through the trigonometric identity:

$$\cos (int-\delta_i-\zeta_i+x_i) \equiv \cos(int-\delta_i)\cos(\zeta_i-x_i) + \sin(int-\delta_i)\sin(\zeta_i-x_i).$$

The basic cycle average equation is subtracted, leaving only a departure equation that is evaluated at $int = \delta_i$ and $int = \delta_i + \pi/2$ to yield two simultaneous, independent equations, where:

$$\tan \zeta_i = \frac{-B_i \sin\beta_i + \Gamma_i \sin\gamma_i + \Psi_i \sin\psi_i + \Phi_i \sin\phi_i + X_i \sin\chi_i}{-B_i \cos\beta_i + \Gamma_i \cos\gamma_i + \Psi_i \cos\psi_i + \Phi_i \cos\phi_i + X_i \cos\chi_i} \tag{8}$$

$$\text{and, } Z_i = -B_i \cos(\zeta_i-\beta_i) + \Gamma_i \cos(\zeta_i-\gamma_i) + \Psi_i \cos(\zeta_i-\psi_i) + \Phi_i \cos(\zeta_i-\varphi_i) + X_i \cos(\zeta_i-\chi_i). \tag{9}$$

In regard to the St. Louis experimental program, it is important to recall that not all of the amplitude and phase terms are obtainable directly from the observations, and hence we need to consider the parameterization of these terms on the basis of identifiable surface features.

Parameterization of the upwelling infrared flux at the surface is straightforward through application of the Stefan-Boltzmann law,

$$LW_o\uparrow = \varepsilon\sigma T_o^4 , \tag{10}$$

where ϵ is the surface emissivity and σ is the universal Stefan-Boltzmann constant (0.813×10^{-7} mly min^{-1} $^{o}K^{-4}$). Upon introducing Eq. (10) into Eq. (3a) and solving for the partial impedance and phase, we obtain

$$\Gamma_1 \cong 4\ \overline{LW_o\uparrow}/\overline{T_o}, \text{ and} \tag{11a}$$

$$\gamma_1 = 0. \tag{11b}$$

The partial impedance B_1 and phase β_1 for the downwelling longwave flux at the surface have not been parameterized here as they were obtained through Fourier analysis of the continuous diurnal pyrgeometer measurements made at the ground station. Parameterization is possible through a wide variety of empirical and theoretical approaches, such as the use of the Angstrom ratio or Swinbank's method[4] as discussed by Dabberdt[5], to mention only two.

The subsurface heat flux density is parameterized through the application of Fourier's law of heat conduction--Eq. (12a)--and the continuity equation for heat in the absence of sources and sinks-- Eq. (12b), where

$$S = -\lambda \frac{\partial T}{\partial z}, \text{ and} \tag{12a}$$

$$\frac{\partial S}{\partial z} = -C \frac{\partial T}{\partial t}. \tag{12b}$$

Here λ is the thermal conductivity (cal cm^{-1} $^{o}K^{-1}$ min^{-1}) and C the volumetric heat capacity (cal $^{o}K^{-1}$ cm^{-3}) of the submedium. Considering the medium as a homogeneous conductor ($\partial\lambda/\partial z = \partial C/\partial z = 0$) with time-independent thermal coefficients ($\partial\lambda/\partial t = \partial C/\partial t = 0$), the partial impedance Ψ_1 and phase ψ_1 are given as

$$\Psi_1 = (\lambda C i n)^{1/2} \equiv \mu (i n)^{1/2}, \text{ and} \tag{12c}$$

$$\psi_1 = \pi/4, \tag{12d}$$

where μ (cal $^{o}K^{-1}$ cm^{-2} $sec^{-1/2}$) is defined as the thermal admittance.

Parameterization of the atmospheric heat flux density is perhaps the most difficult. Lettau[1] presents a type of similarity approach based on the near-surface vertical profile of potential temperature. Both the partial impedance Φ_i and the phase φ_i are given in terms of a characteristic number N_i that is a unique function of the frequency, aerodynamic surface roughness z_o, and the mean friction velocity $\overline{V^*}$, where

$$N_i = \log_{10}\left(\frac{\overline{V^*}}{inz_o}\right). \tag{13}$$

The partial impedance Φ_i is then expressed as

$$\Phi_i = \frac{\rho C_p \overline{V^*}}{(a+bN_i)(1-M^*)}. \tag{14a}$$

The term M^* expresses the magnitude of convective mixing relative to mechanical turbulence; its absolute value is proportional to $\overline{Q_o}/\overline{V^*}$ and is less than unity, and its sign is determined by that of $\overline{Q_o}$. For urban areas, $\overline{V^*}$ will usually be large because of the tall roughness elements and hence M^* will be small. Upon assuming bouyancy effects on turbulent diffusion of heat as small in comparison with mechanical mixing, diurnal variations of M^* are similarly small $[(\tau/iM^*)\partial M^*/\partial t = 0]$ and Eq. (14a) can be simplified accordingly, where

$$\Phi_i \approx \frac{\rho C_p \overline{V^*}}{(a+bN_i)(1-\overline{M^*})} \tag{14b}$$

Lettau also gives an expression for the phase lag,

$$\varphi_i = \tan^{-1}\left(\frac{c}{a+bN_i}\right) \tag{14c}$$

where a, b, and c are semi-empirical constants.

Since it would have been impractical if not impossible to directly determine V^* and z_o along the flight path, these also must be estimated. Values for z_o were derived from an empirical relationship developed by Kung,[8]

$$\log_{10} z_o = -1.24 + 1.19 \log h^*, \tag{15a}$$

where h^* is the characteristic physical height of the roughness elements. The term V^* is, in turn, also derived from an empirical equation from Kung based on the relationship between the geostrophic drag coefficient C_D and the surface Rossby number Ro,

$$C_D \equiv V^*/V_g = 0.174/(\log_{10}\underline{Ro} - 0.81) \tag{15b}$$

$$\underline{Ro} \equiv V_g/z_o f, \tag{15c}$$

where V_g is the geostrophic wind and f the Coriolis parameter.

In this study a simplistic approach toward the parameterization of evaporation has been taken with E_o expressed in terms of Q_o using the inverse Bowen ratio Bo. Thus,

$$X_i = \underline{Bo}\Phi_i, \text{ and} \tag{16a}$$

$$X_i = \varphi_i. \tag{16b}$$

In the following section the reduction of the observations is discussed in terms of the input requirements of the theory as well as its application for the evaluation of the evaporative and thermal properties of the surface throughout the region.

B. Method of Approach

Upon examining all the data collected during the August 1972 and April 1973 experimental periods, it was decided to analyze in detail only those data from 9 August. This decision was based upon one very basic

and important criterion: the theory as outlined earlier is only strictly applicable when the basic (diurnal) cycle is controlled by the surface features, and hence one should avoid periods having significant diurnal trends and of course abrupt changes in the mesoscale atmospheric structure. Only the 9 August data satisfied this requirement.

In review, five basic types of meteorological data obtained on a diurnal basis were available for climatonomical analysis:

- Downwelling longwave radiation at the surface station
- Downwelling solar radiation at the surface station
- Downwelling solar radiation at each of two altitudes from the aircraft
- Upwelling solar radiation at each of two altitudes from the aircraft
- Upwelling window-channel infrared emission (in terms of equivalent blackbody temperature) at each of the two aircraft altitudes.

In addition, available supplemental data sources included:

- Twice-daily boundary layer wind and temperature profiles from the NWS EMSU station located at the Gateway Arch
- Aerial photographs obtained along the flight path by the aircraft.

While the aircraft observations were made continuously along both of the two 90 km segments of each flight, it is desirable to isolate portions of the flight track corresponding to distinctly different yet individually homogeneous surface types and to thus obtain average meteorological conditions representative of each. Figures 13 through 21 are aerial photographs of each of the nine surface sites (see Fig. 2); Table 2 identifies the various sites and briefly describes each. It was considered desirable to choose rural sites on opposite sides of the urban core so as to examine possible skewness in the climatic distribution

that might arise from advection associated with the urban heat island. The sites were carefully evaluated to ensure reasonable homogeneity over a scale of several kilometers, thus minimizing the impact of discontinuities in land use. Digitized records of the hemispheric solar radiation measurements from the aircraft were averaged over 15-sec periods while 5-sec averages were obtained for the higher-resolution infrared radiometer measurements of surface temperature. Summaries of these data over the various sites were used in the analysis of the surface energy budget.

The reduction of the surface observations of downwelling longwave and solar radiation in terms of the requirements of the theory--Eqs. (2a) and (2c)--is quite straightforward and involves only the direct application of harmonic analysis (see for example, Panofsky and Brier)[7]. Upon recalling Eq. (2a) and expressing the absorbed solar radiation at the surface (i.e., the surface forcing function) in terms of the insolation $F_o\downarrow$ and the surface albedo a, we obtain

$$F_o = F_o\downarrow - F_o\uparrow = F_o\downarrow\,(1-a) = \tag{17}$$

$$(1-a)\left[\overline{F_o\downarrow} + \sum_{i=1}^{m} \Delta_i F_o\downarrow \cos(\text{int}-\delta_i)\right],$$

when the albedo is time-independent. Because the 9 August measurements entail solar data on only five of the flights and because these were obtained well above the surface, these aircraft observations were utilized only to determine the albedo of each of the nine representative surface types; the insolation measured at the surface station is used in the evaluation of Eq. (17) under the assumption that spatial variations of $F_o\downarrow$ along the flight track were negligible on this day. Values at 30-min intervals were taken from the analog trace, and the amplitude and phase terms were computed for 24 harmonics; the results are summarized in Table 3. Only the first and second harmonics are listed as together they account for 98.8% of the total variance.

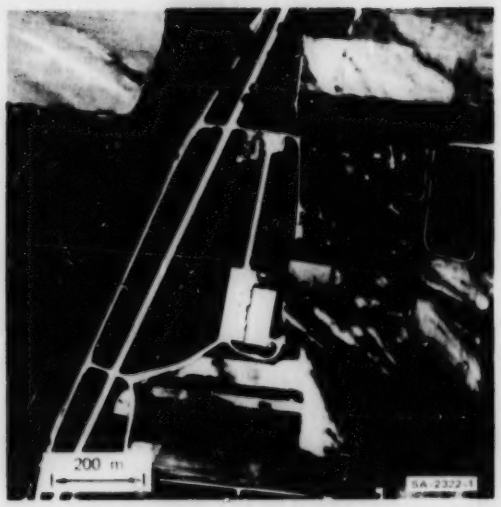

FIGURE 13 SITE R-1

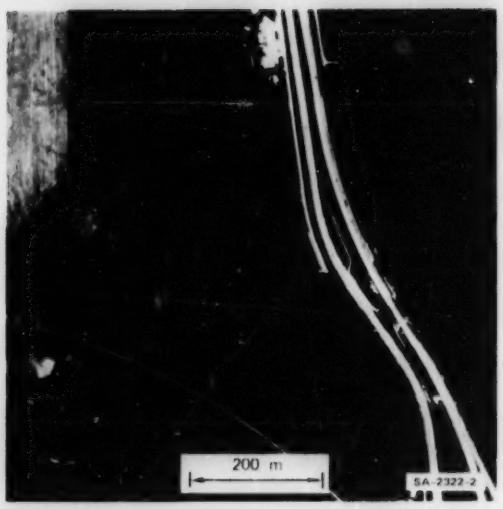

FIGURE 14 SITE R-2

FIGURE 15 SITE R-3

FIGURE 16 SITE R-4

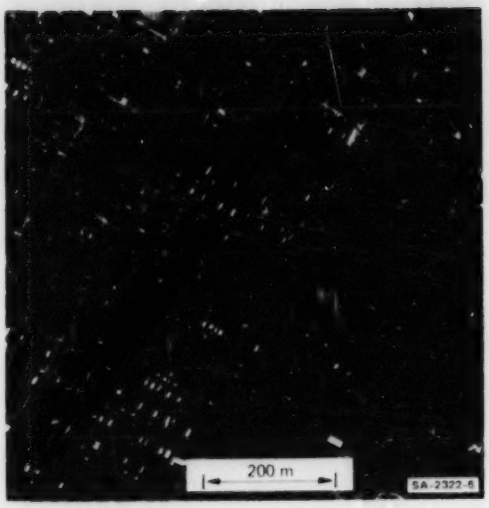

FIGURE 17 SITE R-5

FIGURE 18 SITE R-6

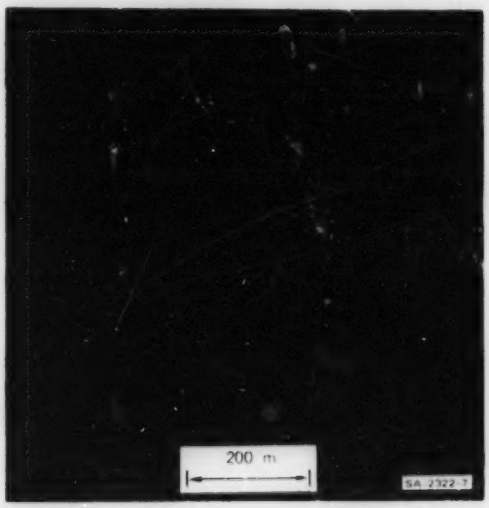

FIGURE 19 SITE R-7

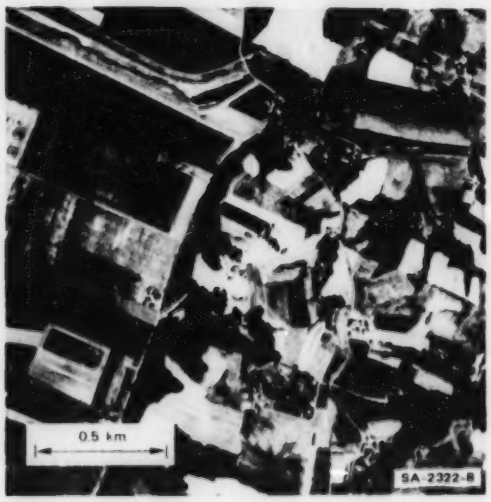

FIGURE 20 SITE R-8

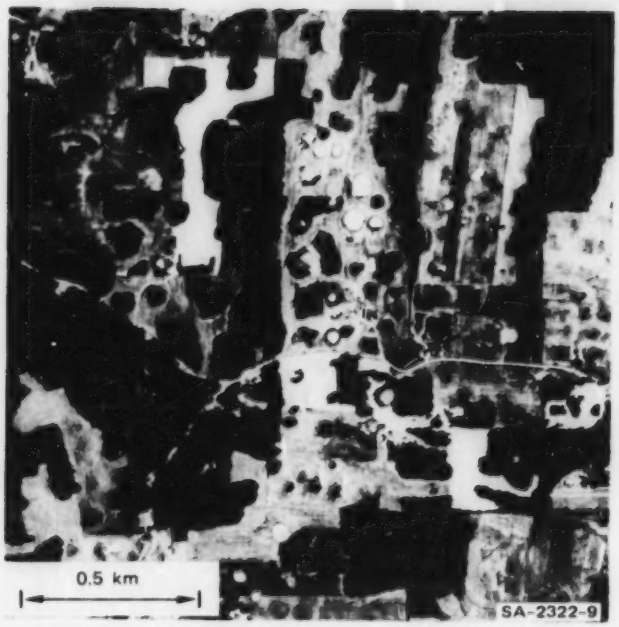

FIGURE 21 SITE R-9

Table 2

DESCRIPTION OF SURFACE AREAS SELECTED FOR ANALYSIS

Site*	Description	Range (km)†
R-1	Mostly farmland; roadway; some trees	23.8N
R-2	Mostly woods, some fields; roadways	19.9N
R-3	New suburban housing tract	13.0N
R-4	Commercial-industrial; old residential	7.8N
R-5	Old urban residential	3.7N
R-6	Old urban residential; some light commercial	3.7S
R-7	Farmland	12.5S
R-8	Mostly woods and fields; some farmland	23.8S
R-9	Mostly woods, some fields	33.7S

*Locations shown in Figure 2

†Distance (north or south) of city center

The downwelling infrared flux density as recorded at the surface station was also assumed representative of conditions at each of the nine sites. As above, the harmonic analysis of values at 30-min intervals was performed in the evaluation of Eq. (2c); the results are also listed in Table 3. In general agreement with the solar data, 95.6% of the variance is specified by the first and second harmonics.

Table 3

RESULTS OF HARMONIC ANALYSIS OF 9 AUGUST 1972 SURFACE OBSERVATIONS OF DOWNWELLING SHORT- AND LONGWAVE RADIATION AT GRANITE CITY, ILLINOIS

Parameter	Mean	i=1	i=2
$F_o\downarrow$ (ly/min)	0.428	---	---
$\Delta_i F_o\downarrow$ (ly/min)	---	0.646	0.235
β_i (rad)	---	3.429	0.555
$LW_o\downarrow$ (ly/min)	0.515	---	---
$\Delta_i LW_o\downarrow$ (ly/min)	---	0.060	0.019
β^*_i (rad)	---	- 0.305	- 0.405

Determination of a daily average and the harmonics for the aircraft observations cannot be obtained through standard harmonic analysis due to the irregular spacing of the seven averaged data points representative of each surface region as measured at each of the two altitudes. Furthermore, the small number of data points, and hence relatively large time intervals, prevented the use of extrapolation methods. Hence we evaluated the applicability of a nonlinear regression routine available at the Institute. In this manner we specified the form of the Fourier series

and obtained the mean, amplitude, and phase that best fit the data. A two-harmonic function was chosen, resulting in a five-parameter fit to the data:

$$G(t) = R_1 + R_2 \cos(0.2618t - R_3) + R_4 \cos(0.5236t - R_5), \qquad (18)$$

where,

R_1 = average value over the period (°C)

R_2 = amplitude of 1st harmonic (°C)

R_3 = phase of 1st harmonic (rad)

R_4 = amplitude of 2nd harmonic (°C)

R_5 = phase of 2nd harmonic (rad).

The form of the equation is directly analagous to that of Eqs. (2a) through (2f). Prior to applying the method to the reduction of the aircraft data, the method was first applied in several test cases to evaluate its validity. As a simple first trial, 14 irregularly spaced points along a pure cosine wave with origin at 00 hours were analyzed using a three-harmonic form of Eq. (18). The regression method requires initial guesses (R^*_J) of each parameter; these were purposely chosen poorly: $R_1^* = 0.9$, $R_2^* = 0.1$; $R_3^* = 0.15$ rad, $R_4^* = 0.2$, $R_5^* = 0.5$ rad, $R_6^* = 0.2$, and $R_7^* = 0.5$ rad. In spite of the "bad" initial values, the routine converged rapidly to provide the following results: $R_1 = 1.2 \times 10^{-4}$, $R_2 = 1.000$, $R_3 = -0.9 \times 10^{-5}$ rad, $R_4 = 2.2 \times 10^{-4}$, $R_5 = 0.6$ rad, $R_6 = 1.6 \times 10^{-4}$, and $R_7 = 7.3$ rad. Although a good test of the method's validity in simulating a harmonic analysis, a more realistic evaluation entails the use of observed diurnal near-surface temperatures under essentially stationary conditions. Meteorological conditions on 9 August in the St. Louis area satisfied this criterion. Thermograph data

for this period were obtained from seven instrument shelters in the area (see Fig. 22) of our operations; the shelters were maintained by the Illinois State Water Survey (ISWS) as a part of Project METROMEX.[8] These strip chart data were reduced to provide 24-hourly temperature values at each station and then analyzed using both the conventional harmonic analysis method for all 24 values and the regression method with only eight values. Data points chosen at times corresponding to the times of the seven aircraft flights plus an additional value at midnight. The results of the two sets of analyses are summarized in Table 4. Comparison of the two methods shows that results obtained from the regression method for all seven cases are in excellent agreement with those of the harmonic analysis for both the mean values and the first harmonics while the second harmonic values agree quite satisfactorily.

In all cases, the "computed" (i.e., regression method) diurnal average temperature is within 0.2°C of the "observed" (i.e., harmonic analysis) and the root-mean-square-difference (RMSD) is only about 0.1°C. The computed amplitudes of the first harmonic are all within 7.6% of the observed, while the RMSD is 4.3% of the observed mean; four of the seven stations show agreement within 0.06 rad (15 min in time) between computed and observed phase lags in the first harmonic, while the differences in the other three range from 0.14 to 0.23 rad (~ 35 to 60 min). Agreement among the amplitude and phase terms is less consistent in the second harmonic, although still encouraging. Five of the amplitude terms agree within 0.2°C or about 30%, although two differ by up to 0.4°C; similarly, most phase terms are within 0.4 rad (about 45 min) except two that differ up to 1 rad. However, the overall agreement is good as the first harmonic explains over 95% of the total variance.

As a result of these tests, the regression method was applied for the analysis of the effective surface temperature data obtained from the aircraft PRT-5 measurements. To evaluate this application, the seven

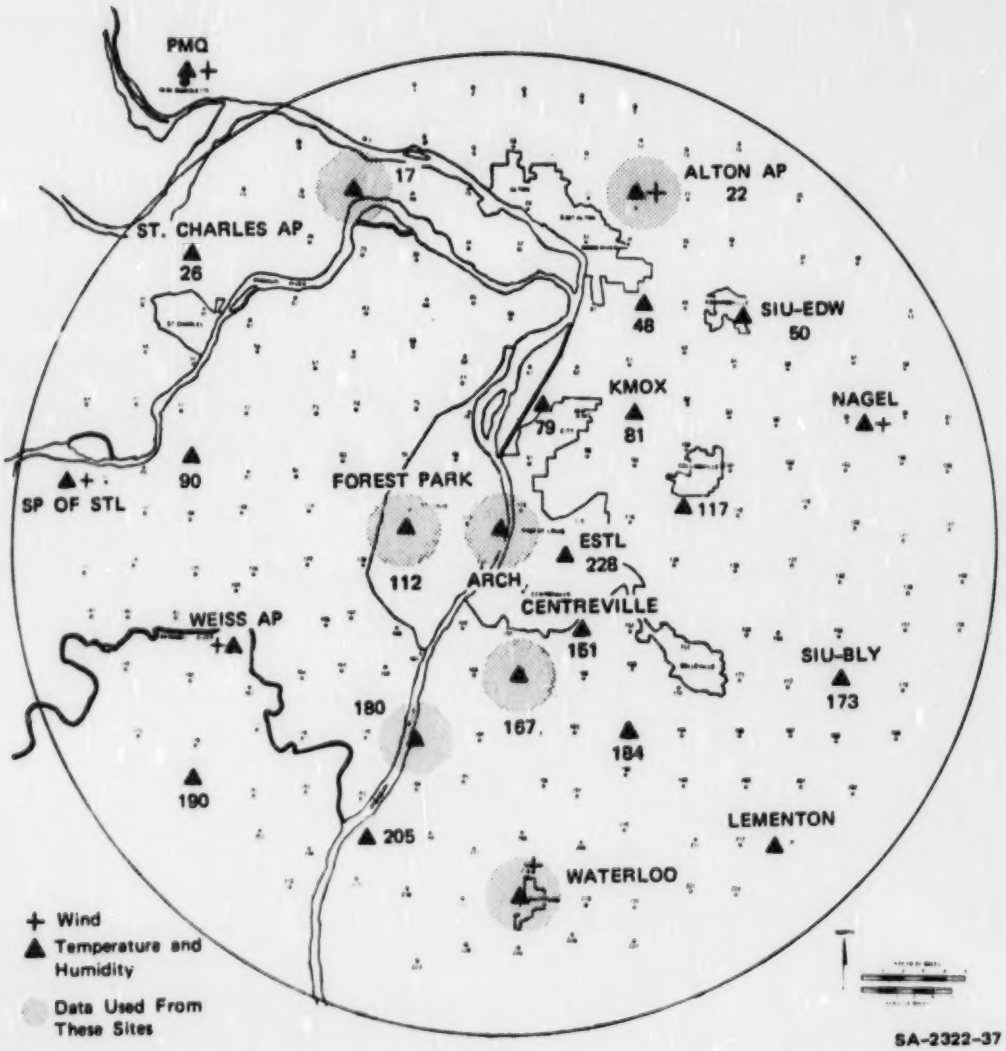

FIGURE 22 NEAR-SURFACE METEOROLOGICAL STATIONS OPERATED BY ILLINOIS STATE WATER SURVEY, AUGUST 1972

Table 4

COMPARISON OF THE 24-POINT HARMONIC AND 8-POINT REGRESSION ANALYSES OF THE NEAR-SURFACE AMBIENT TEMPERATURE (T) ON 9 AUGUST 1972 IN THE GREATER ST. LOUIS AREA

Station*	Harmonic Analysis					Regression Analysis				
	$\bar{T}$	$\Delta_1 T$	δ_1^*	$\Delta_2 T$	δ_2^*	$\bar{T}$	$\Delta_1 T$	δ_1^*	$\Delta_2 T$	δ_2^*
No. 167	19.6°C	5.13°C	4.13rad	0.64°C	1.08rad	19.3°C	4.73°C	3.90rad	0.67°C	2.10rad
No. 180	17.2	6.22	3.90	0.88	0.50	17.1	6.00	3.65	0.67	1.84
Waterloo	17.7	5.47	4.33	0.60	1.57	17.6	5.06	4.19	1.12	1.87
Gateway Arch	20.4	3.66	4.56	0.71	1.36	20.3	3.48	4.50	0.67	1.73
No. 112	18.6	4.62	4.37	0.82	0.93	18.7	4.68	4.40	0.67	0.97
No. 017	16.6	6.94	3.98	0.84	1.07	16.7	6.67	3.95	0.51	1.07
No. 022	19.8	4.87	4.27	0.80	1.66	19.8	4.83	4.30	0.80	1.68
Mean	18.5	5.27	4.22	0.76	1.17	18.5	5.07	4.13	0.74	1.61

	$\bar{T}$	$\Delta_1 T$	δ_1^*	$\Delta_2 T$	δ_2^*
RMSD	0.13	0.27	0.16	0.25	0.66

*Station locations are shown on Figure 22

space-averaged temperatures obtained from the upper altitude for site R-1 were analyzed first; the resulting five-parameter fit is illustrated in Figure 23. The fitted curve looks quite reasonable for the daytime period, but the nighttime portion is unrepresentative in comparison with the shape of the near-surface ambient temperature curves for the seven ISWS stations; the fitted ambient temperature curve for station number 022 is also shown in the figure. The discrepancy undoubtedly resulted from the large time interval between the last evening datum and the first morning value. The importance of one or more measurements during this period was anticipated, but as noted earlier we were unable to obtain these due to mechanical failure of the aircraft. In lieu of an intermediate measurement, we estimated a reasonable value in order to inhibit dominance of the nighttime regime by the second harmonic, as illustrated in Figure 23. The interpolation is necessarily subjective, although consistent among sites: a value (T_{INT}) is obtained midway between the 2000 and 0400 CDT measurements by assuming that 60% of the surface cooling occurs during the first half of the interval. This rate reflects nighttime surface cooling typical of cloud-free conditions as experienced during the experimental period. The temperature change over this interval ranged on the order of 10°C at the nine sites. It is felt that the magnitude of the uncertainty of the interpolated value is on the order of 1°C. An error analysis was then made to evaluate the impact of the upper level PRT-5 data for site R-1 and to vary the magnitude of the interpolated value over 0.5°C increments through ±2°C. The rate of change with temperature in each of the parameters of the regression analysis was essentially constant, where

$$\frac{\Delta \bar{T}}{\Delta T_{INT}} = 0.20,$$

$$\frac{\Delta[\Delta_1 T]}{\Delta T_{INT}} = -0.22,$$

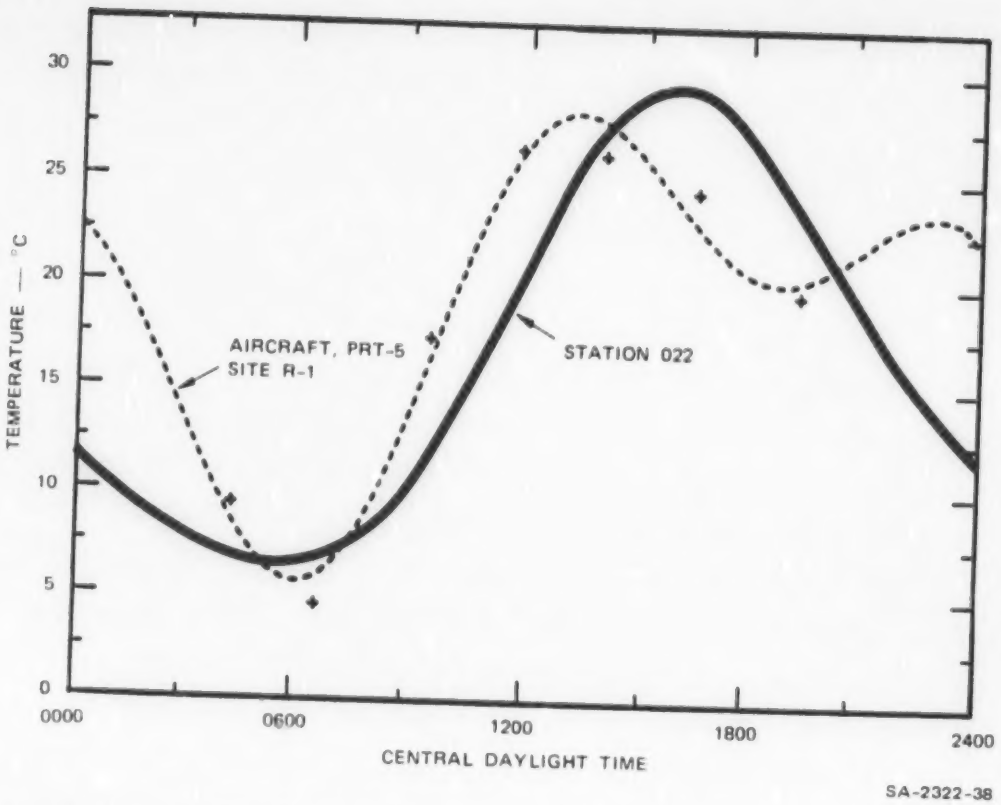

FIGURE 23 COMPARISON OF TWO-HARMONIC TEMPERATURE WAVE AT STATION 022 AND TWO-HARMONIC REGRESSION ANALYSIS FOR SITE R-1 USING SEVEN DATA POINTS

$$\frac{\Delta\delta_1^*}{\Delta T_{INT}} = 0.03 \text{ rad/}^{o}\text{C},$$

$$\frac{\Delta[\Delta_2 T]}{\Delta T_{INT}} = 0.26,$$

$$\frac{\Delta\delta_2^*}{\Delta T_{INT}} = -0.04 \text{ rad/}^{o}\text{C}.$$

In view of relatively small impact of "errors" as large as 1°C we feel confident in the representativeness of the regression analysis employing the single interpolated value. Certainly the resultant diurnal curve is more consistent with both the near-surface ambient conditions and what one would expect on the basis of the meteorological state. Figure 24 illustrates the five-parameter (two-harmonic) fit for the PRT-5 data at each of the two levels for the nine surface sites; Table 6 in the next section lists the mean, amplitude and phase values.

C. Application and Results

In view of the available experimental data and the basic objective of the study to evaluate effective surface geophysical features, the specific aim of the analysis program was to determine the feasibility of obtaining the thermal (i.e., thermal admittance) and evaporative (inverse Bowen ratio) descriptors of a variety of land-use types through the application of climatonomic theory to direct and remote observations. The first step in the analysis is the procedure to specify the solar forcing function at each of the sites and then the primary response function (i.e., surface temperature); through parameterization, the secondary responses are specified or evaluated, and then the descriptors are determined.

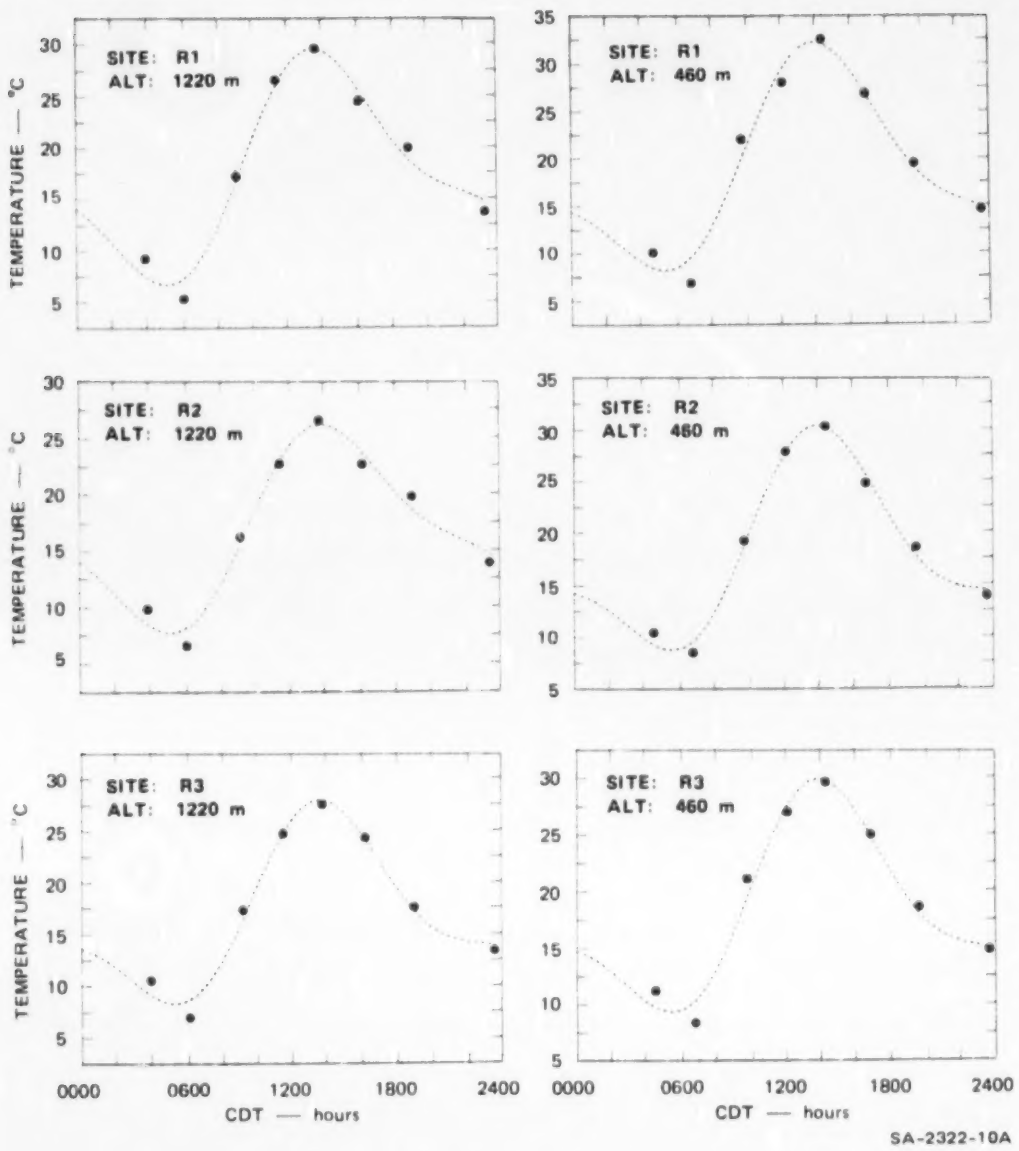

FIGURE 24 EFFECTIVE SURFACE RADIATIVE TEMPERATURE FROM TWO AIRCRAFT ALTITUDES AT NINE SITES ON 9 AUGUST 1972

Curve is from 2-harmonic regression analysis

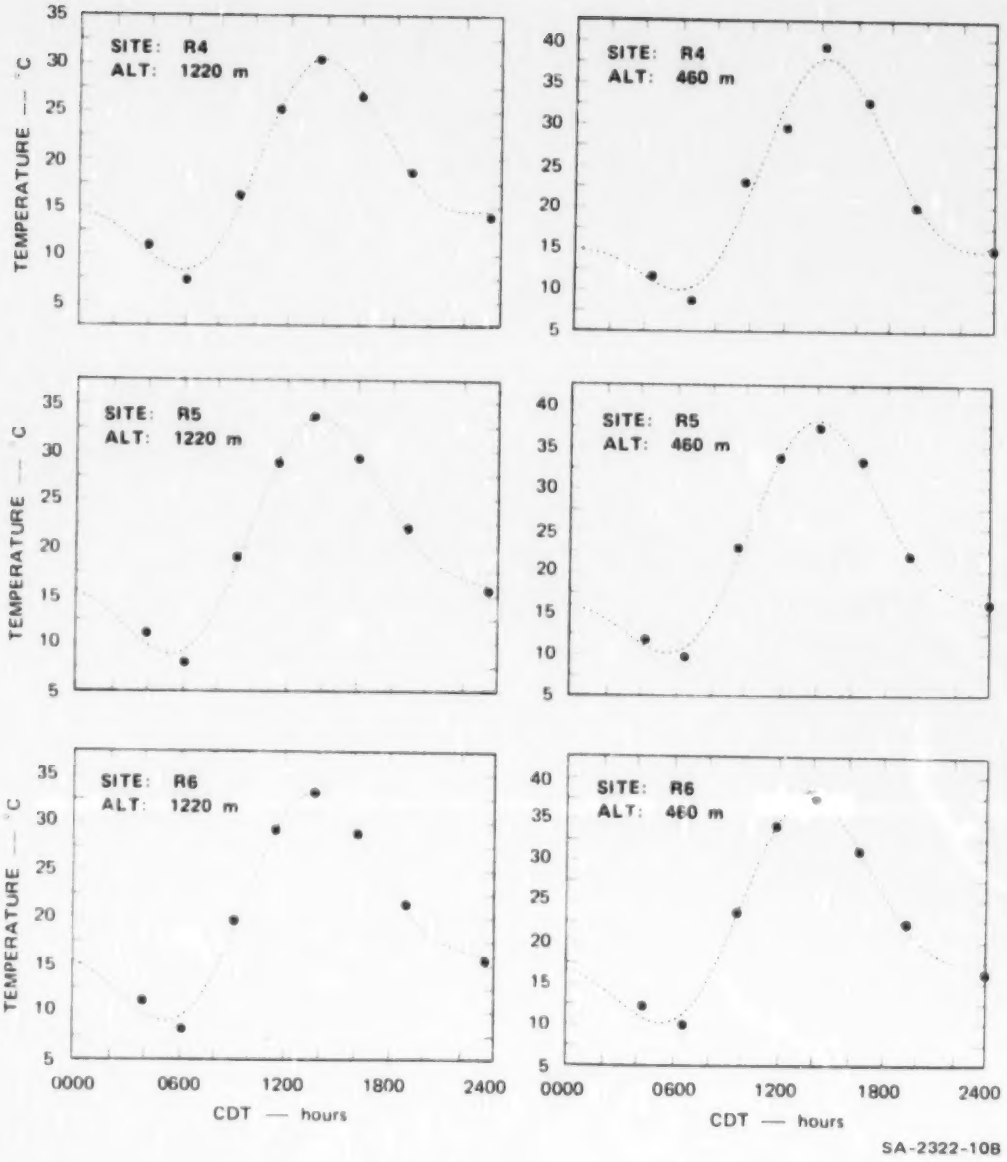

FIGURE 24 EFFECTIVE SURFACE RADIATIVE TEMPERATURE FROM TWO AIRCRAFT ALTITUDES AT NINE SITES ON 9 AUGUST 1972

Curve is from 2-harmonic regression analysis (Continued)

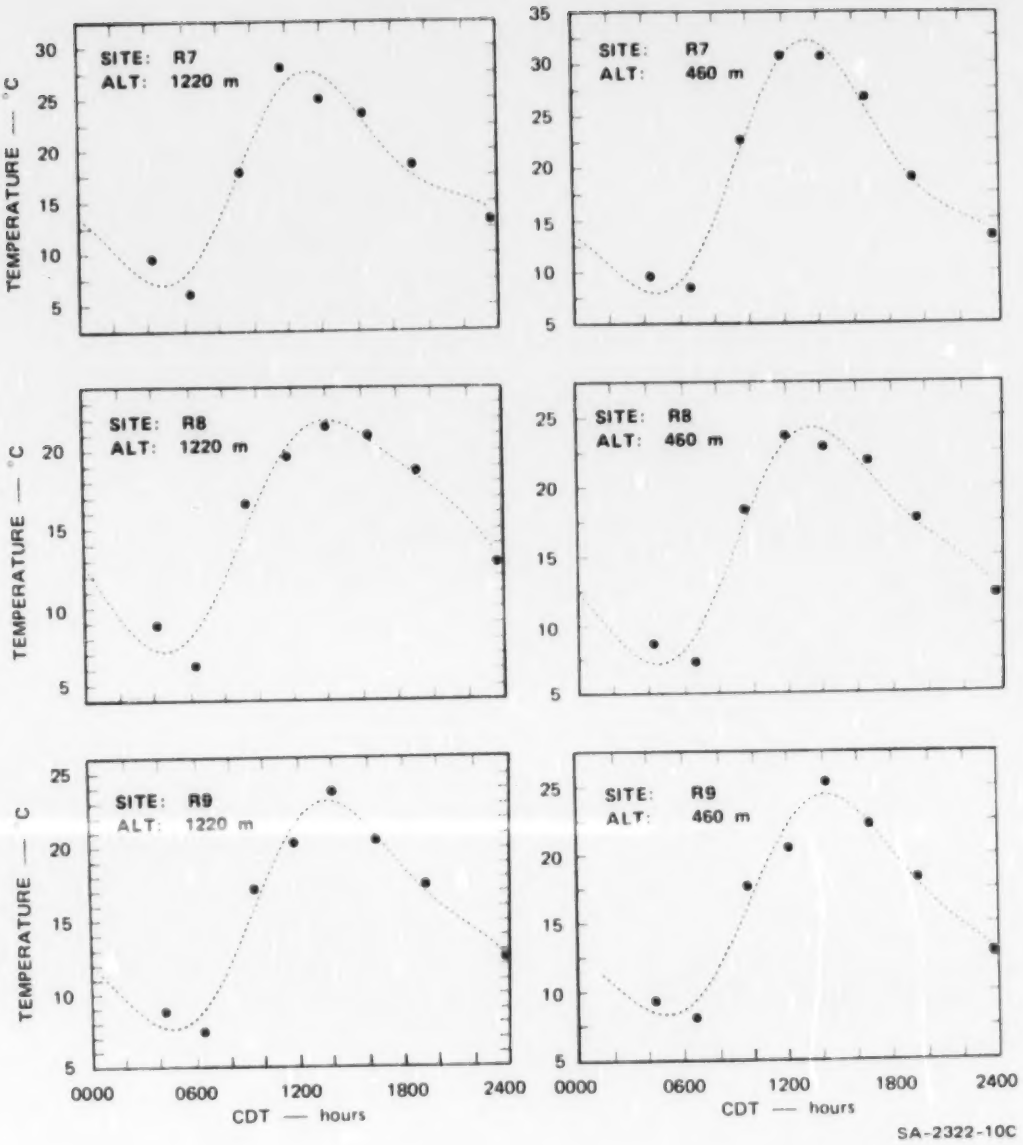

FIGURE 24 EFFECTIVE SURFACE RADIATIVE TEMPERATURE FROM TWO AIRCRAFT ALTITUDES AT NINE SITES ON 9 AUGUST 1972

Curve is from 2-harmonic regression analysis (Concluded)

Table 3 listed the mean, amplitude, and phase terms for the insolation on 9 August. The surface reflectivity then determines the form of the forcing function at each site. Table 5 lists the albedo values observed at each site for all of the daytime flights on 9 August. In Table 6, the albedo and forcing function are summarized according to site and aircraft altitude; for convenience, the downwelling longwave flux given earler in Table 2 is also summarized in Table 6.

The diurnal surface temperature variations discussed earlier and illustrated in Figure 24 are the effective surface radiative temperature values deduced from the aircraft bolometer measurements and an assumed constant surface emissivity of unity. To obtain some insight into the magnitude of possible variations in surface emissivity (ε), we evaluated relative ε-variations among the nine sites by assuming that the actual mean surface temperature was indeed the same for all sites. Thus differences in the effective mean surface temperatures are essentially attributable to variations in the emissivity. Using the upper level measurements first, it was found that the relative ε-variations are on the order of 7%; the largest ε-values are associated with the more urbanized sites. The lower level data resulted in similar findings with relative ε-variations less than 9%. The possible error introduced by assuming $\varepsilon = 1$ in the climatonomic determination of Γ_i and $\Delta_i T_o$ (and subsequently, the other second order responses) is minimal; thus, for the lack of an objective determination of absolute emissivity at the various sites, the unity value has been used throughout. The mean, amplitude, and phase terms for the primary response function (T_o) and the upwelling longwave flux ($LW_o\uparrow$) are summarized in Table 6.

As discussed earlier, the B_i and β_i terms describing the downwelling longwave flux are derived from the harmonic analysis of the pyrgeometer measurements at the surface station. These values have been taken as representative of conditions at all nine surface test areas.

Table 5

ALBEDO VALUES FOR THE NINE SURFACE AREAS AS MEASURED
ON 9 AUGUST 1972 FROM THE TWO AIRCRAFT ALTITUDES

Flight Time (approx.)	Site Number R-1	R-2	R-3	R-4	R-5	R-6	R-7	R-8	R-9
Altitude: 1220 m									
0900CDT	16.3	16.8	16.1	13.5	11.9	12.1	14.9	16.4	16.5
1130	15.9	16.6	16.8	14.0	12.5	12.9	15.0	16.2	16.6
1330	15.2	15.5	15.6	13.3	11.9	12.6	15.2	16.2	16.6
1600	15.6	15.6	16.4	14.3	13.3	15.1	17.5	19.0	16.7
1900	13.8	17.9	16.1	14.2	13.1	13.4	14.4	16.6	15.4
Average	15.4	16.5	16.2	13.9	12.6	13.3	15.4	16.9	16.4
Altitude: 460 m									
0900CDT	15.9	16.2	16.3	13.8	12.0	11.9	15.1	16.2	14.9
1130	15.1	15.5	16.0	13.8	11.6	12.0	14.5	16.8	16.7
1330	14.8	17.3	16.5	13.4	12.1	12.0	14.3	16.8	16.5
1600	15.7	17.3	17.4	14.3	13.1	12.5	14.9	16.3	16.6
Average	15.4	16.6	16.6	13.8	12.2	12.1	14.7	16.5	16.2

Table 6

CLIMATONOMIC PARAMETERS FOR 9 AUGUST 1972, IN THE GREATER ST. LOUIS AREA

Site: Altitude*	$\bar{F}_o$ (ly/min)	ΔF_{1o} (ly/min)	δ_1 (rad)	ΔF_{2o} (ly/min)	δ_2 (rad)	$\bar{T}_o$ (°K)	ΔT_{1o} (°K)	ζ_1 (rad)	ΔT_{2o} (°K)	ζ_2 (rad)	Σ_1 (mly/min-°K)	Σ_2 (mly/min-°K)	$\Gamma_{1,2}$ (mly/min-°K)	$\gamma_{1,2}$ (rad)	B_1 (mly/min-°K)	β_1 (rad)
R1:U	0.362	0.547	3.429	0.199	0.555	290.2	9.65	0.50	3.58	-0.24	59.3	62.5	7.9	0	6.2	0.20
R1:L	0.362	0.547	3.429	0.199	0.555	291.8	10.44	0.50	3.62	0.07	55.4	67.4	8.1	0	5.7	0.20
R2:U	0.357	0.540	3.429	0.196	0.555	289.8	7.99	0.59	2.61	-0.22	67.0	72.1	7.9	0	7.5	0.29
R2:L	0.357	0.540	3.429	0.196	0.555	291.3	9.23	0.48	3.62	0.14	57.2	48.7	8.1	0	6.5	0.18
R3:U	0.358	0.542	3.429	0.197	0.555	289.8	8.26	0.43	3.34	-0.04	65.2	65.2	7.9	0	7.3	0.13
R3:L	0.357	0.540	3.429	0.196	0.555	291.3	8.76	0.46	3.34	0.04	62.9	57.1	8.0	0	6.8	0.16
R4:U	0.369	0.557	3.429	0.203	0.555	291.0	9.00	0.51	4.19	0.21	61.9	47.6	8.0	0	6.7	0.21
R4:L	0.369	0.557	3.429	0.203	0.555	294.5	12.26	0.48	4.96	0.47	44.2	39.1	8.3	0	4.9	0.18
R5:U	0.374	0.565	3.429	0.205	0.555	293.0	10.65	0.51	3.80	0.05	52.7	54.0	8.2	0	5.6	0.21
R5:L	0.376	0.568	3.429	0.206	0.555	294.9	12.33	0.48	4.49	0.29	45.9	44.9	8.3	0	4.9	0.18
R6:U	0.371	0.561	3.429	0.204	0.555	293.2	10.40	0.47	3.78	-0.00	52.7	49.8	8.2	0	5.8	0.17
R6:L	0.376	0.568	3.429	0.206	0.555	295.6	11.88	0.45	4.46	0.12	44.4	38.7	8.4	0	5.1	0.15
R7:U	0.362	0.547	3.429	0.199	0.555	289.8	8.68	0.44	3.26	-0.42	61.5	57.4	7.9	0	6.8	0.14
R7:L	0.365	0.552	3.429	0.200	0.555	292.2	10.69	0.38	3.42	-0.23	51.4	58.4	8.1	0	5.6	0.08
R8:U	0.356	0.538	3.429	0.196	0.555	288.3	6.90	0.67	1.52	-0.75	80.3	113.5	7.8	0	8.7	0.37
R8:L	0.357	0.540	3.429	0.196	0.555	288.9	7.67	0.51	2.10	-0.57	71.9	99.6	7.8	0	7.8	0.21
R9:U	0.358	0.542	3.429	0.197	0.555	288.5	7.00	0.52	1.80	-0.39	76.5	96.3	7.8	0	8.6	0.22
R9:L	0.358	0.542	3.429	0.197	0.555	289.1	7.38	0.57	1.72	-0.14	74.1	125.4	7.9	0	8.1	0.27

*U = upper (1220 m)

L = lower (460 m)

Table 6 (Concluded)

Site: Altitude	B_2 (mly/min-°K)	β_2 (rad)	z_o (cm)	$\overline{V^*}$ (cm/sec)	ϕ_1 (mly/min-°K)	$\varphi_1 = \chi_1$ (rad)	ϕ_2 (mly/min-°K)	$\varphi_2 = \chi_2$ (rad)	$\phi_{1,2}$ (rad)	V_1 (mly/min-°K)	V_2	μ (mly/sec$^{1/2}$-°K)	Bo (n.d.)
R1:U	5.3	-0.65	15	23	10.7	0.36	11.4	0.38	0.79	23.7	-86.0	46	2.10
R1:L	5.2	-0.34	15	23	10.7	0.36	11.4	0.38	0.79	22.5	-44.0	44	1.74
R2:U	7.3	-0.63	50	26	13.2	0.39	14.1	0.41	0.79	40.7	-132.0	80	1.18
R2:L	5.2	-0.27	50	26	13.2	0.39	14.1	0.41	0.79	18.0	-41.3	35	2.06
R3:U	5.7	-0.45	100	28	15.0	0.41	16.1	0.44	0.79	6.6	-83.1	13	2.94
R3:L	5.7	-0.37	100	28	15.0	0.41	16.1	0.44	0.79	12.4	-69.2	24	2.27
R4:U	4.5	-0.19	200	30	17.2	0.43	18.5	0.46	0.79	19.3	-34.6	38	1.48
R4:L	3.8	0.06	200	30	17.2	0.43	18.5	0.46	0.79	12.7	7.3	25	0.78
R5:U	5.0	-0.35	200	30	17.2	0.43	18.5	0.46	0.79	18.2	-67.2	36	0.97
R5:L	4.2	-0.12	200	30	17.2	0.43	18.5	0.46	0.79	12.9	-21.1	25	0.80
R6:U	5.0	-0.41	200	30	17.2	0.43	18.5	0.46	0.79	11.4	-76.9	22	1.40
R6:L	4.3	-0.29	200	30	17.2	0.43	18.5	0.46	0.79	8.5	-46.9	17	1.15
R7:U	5.8	-0.83	10	22	10.0	0.35	10.6	0.37	0.79	16.6	-113.5	32	3.68
R7:L	5.6	-0.64	10	22	10.0	0.35	10.6	0.37	0.79	6.5	-86.4	13	3.29
R8:U	12.5	-1.16	50	26	13.2	0.39	14.1	0.41	0.79	63.1	-351.4	123	0.36
R8:L	9.0	-0.98	50	26	13.2	0.39	14.1	0.41	0.79	26.0	-230.8	51	2.51
R9:U	10.6	-0.80	100	28	15.0	0.41	16.1	0.44	0.79	27.1	-255.6	53	2.51
R9:L	11.0	-0.55	100	28	15.0	0.41	16.1	0.44	0.79	37.3	-201.4	73	1.57

Estimates of the amplitude and phase terms for the atmospheric flux of sensible heat follow from Eqs. (13) through (15). The aerodynamic surface roughness is computed with Eq. (15a) using characteristic physical heights estimated from the aerial photographs for the various sites (see Figs. 13 through 21). The geostrophic wind was estimated from the two NWS low-level EMSU soundings (0600 and 1130 CST) to be about 6.5 m sec^{-1}. After computing the surface Rossby number at each site, the geostrophic drag coefficient and the surface friction velocity are determined from Eq. (15). Terms Φ and φ have been tabulated in Table 6 based on Eq. (14) and the following constant values: $a = b = 8.5$; $c = 17$, and $\overline{M}^* = 0.2$.

Having parameterized the radiative fluxes and the atmospheric sensible heat flux, the solutions for both the evaporative and the subsurface heat fluxes are obtained by using the known amplitude and phase terms together with Eqs. (8) and (9). Since Φ and χ are known, both Ψ' and X, and subsequently μ and Bo can be evaluated with Eqs. (12c) and (16a), respectively. In the case of the partial impedance for evaporation the sum of Φ and X has been evaluated using Eqs. (8) and (9); the X-values are then obtained as the residual using the Φ-values as discussed above. The thermal admittance μ follows from Ψ' using Eq. (12c). The values for Ψ', Bo, and μ evaluated in this manner using first harmonic amplitude and phase terms were summarized in Table 6.

In summary, we have taken measured radiative parameters and certain parameterized (synthesized) values and through the application of climatonomy have determined two important geophysical features of the sites: the thermal admittance (μ) is obtained through consideration of the submedium at each site as a homogeneous conductor of heat; the inverse Bowen ratio (Bo) expresses the magnitude of the evaporative heat flux as a fraction of the sensible flux of heat to/from the atmosphere at the earth/air interface. Keeping in mind the limitations noted both

in the measured and parameterized values, it is possible to subjectively evaluate the representativeness and significance of the results. It is encouraging to note that all sites have μ- and Bo- values that are in the range of what might be anticipated. For example, μ ranges from a minimum of 22 mly $sec^{-1/2}$ $^{o}K^{-1}$ in open farm country (R-7) to a maximum of about 87 at the wooded sites (R-8 and R-9); the mean value for all sites is 42. Lettau[9] lists typical μ-values determined for a variety of homogeneous media: soils range from 14 mly $sec^{-1/2}$ $^{o}K^{-1}$ for fine, dry quartz sand to 47 for the same sand with 22% moisture; μ for "sandy clay (15% moisture)" is given as 36 while "swamp land (90% moisture)" is 44. Rocks range from 45 for basalt to 56 for granite and concrete. Regarding heterogeneous surfaces, Lettau estimates "fields, weedy swamp, still water, and hilly woods" to have μ-values of 35. Examining our results in view of this background, several conclusions may be drawn. First, the absolute values of the computed thermal admittances are reasonable. Second, the highest values occur at sites R-2, R-8, and R-9. These three sites share one common feature not typical of any of the other six sites: they are all dominated by a high percentage of wooded areas. It is interesting, however, that Lettau estimates μ to be smaller by a factor of 1.5 to 2 for similar terrain, although he does not state whether his estimate is a summer or winter value. It is quite conceivable that the presence or absence of foliage significantly alters the effective thermal conductivity of a wooded area and that the former situation may lead to larger values of μ as a result of the increased surface area and concurrent increase in mixing and the transfer of heat away from the canopy.

The "developed" sites (R-3, -4, -5, and -6) all have quite similar values of the thermal admittance, around 25 mly $sec^{-1/2}$ $^{o}K^{-1}$. There does not seem to be any noticeable difference in μ among the various building-zone types; i.e., new and old residential and commercial all appear

similar. One possible exception is site R-6, where μ computed from the lower level aircraft data seems somewhat low. No conjecture is offered in explanation.

Site R-7 is a good check on the method as the site is simple, homogeneous and extensive, and experience dictates a low value for μ-- Lettau[9] estimates 35. The two μ-values for this site are 32 and 13, averaging out to 23.

Without supporting surface observations, it is difficult to evaluate all of the Bo-values. Most values are less than 2.5, with site R-7 the maximum, having an average Bo of 3.5. There had been showers in the area on 8 August and hence the Bo-values are not unreasonably large. It is significant that the lowest values are found for three of the four developed sites, R-4, -5, and -6. This is to be expected due to the increased runoff in urban and suburban areas and the corresponding decrease in evaporation.

A final observation is in order regarding the distribution of μ and Bo at the nine sites: although the theoretical formulation used in evaluating the surface energy budget explicitly ignored energy fluxes associated with photosynthesis (or anthropogenesis), the impact, if any, of such fluxes is reflected in the measured values. Hence in using the climatonic theory in the valuation of μ and Bo as (essentially) residuals, we have implicitly accounted for the impact of such other fluxes in the determination of these parameters. Thus, for example, it is not unlikely that the large Bo-values determined for the undeveloped sites relects some impact of photosynthesis. This may in part explain why the largest Bo-values were found for the agricultural site.

The μ- and Bo-values tabulated in Table 6 are the result of the analysis of the first-harmonic data. Since μ and Bo are frequency-independent, all harmonics should yield similar results. Difficulties

were encountered in attempting to evaluate both parameters on the basis of the second-harmonic data: μ-values became negative, while Bo was excessively large in many cases (up to 25). There are three possible explanations for these discrepancies: (1) errors in the regression analysis used to infer the amplitude and phase terms from the surface temperature data, (2) experimental inaccuracies such as instrument drift or (more likely) wander of the flight track, and (3) limitations in the theory--particularly in the neglect of photosynthetic and anthropogenic fluxes. Most likely, each contributes to the problem. On the assumption that the cause lay in the data and particularly in the determination of the second-harmonic terms, a simple feedback analysis was pursued wherein effective $\Delta_2 T_o$- and δ_2-values were derived that forced the determination of μ- and Bo-values equal to the first-harmonic results. In 16 of the 18 cases, the "effective" temperature amplitude ($\Delta_2 T_o$) differed from the original (Table 6) by less than 0.7°C; phase differences were generally larger, averaging about 0.6 rad or 70 min. Differences in both terms are certainly within the range of possible errors associated with the regression method for determining Fourier coefficients (see Section V-B) and/or with departures from the aircraft flight track (leading to differences in scene at the nine sites from flight to flight).

Table 7 then summarizes the amplitudes of the atmospheric sensible and latent heat flux densities and the subsurface heat flux density on the basis of (1) the first-harmonic μ- and Bo-values, as derived above, and (2) the temperature amplitudes ($\Delta_1 T_o$) determined earlier from the regression approach. To illustrate the diurnal fluctuations of these fluxes and their variations among land-use types, Figure 25 illustrates these differences for three sites: farmland (R-7), commercial/industrial (R-4), and new suburban residential (R-3). The curves have been derived from Eqs. (2d through f) using averaged amplitude terms from Table 7 and phase terms from Table 6.

Table 7

DERIVED AMPLITUDE TERMS FOR ATMOSPHERIC SENSIBLE ($\Delta_1 Q_o$), LATENT ($\Delta_1 E_o$), AND SUBSURFACE ($\Delta_1 S_o$) HEAT FLUX DENSITIES
Units: mly/min

Site: Altitude*	$\Delta_1 Q_o$	$\Delta_2 Q_o$	$\Delta_1 E_o$	$\Delta_2 E_o$	$\Delta_1 S_o$	$\Delta_2 S_o$
R1:U	103	36	217	76	229	107
R1:L	112	34	194	59	235	94
R2:U	106	38	125	45	325	157
R2:L	122	57	251	117	166	103
R3:U	124	49	364	143	55	28
R3:L	131	55	298	125	109	60
R4LU	155	79	229	116	174	116
R3:L	211	96	165	75	156	93
R5:U	183	70	178	68	194	98
R5:L	212	85	170	68	159	84
R6:U	179	76	250	106	119	66
R6:L	204	99	235	114	101	64
R7:U	87	37	319	135	144	81
R7:L	107	36	352	120	73	33
R8:U	91	24	33	9	435	154
R8:L	101	28	254	70	199	72
R9:U	105	33	264	82	190	80
R9:L	111	25	174	40	275	83

* U = upper (1220 m mgl)

L = lower (460 m mgl)

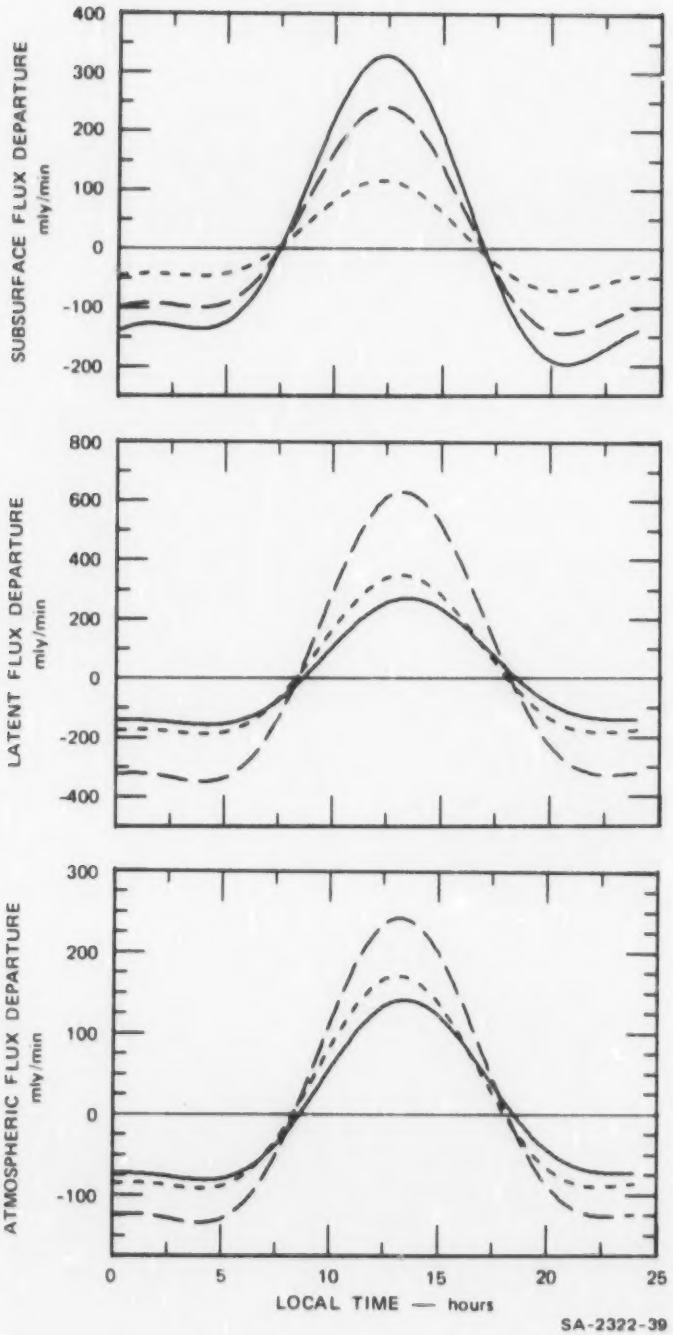

FIGURE 25 DIURNAL VARIATION OF DERIVED DEPARTURES (FROM DAILY AVERAGE) OF ATMOSPHERIC, LATENT, AND SUBSURFACE HEAT FLUX DENSITIES FOR THREE LAND-USE TYPES: FARMLAND (——), COMMERCIAL/INDUSTRIAL (— —), AND SUBURBAN RESIDENTIAL (- - - -)

VI CONCLUSIONS AND RECOMMENDATIONS

All of the data collected during the experimental programs in St. Louis have not been fully exploited for information content. Additional analyses would include not only the aircraft observations but also a variety of surface observations collected during the same period under other observation programs. Detailed photographic analysis was limited by the scope of the present study. Nevertheless, the program demonstrated the feasibility of acquiring observations of the time changes in the solar forcing function and the primary response function (surface temperature) and for inferring, in conjunction with climatonomic theory, secondary responses as a function of surface type. In this way variations in the surface energy budget are described. Magnitudes and variations in both observed and derived quantities were established by the program, and a useful evaluation of program requirements for future applications is now possible.

Considerable rechecking of both observational and theoretical results with independent data is of course, desirable. Improvements in data acquisition and processing techniques would be introduced as a result of past experience. Although it is easy to expand an observational program, certain improvements must be given priority. From the aircraft platform, measurements of reflected solar radiation and surface infrared emission should be obtained with the same field of view, and over a complete 24-hour period (with overlap). Furthermore, solar radiation measurements (in both directions) should be expanded so as to permit a separation of visible and near-infrared contributions.

The program for the analysis of other standard aircraft data could be expanded considerably with a good payoff to a study of the type

conducted. Because of the importance of small changes in the surface albedo and surface temperature, more effort is required to assess the magnitude of the atmospheric influence on these measurements (by virtue of observed changes with altitude). A more careful analysis of the air temperature data collected at each of the two flight altitudes provides information on changes in stability and advection within the boundary layer; corrections for cooling or heating during each traverse can be accomplished with the observations themselves. In addition, harmonic analyses of the aircraft-measured temperature in the boundary layer over each site of interest would assist in the analyses of the secondary response terms in the climatonomical analysis of the surface energy budget. Finally, inasmuch as ground-speed determinations between check points are documented, wind estimates at two altitudes along the flight track could be obtained from the indicated air speed, ambient temperatue, and drift angle. Because of the need for a more careful representation of flow conditions, this wind information should be supplemented with additional surface wind observations at locations along the track and with at least four balloon soundings per day at one location. Together these data would provide a more detailed assessment of the temporal and spatial variations in the atmospheric flux of sensible heat.

Surface radiation observations (along with temperature, humidity, and wind) should be expanded to cover several preselected sites of different types along the flight track. Better descriptions of surface structure with improved input information on roughness and potential evapotranspiration are required. Inventories also are required on photosynthetic and anthropogenic heat sources, both of which have been neglected thus far.

Lastly, several important improvements need to be made in the aircraft operations. First, more frequent flights over a 24-hour period need to be made: on the order of 10 to 12. This is necessary to over-

come potential difficulties in the determination of Fourier coefficients. Secondly, more active control of the aircraft flight path needs to be implemented to assure repeated overflights of the identical surface scene.

The results to date are encouraging: the study has demonstrated the feasibility of this method for evaluating the structure of the surface energy budget. Incorporating experiences and the recommendations herein, we recommend the program be expanded to evaluate in a systematic fashion the geophysical surface features of a broad range of typical land-use types under varying meteorological conditions. In this way we will be able to look at such interactions as the impact of soil moisture on thermal admittance, foilage and its effect on albedo, and so forth.

Appendix A

AIRCRAFT DATA SUMMARY

Most of the aircraft measurements of solar radiation, surface temperature, and air temperature are summarized graphically in this appendix (Figures A-1 through A-14).* All data are plotted as a function of flight track range. The origin of the range for August 1972 data coincides with the northernmost checkpoint of the August 1972 flight track shown in Figure 2 of the text; the range for April 1973 data originates at the westernmost checkpoint shown in Figure 2. These origins are maintained regardless of the direction of motion of the aircraft at either of the two flight altitudes. The major urban area for August flights falls between about 33 and 45 km range while the major rural areas occur over the last two-fifths of the track. Along the April flight track the urban area is more varied; the major portion of the urban areas occur between about 26 and 47 km range while the major rural areas occur over the last third of each flight track.

Solar data are presented for the August flights only. The characteristic dip in the albedo traces near the origin results from crossing a broad section of the Mississippi River (see Figure A-1); a broad dip in the albedo curves occurs over the urban area. Irregularities in the measured downwelling solar irradiance (solid curve) are produced by clouds above the aircraft and are frequently associated with irregularities in the albedo curves as well, especially when the aircraft pyranometer is shaded but the surface directly beneath the aircraft is not shaded. Variations in incident solar radiation with changes in solar zenith angle also are revealed by time changes in the solid curves. Especially characteristic of convective activity are the data for the 1630 CDT flight on 11 August 1972 (Figure A-9);

*For convenience, the illustrations for this appendix are grouped after this discussion.

Pages A-1 and A-2 are Blank

showers forced cessation of the observational sequence at this time.

The sequence of radiometric surface temperatures for 9 August 1972 (Figure A-10) clearly shows the pronounced increase in surface temperature variability associated with daytime solar heating. At night the surface temperatures are relatively uniform except for water bodies (rivers), which appear as pronounced warm spikes. These spikes provide an excellent nighttime check on the actual flight track. The low-level flights of 0400 and 0630 CDT actually strayed too far to the east as evidenced by the double spikes appearing between 25 and 31 km range; these correspond to two crossings of a bend in a Mississippi River channel along the northeastern border of St. Louis (cf., Figure 2). As the land areas heat to their maximum temperatures, the water bodies appear as minima on the temperature curves.

Figure A-11 portrays graphically the air temperature as a function of range at both altitudes; a comparison of the traces provides an immediate indication of stability (above 460 m). These records are sensitive to slight changes in aircraft altitude; unfortunately, a precise altitude record was not available for the data. If it is assumed that the data have been properly calibrated and that the aircraft altitude was essentially uniform along each leg, then it appears that at the start of the period cold air advection (with northerly flow) was still occurring, with greater stability between 460 m and 1220 m over the rural area along the southern portion of the track (beyond 50 km range). By afternoon the temperatures have become more uniform and the stability has decreased.

Data in Figure A-12 for 11 August 1972 are similar to those in Figure A-10 for 9 August 1972. In Figure A-13 (11 August 1972), the air temperature data contain many noise spikes; these spikes should be ignored. Nighttime data for 11 August suggest less stability beyond 50 km range in contrast to the observations of 9 August. Of course, from

the surface temperature measurements it is also clear that the same region has much greater stability below the 460 m altitude. Nevertheless, the trend of the airborne air temperature data is disturbing, showing an increase with flight time (460 m flown first on this flight sequence). Therefore, a firm picture of the air temperature fields in the early morning periods cannot be established without more observations supplying accurate calibrations and a careful check on flight altitudes.

The surface temperature measurements from the April 1973 flights (Figure A-14) shows the extensive flooded area around the Mississippi River near the origin of the flight track. This region is relatively cool during the 1700 CST flight but, as the land cools, appears relatively warm in the early morning hours. The large dip in the dashed trace at 0130 CST should be ignored (10°C not added).

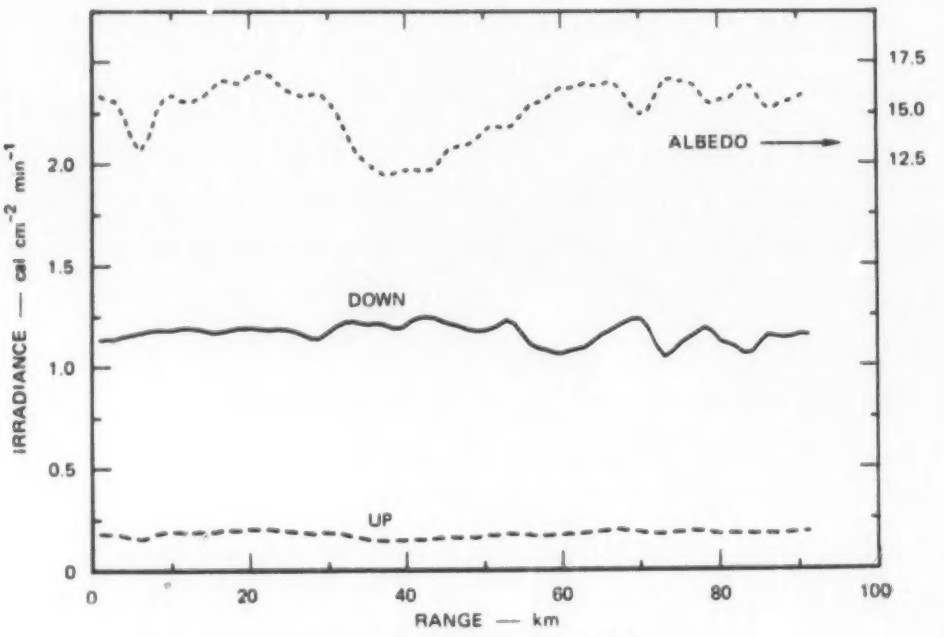

(a) FLIGHT ALTITUDE 1220 METERS

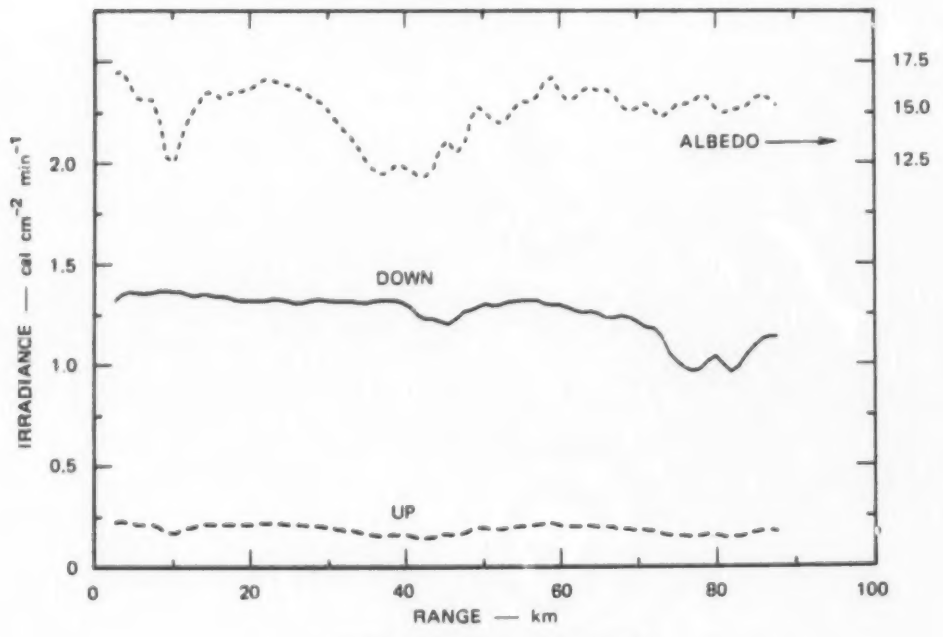

(b) FLIGHT ALTITUDE 460 METERS

SA-2322-24

FIGURE A-1 AIRCRAFT SOLAR MEASUREMENTS, 0930 CDT FLIGHT, 9 AUGUST 1972

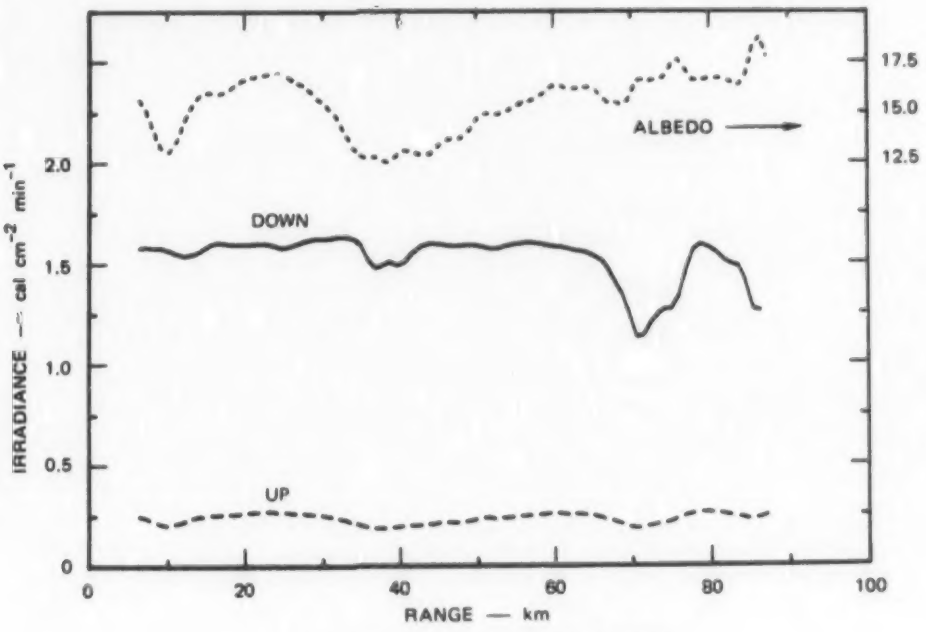

(a) FLIGHT ALTITUDE 1220 METERS

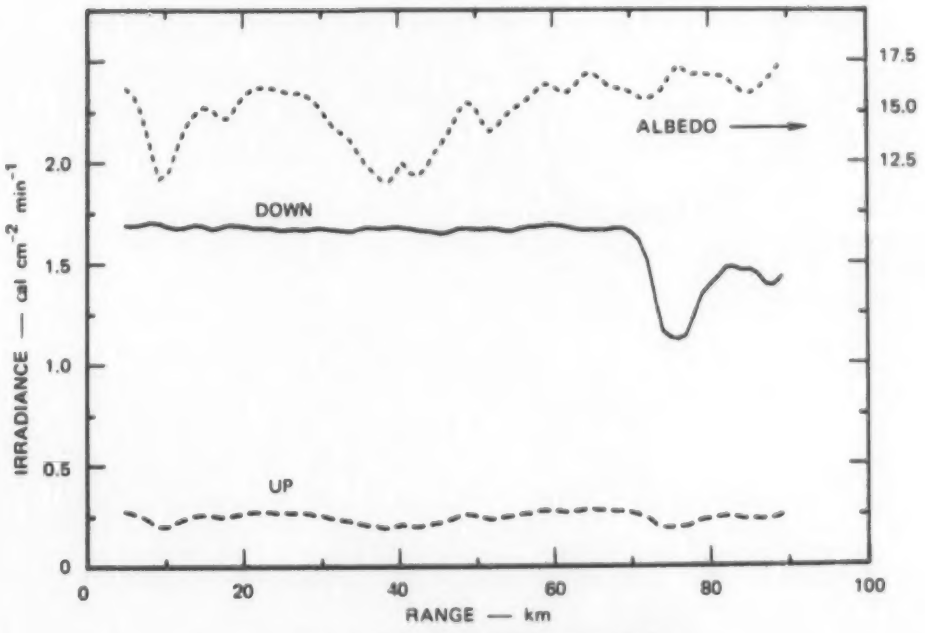

(b) FLIGHT ALTITUDE 460 METERS

SA-2322-25

FIGURE A-2 AIRCRAFT SOLAR MEASUREMENTS, 1145 CDT FLIGHT, 9 AUGUST 1972

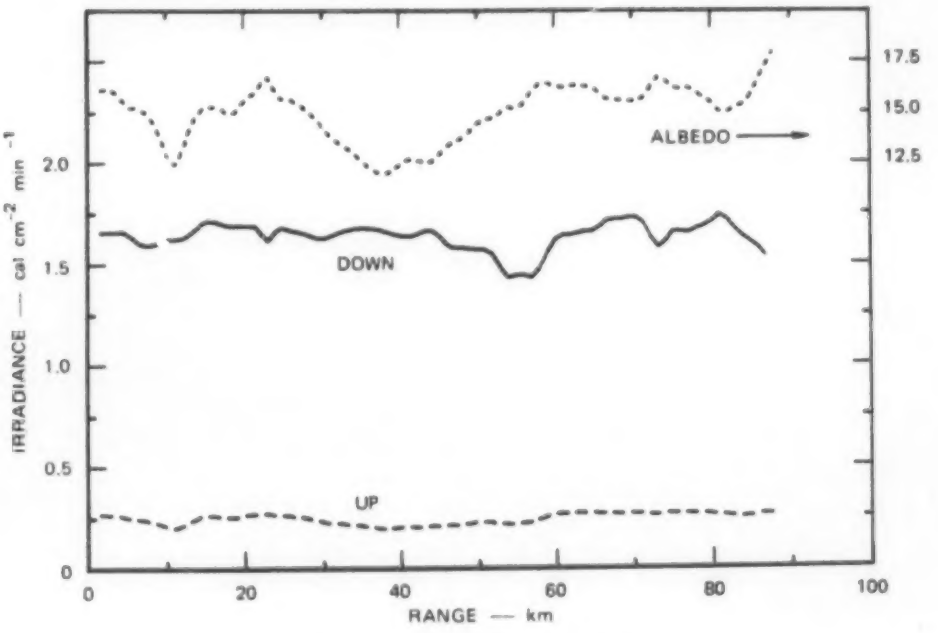

(a) FLIGHT ALTITUDE 1220 METERS

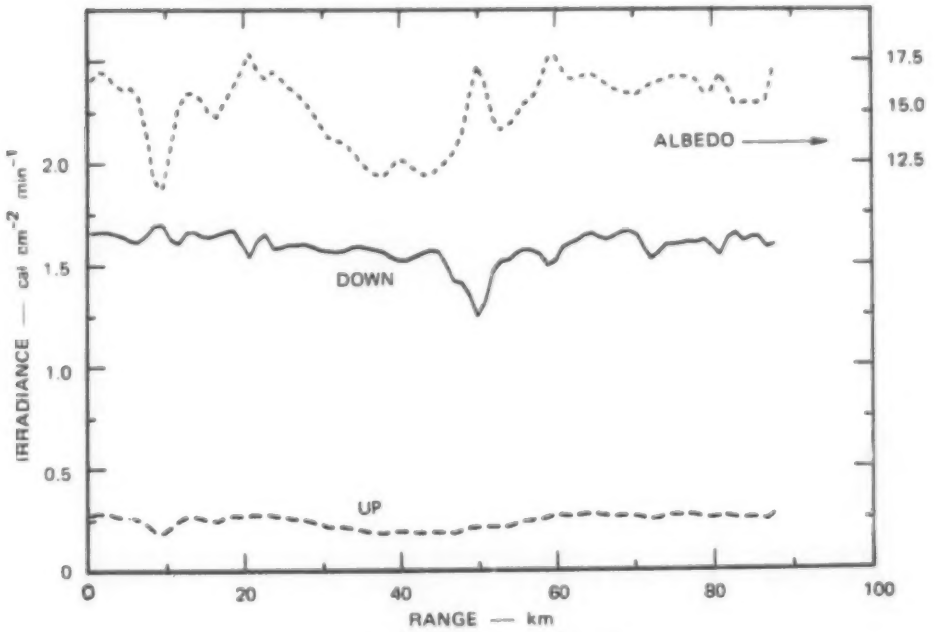

(b) FLIGHT ALTITUDE 460 METERS

SA-2322-26

FIGURE A-3 AIRCRAFT SOLAR MEASUREMENTS, 1400 CDT FLIGHT, 9 AUGUST 1972

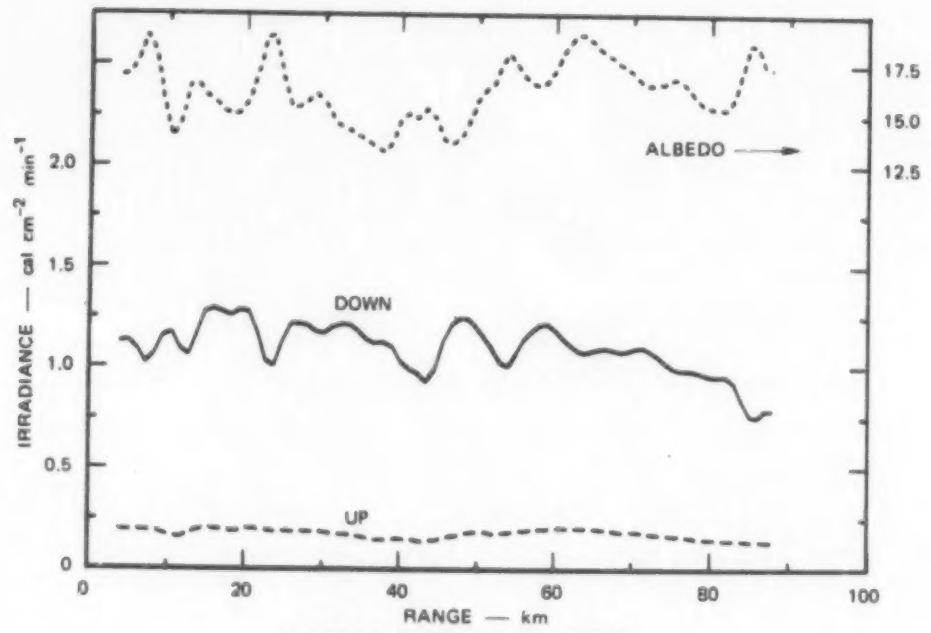

(a) FLIGHT ALTITUDE 1220 METERS

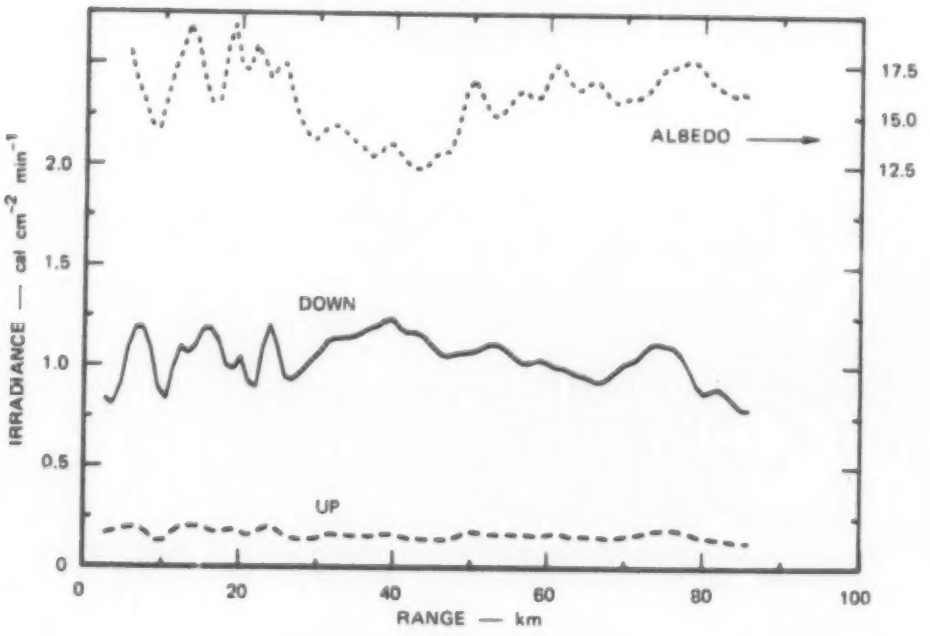

(b) FLIGHT ALTITUDE 460 METERS

SA-2322-27

FIGURE A-4 AIRCRAFT SOLAR MEASUREMENTS, 1630 CDT FLIGHT, 9 AUGUST 1972

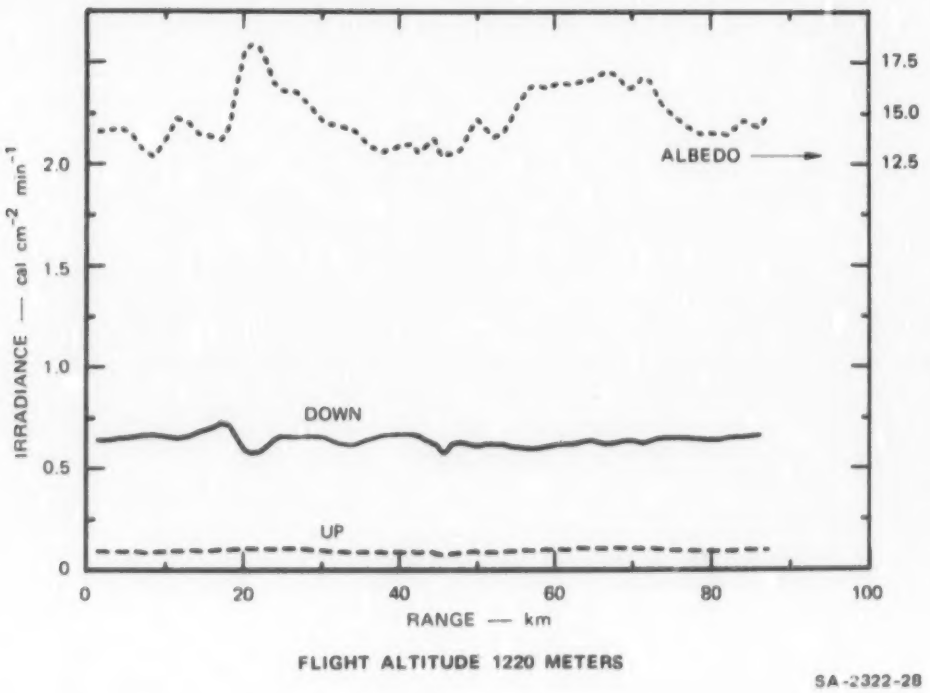

FIGURE A-5 AIRCRAFT SOLAR MEASUREMENTS, 1915 CDT FLIGHT, 9 AUGUST 1972

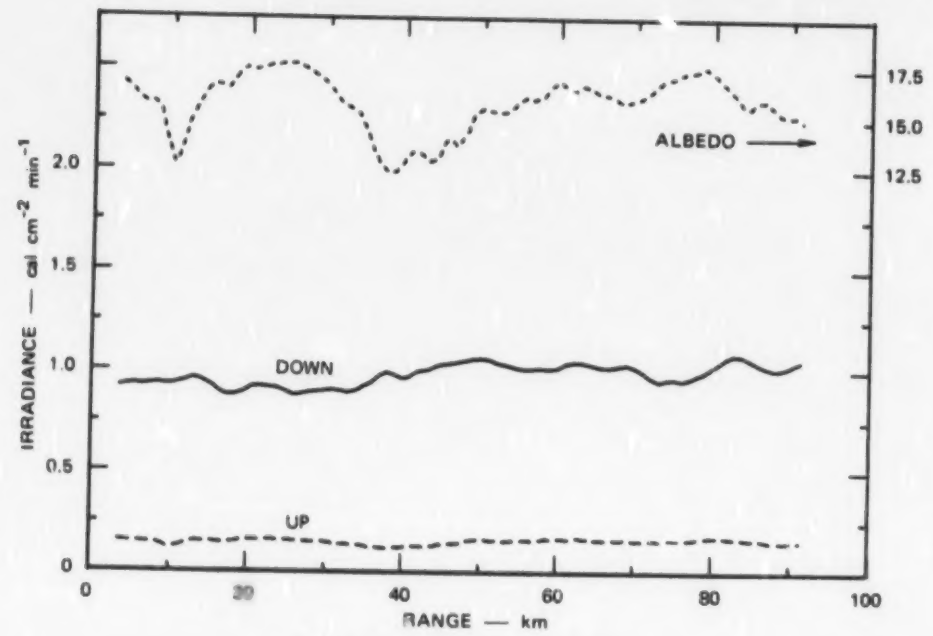

(a) FLIGHT ALTITUDE 460 METERS

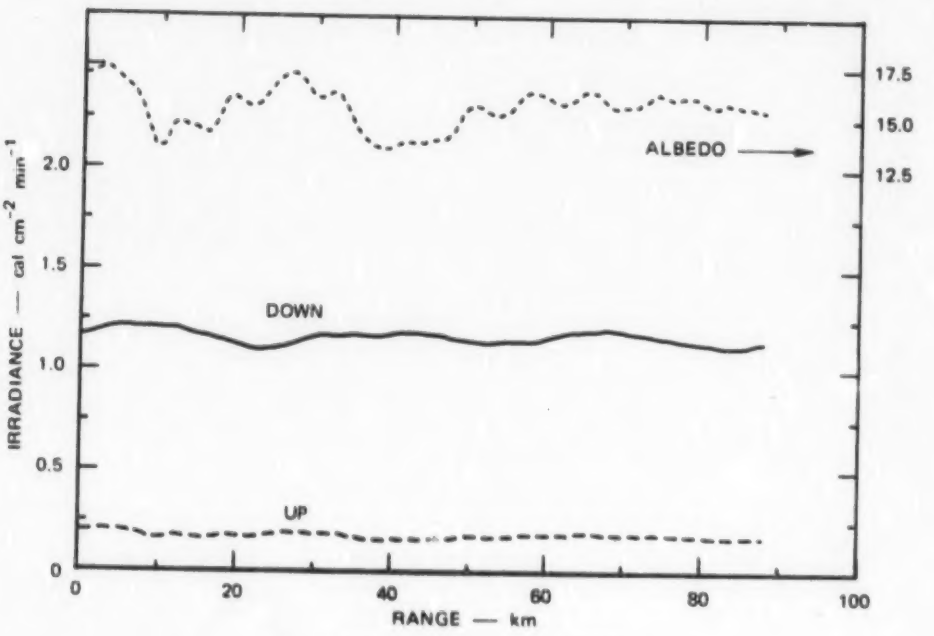

(b) FLIGHT ALTITUDE 1220 METERS

SA-2322-29

FIGURE A-6 AIRCRAFT SOLAR MEASUREMENTS, 0900 CDT FLIGHT, 11 AUGUST 1972

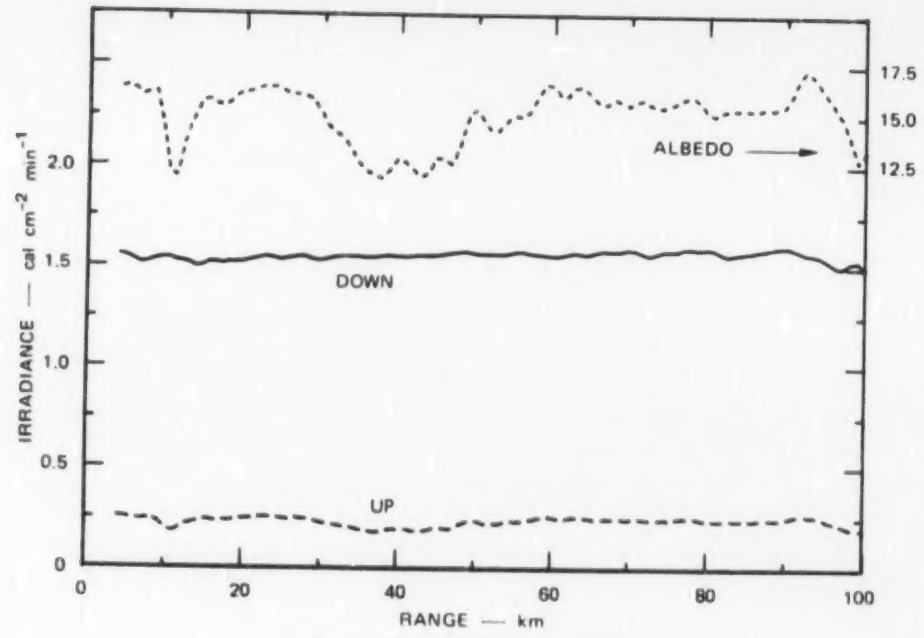

(a) FLIGHT ALTITUDE 460 METERS

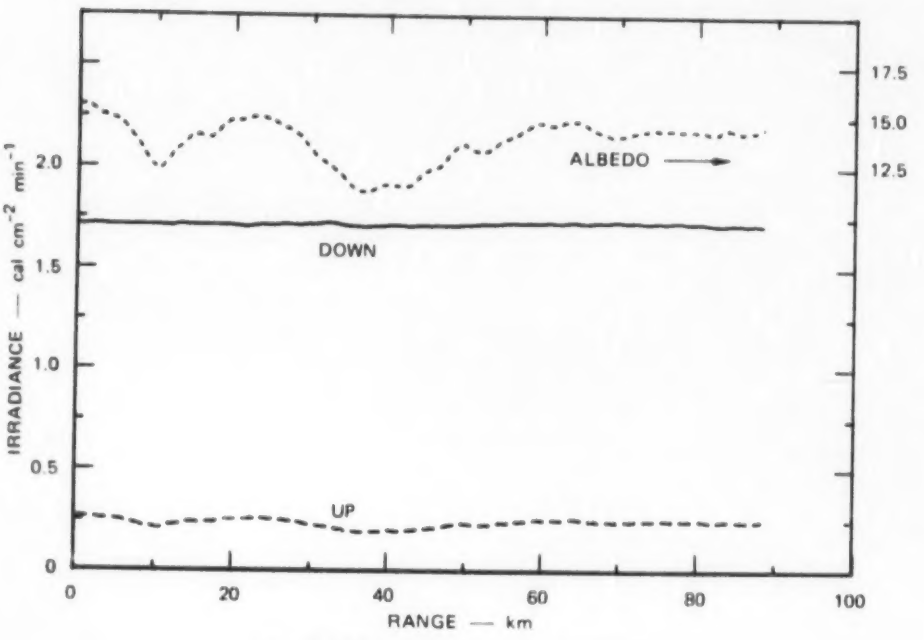

(b) FLIGHT ALTITUDE 1220 METERS

SA-2322-30

FIGURE A-7 AIRCRAFT SOLAR MEASUREMENTS, 1130 CDT FLIGHT, 11 AUGUST 1972

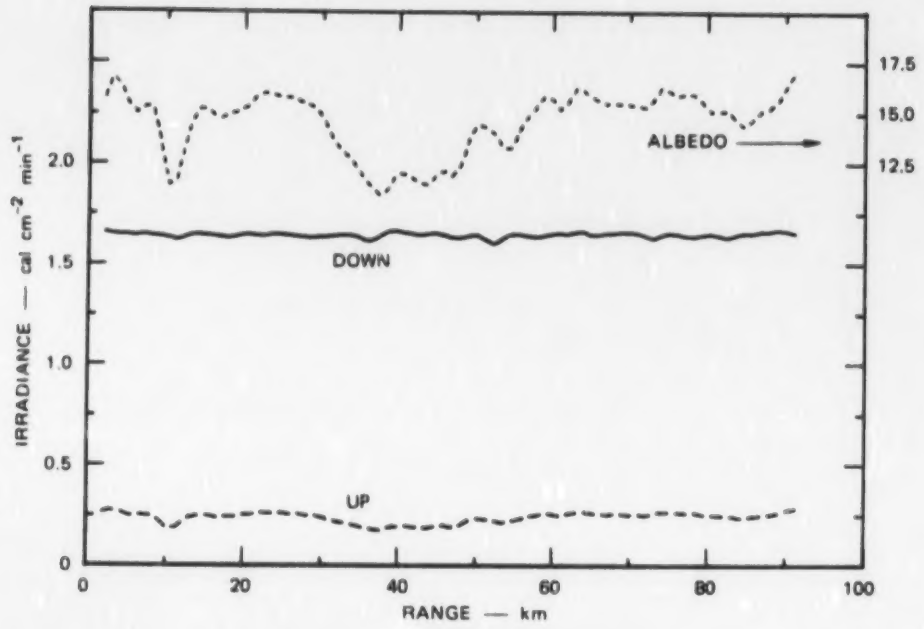

(a) FLIGH ALTITUDE 460 METERS

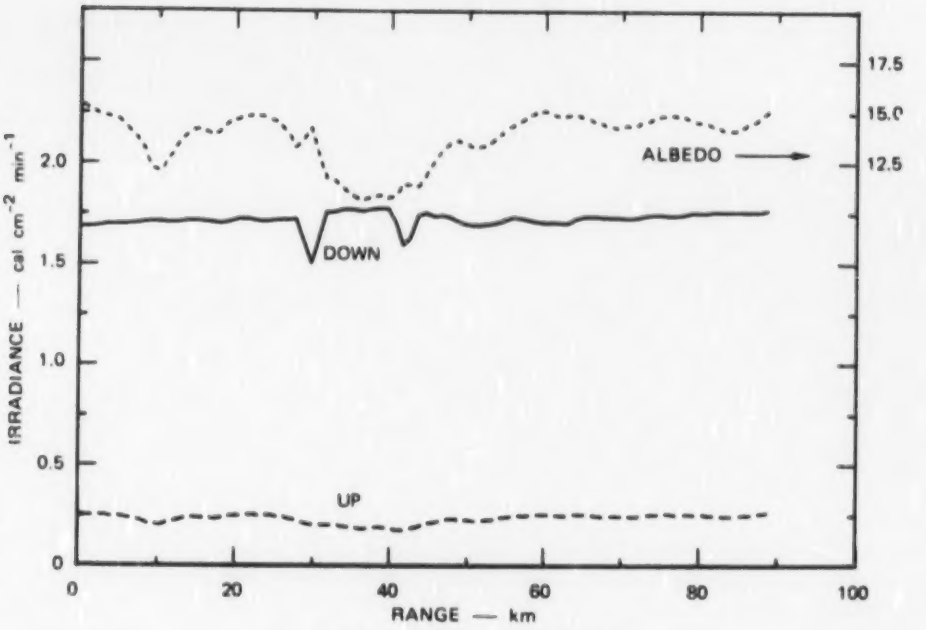

(b) FLIGHT ALTITUDE 1220 METERS

SA-2322-31

FIGURE A-8 AIRCRAFT SOLAR MEASUREMENTS, 1400 CDT FLIGHT, 11 AUGUST 1973

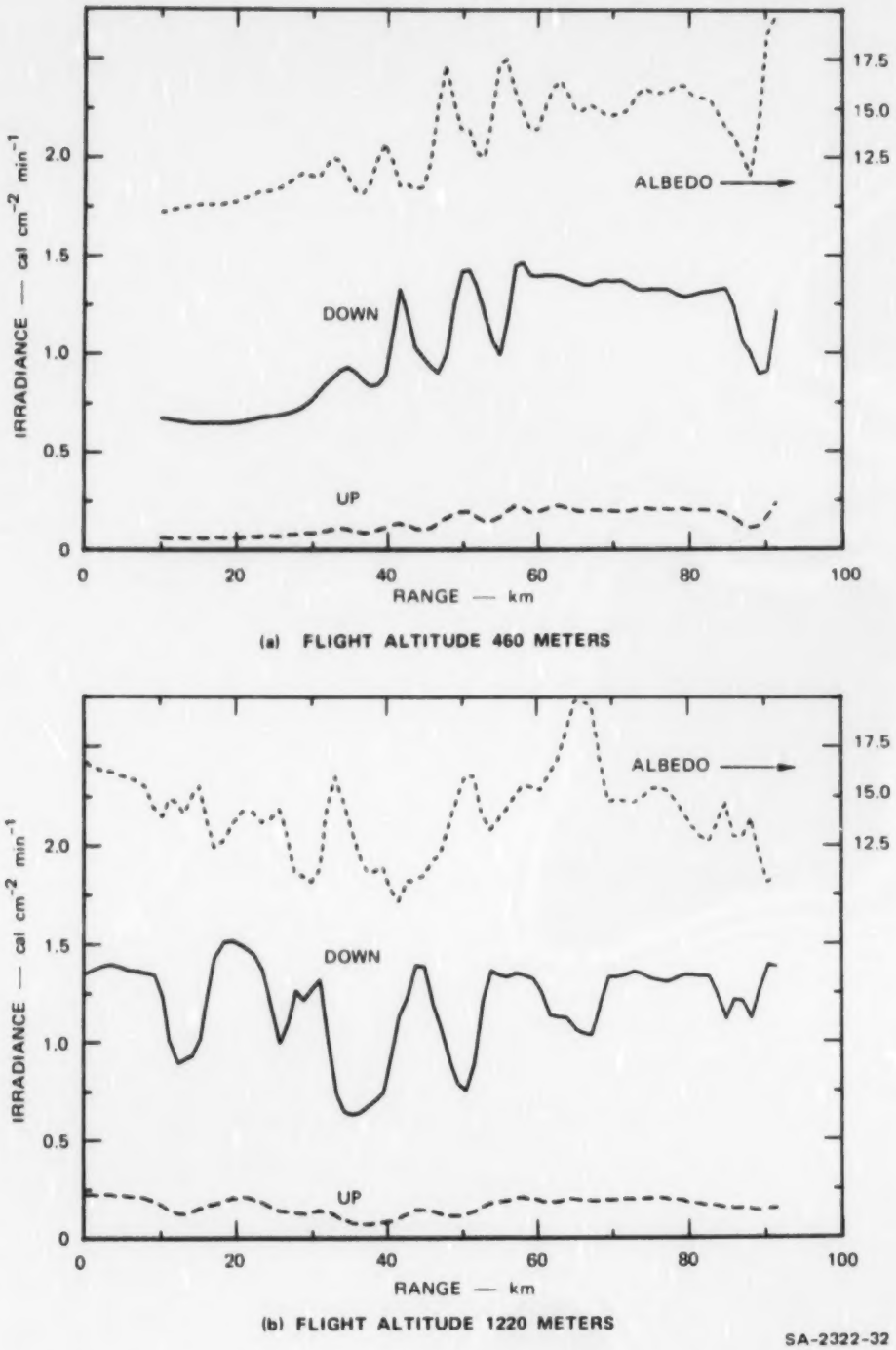

FIGURE A-9 AIRCRAFT SOLAR MEASUREMENTS, 1630 CDT FLIGHT, 11 AUGUST 1973

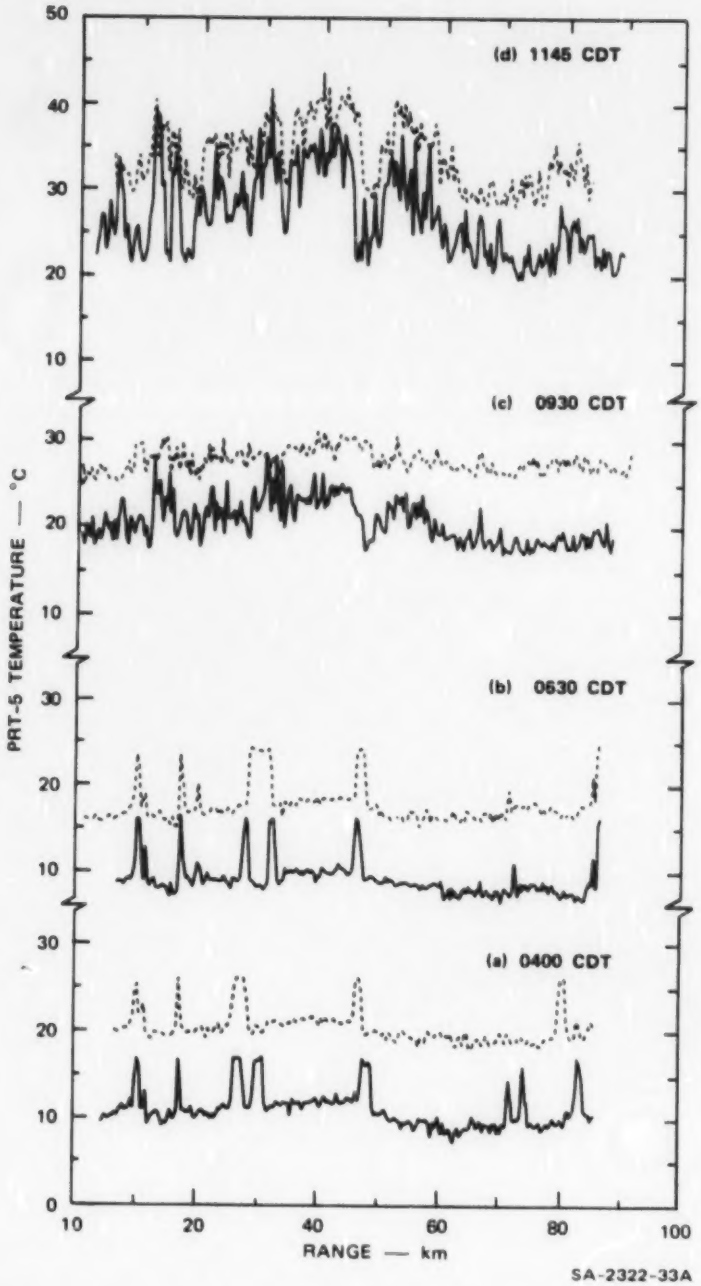

FIGURE A-10 AIRCRAFT RADIOMETRIC SURFACE TEMPERATURE MEASUREMENTS, 9 AUGUST 1972

Solid curve: measurements from 460 m
Dashed curve: measurements from 1220 m, 10°C added.

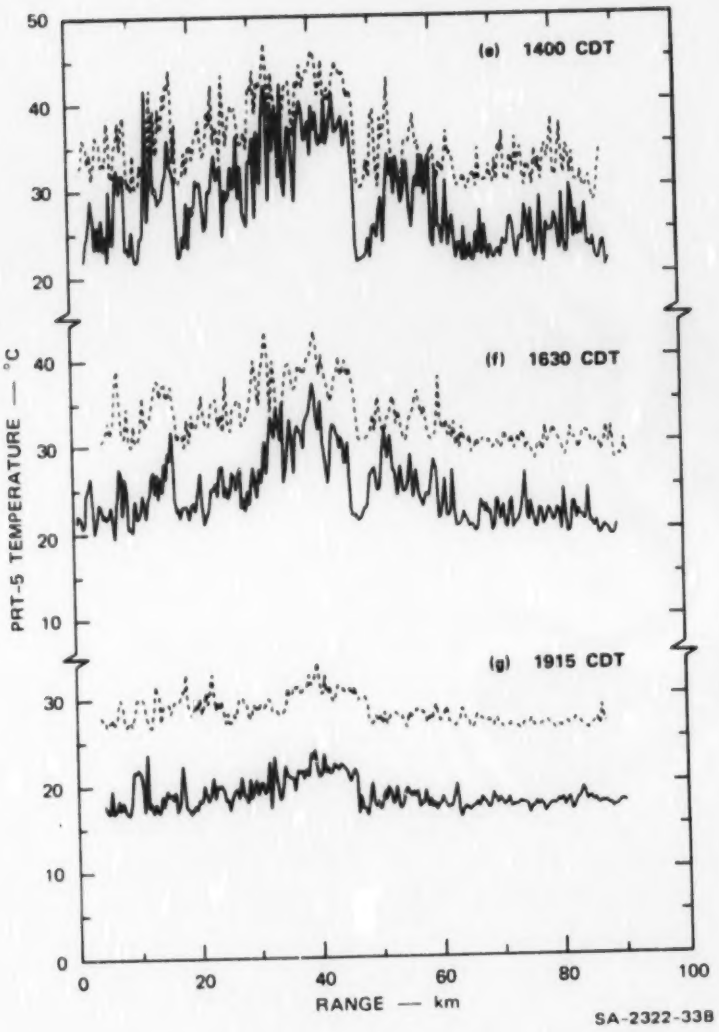

FIGURE A-10 AIRCRAFT RADIOMETRIC SURFACE TEMPERATURE MEASUREMENTS, 9 AUGUST 1972 (Concluded)

Solid curve: measurements from 460 m
Dashed curve: measurements from 1220 m, 10°C added

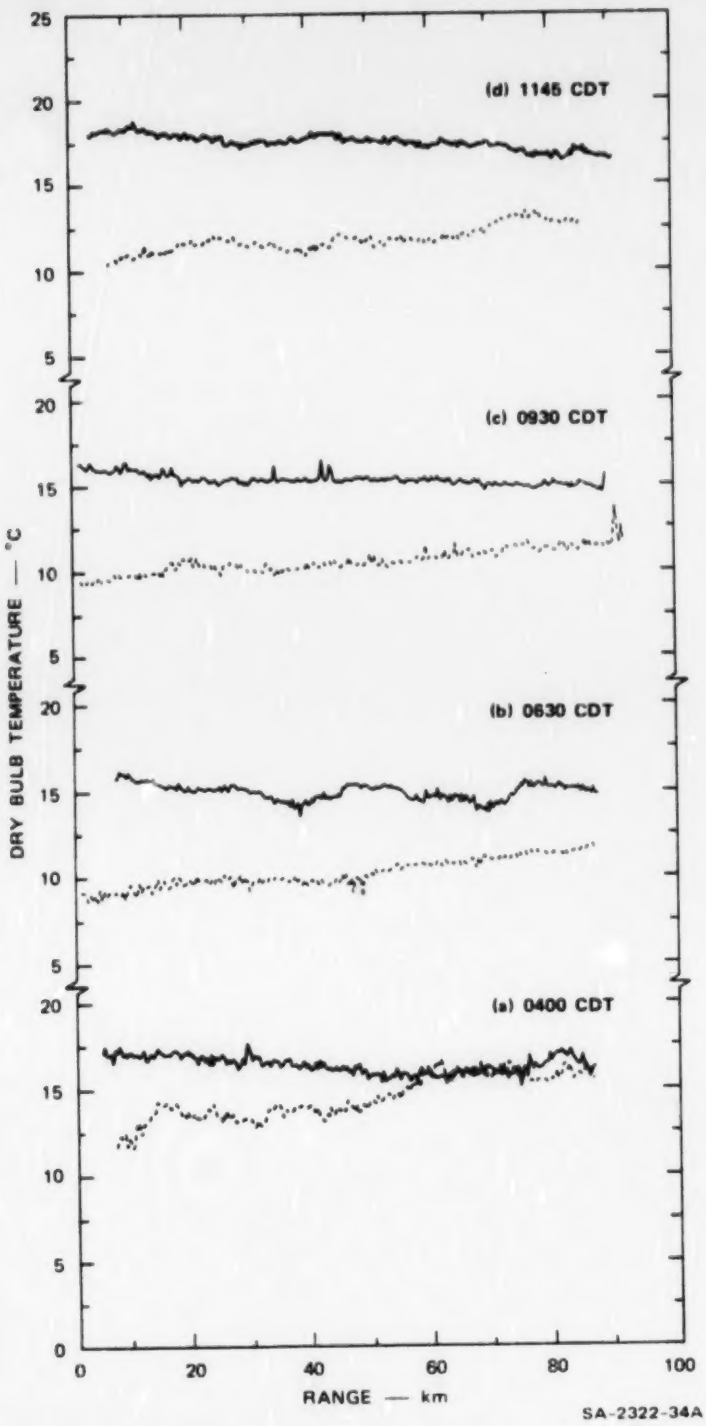

FIGURE A-11 AIRCRAFT AIR TEMPERATURE MEASUREMENTS, 9 AUGUST 1972

Altitudes: 460 m (solid) and 1220 m (dashed)

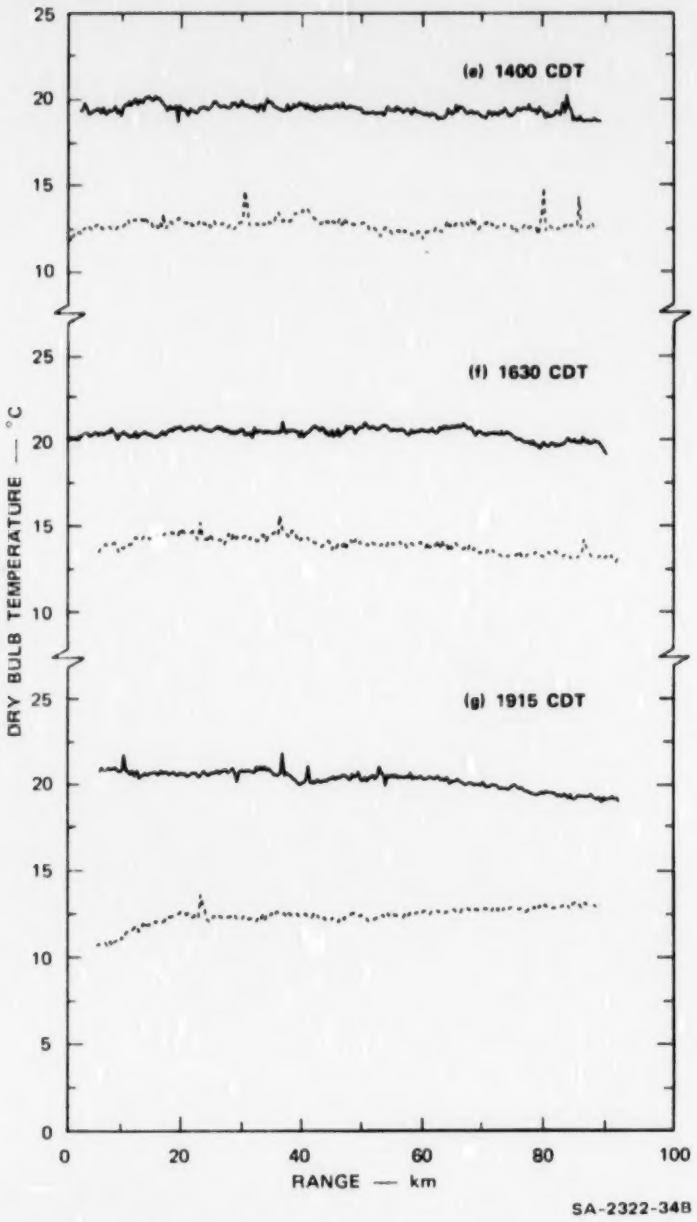

FIGURE A-11 AIRCRAFT AIR TEMPERATURE MEASUREMENTS, 9 AUGUST 1972 (Concluded)

Altitudes: 460 m (solid) and 1220 m (dashed)

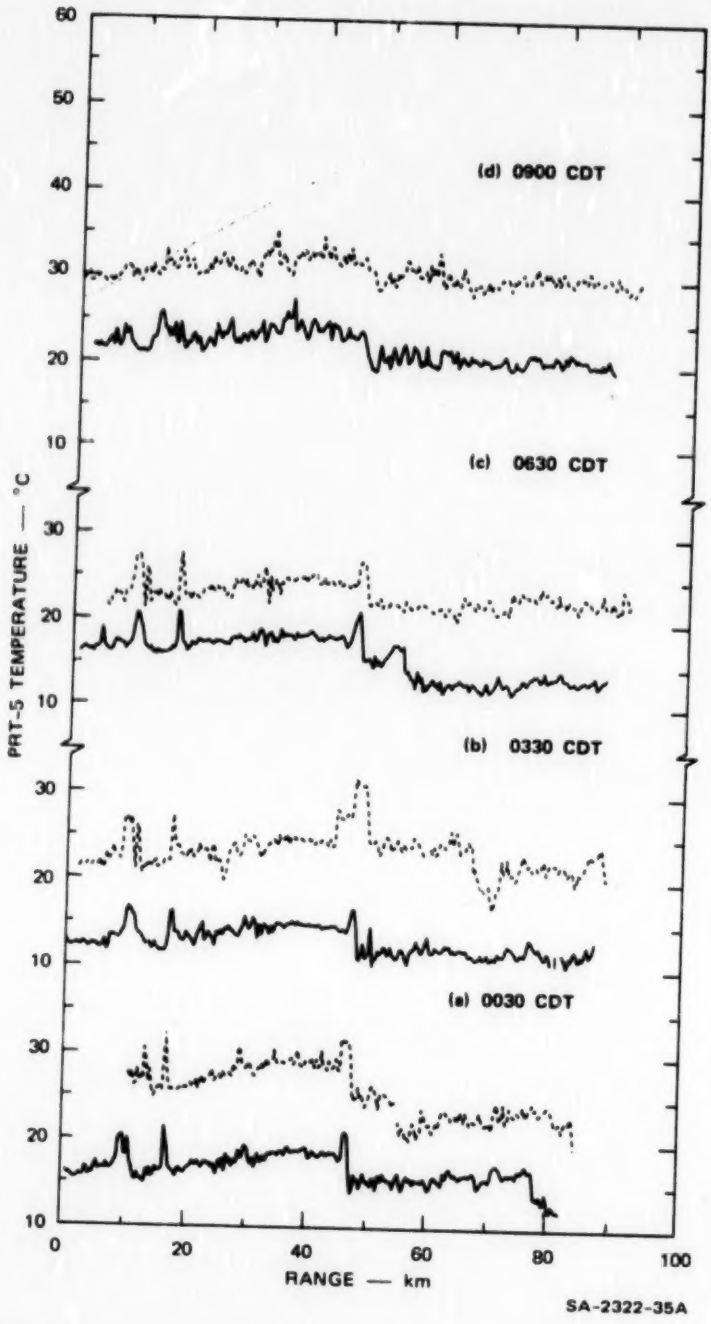

FIGURE A-12 AIRCRAFT RADIOMETRIC SURFACE TEMPERATURE MEASUREMENTS, 11 AUGUST 1972

Dashed curve: measurements from 460 m, 10°C added
Solid curve: measurements from 1220 m

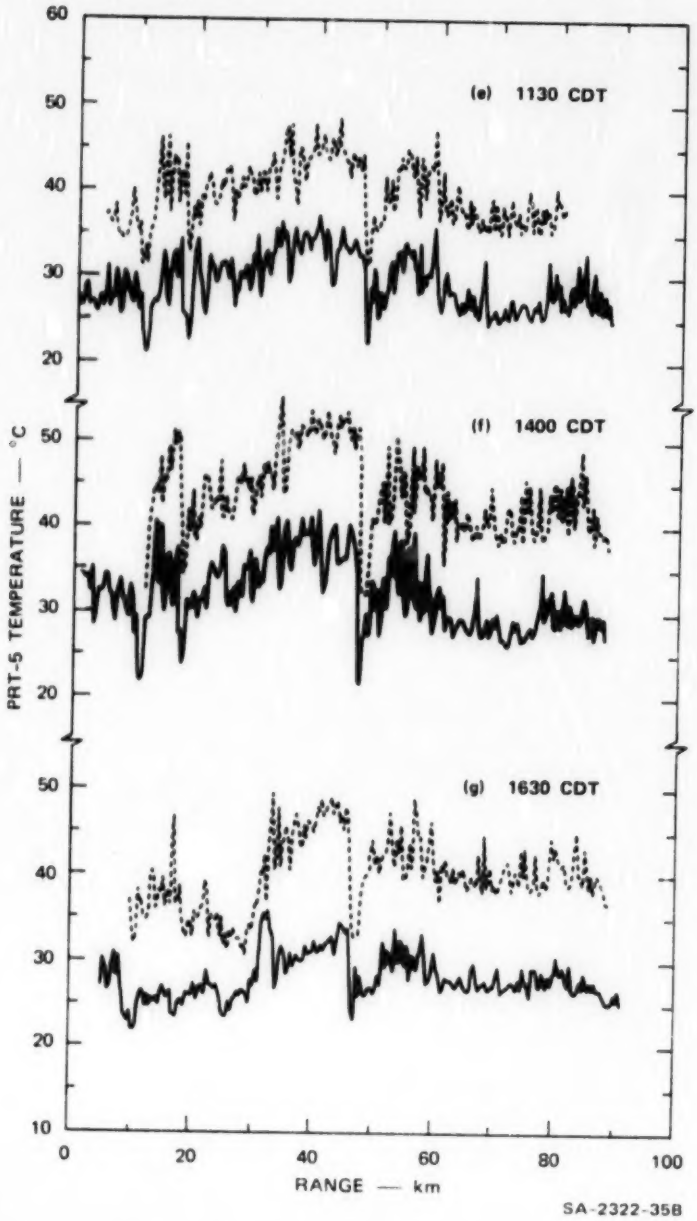

FIGURE A-12 AIRCRAFT RADIOMETRIC SURFACE TEMPERATURE MEASUREMENTS, 11 AUGUST 1972 (Concluded)

Dashed curve: measurements from 460 m, 10°C added
Solid curve: measurements from 1220 m

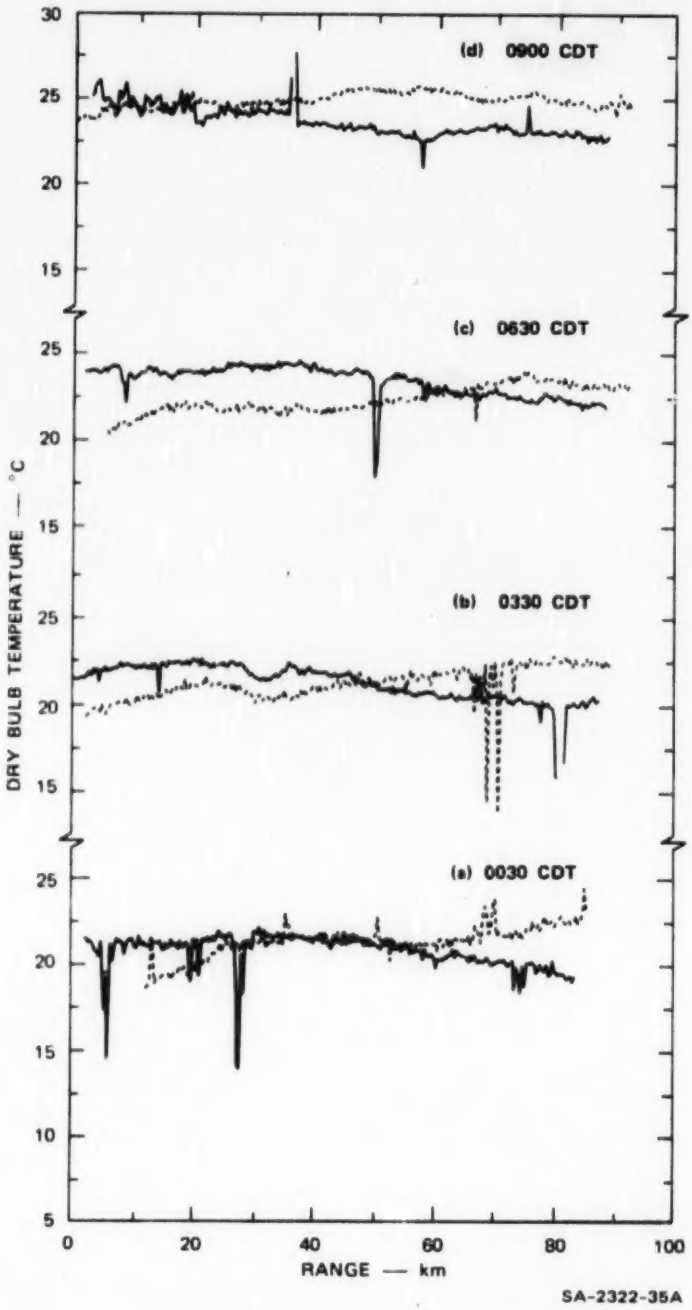

FIGURE A-13 AIRCRAFT AIR TEMPERATURE MEASUREMENTS, 11 AUGUST 1972

Altitudes: 460 m (dashed) and 1220 m (solid)

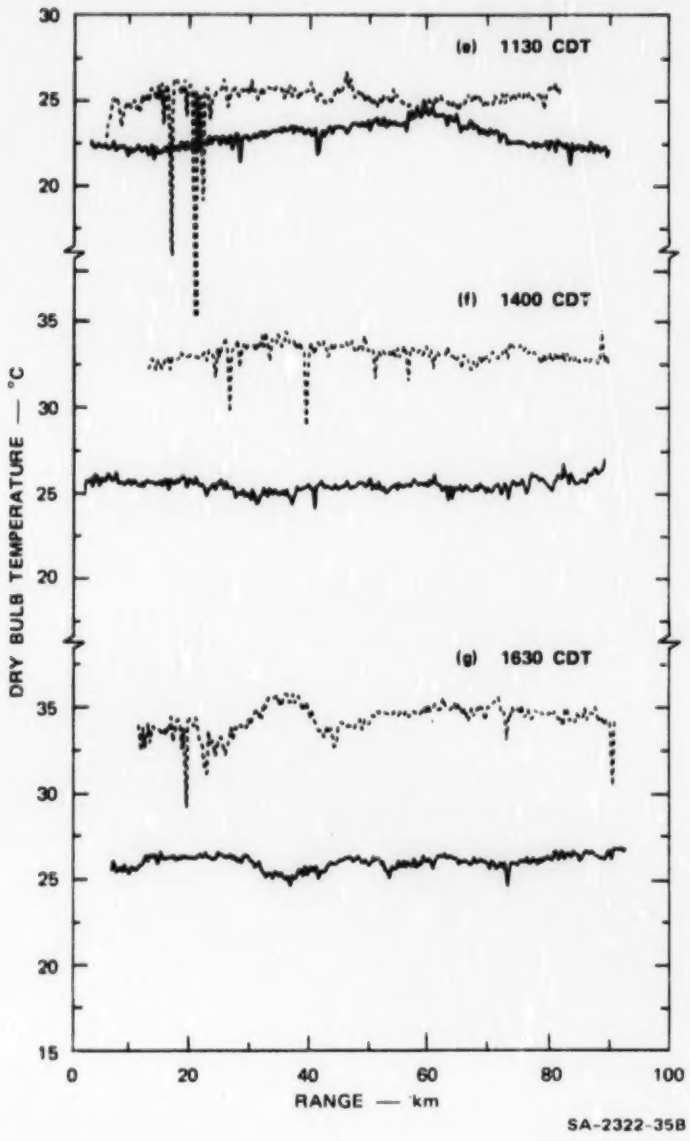

FIGURE A-13 AIRCRAFT AIR TEMPERATURE MEASUREMENTS, 11 AUGUST 1972 (Concluded)

Altitudes: 460 m (dashed) and 1220 m (solid)

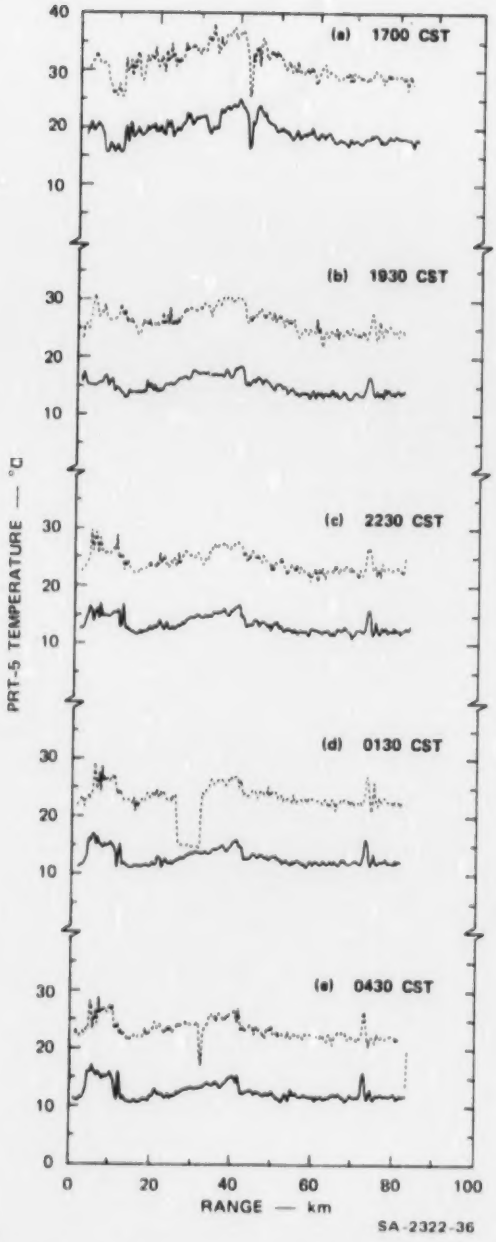

FIGURE A-14 AIRCRAFT RADIOMETRIC SURFACE TEMPERATURE MEASUREMENTS, 23-24 APRIL 1973

Dashed curve: measurements from 460 m, 10°C added
Solid curve: measurements from 1220 m

REFERENCES

1. H. H. and K. Lettau, "Exploring the World's Driest Climate: Scientific Results of the University of Wisconsin Field Studies during July 1964, in the Peruvian Dessert (Pampa de la Joya), pre-publication draft, Madison, Wisconsin (1971).

2. E. E. Uthe, "Lidar-Derived Aerosol Structure over St. Louis, Missouri, during METROMEX 1972", Interim Report, NSF Grant GI-34770, Stanford Research Institute, Menlo Park, California (1972).

3. Physics of Plant Environment, W. R. VanWijk, Ed., (North-Holland Publishing Company, Amsterdam, 382 pp, 1963).

4. W. C. Swinbank, "Long-Wave Radiation from Clear Skies" Quarterly Journal of the Royal Meteorological Society, 381, 339-348 (1963).

5. W. F. Dabberdt, "Climatonomy of the Antarctic Plateau," paper presented at the Conference on Planetary Boundary Layers, 18-21 March 1970, sponsored by IUGG, IAMAP, and AMS, Boulder, Colorado.

6. E. Kung, "Climatology of Aerodynamic Roughness Parameter and Energy Dissipation in the Planetary Boundary Layer over the Northern Hemisphere, Section 2 of Studies of the Effects of Variations in Boundary Conditions on the Atmospheric Boundary Layer, Department of Meteorology, University of Wisconsin, Annual Report Contract DA-36-039-AMC-00878, USAERDA, Ft. Huachuca, Arizona (1963).

7. H. Panofsky, and G. N. Brier, Some Applications of Statistics to Meteorology, (Mineral Industries Continuing Education, Pennsylvania State University, University Park, Pa. 224 pp, 1965).

8. S. Changnon, "1972 Operational Report for METROMEX", Illinois State Water Survey, Urbana, Illinois (1972).

9. H. H. Lettau, Micrometeorology Syllabus, Meteorology 403, Department of Meteorology, University of Wisconsin, Madison, Wisconsin (1968).